T

SN251 74-17

~~配付禁止~~

~~Not For Publication~~

本資料は H13年 11 月 30 日付けで登録区分変更する。

〔技術情報グループ〕

Thermo-Hydraulic Dynamics by Release of Molten Fuel in a Fuel Assembly

July, 1974

POWER REACTOR AND NUCLEAR FUEL DEVELOPMENT CORPORATION

SN251 74-17
July, 1974

Thermo-Hydraulic Dynamics by Release of Molten Fuel in a Fuel Assembly*

Masaji Tezuka**
Shuichi Ohta** and
Hikaru Kajiwara**

Abstract

For the purpose of evaluating the safety and studying the safety measures against accidents in a nuclear reactor core which present serious problems in designing a fast breeder reactor today, analytical evaluation was conducted on the monitoring system as to its feasible conditions and the extent for the monitoring of in-pile irregularities which may be a possible cause for accidents in a fuel assembly. For the target accident for the evaluation of the monitoring system, local release of molten fuel which is assumed to be a cause for channel blockage in a fuel assembly was taken up. The respondency of the flowmeter at the outlet to the coolant flow fluctuations by the fuel-sodium interaction, and the respondency of the thermometer at the outlet to the heat transmission behavior in a fuel assembly by a heat release from fuel to sodium were studied respectively from the standpoint of safety analysis.

This is the translation of the report, No. SJ201 74-14, issued in February, 1974.

* Work programed by Tokyo Shibaura Electric Co., Ltd. under contract with Power Reactor and Nuclear Fuel Development Corporation.

** Tokyo Shibaura Electric Co., Ltd.

CONTENTS

I. Introduction

Safety evaluation and safety measures against localized accidents in a fast breeder reactor core are being taken up as an important problematic point in the safety design of reactor core. For the major reason of this, it may well be said that the possibility of localized accident in a localized channel blockage and the propagation of the accident has not yet been completely eliminated at this stage of the research and development effort, and also that since the possible location of accident is quite localized, it is difficult to detect or find it out at its earliest stage. Therefore, in order to provide sufficient safety measures to any section where exists a potentiality of accident in a fuel assembly, the physical aspect of accident occurrence, its mechanism and the propagation process therefore must be first correctly grasped and then must be developed an accident evaluation. It is also necessary to sufficiently study the detection and monitoring conditions including whether the monitoring system is able to monitor and detect an accident at the time of an irregularity warning signal, and further, how such warning signals should be handled and how to prevent such a localized accident from propagating to the adjacent fuel assemblies.

Consequently, in this study, in order to give a better and correct respondency between the actual occurrence phenomena of localized accident in the fuel assembly and the detector's detection condition and extent, localized molten fuel release accidents inside the fuel assembly were taken up as the subject of detection evaluation for accident analysis, and on this basis, the respondency of the monitoring system was studied.

The potentiality of occurrence of this type of accident is considerred to be as the result of a fuel burst caused by localized channel

blockage. When the molten fuel is released locally into the flow channel in the fuel assembly, the sodium will suddenly boils up by the thermal interaction of the released fuel and sodium, and thus the surrounding coolant flow will be greatly disturbed. Also it is well expected that by the massive release of thermal energy from the molten fuel into sodium, the surrounding coolant temperature may rise considerably high. Consequently, it is thought that the flow fluctuations caused by sudden generation of sodium voids are responded by the outlet flowmeter, while the released thermal energy into the coolant from the released fuel may be responded by the outlet thermometer via the thermal transmission process in the fuel assembly.

For the method of analysis, studies were undertaken with the following two independent analytical models relating to evaluation of respondency of both the outlet flowmeters and outlet thermometers:

In this study, the prototype reactor "MONJU" (power output 300 MWe) which is under design development at present is taken up as the subject of analysis.

II. Analysis of Coolant Flow Behavior by Localized Molten Fuel-Sodium Interaction

In the event that a localized fusion of fuel takes place in the fuel pin and is released into the coolant flow channel, a violent sodium vaporization will be caused by thermal interaction of the remaining sodium and the released molten fuel inside the channel, which in turn will cause a large flow turbulence of the coolant in its vicinity. But if the released molten fuel is quite localized and in small quantity, the once generated Na voids are cooled by the coolant in the vicinity where an interaction takes place and on the surface of the fuel pins, and it is considerable that these produced voids are again condensed and disappear in a short time.

Consequently, the following analytical study was conducted to determine what would be the amount of molten fuel to contribute to UO_2-Na interaction in a localized molten fuel release accident for which the present flowmeters are designed, what detectable flow fluctuation would be caused to the coolant, and further whether the detection rate is sufficient to warrant safety.

II-1. Analytical Method

For the analysis of the coolant flow behavior by sodium voids following a localized molten fuel release, our calculation code "SUGAR"[2] was used This code was developed based on the Cho-Wright Model[1] which is most generally employed today for analysis of UO_2-Na interaction.

The analytical model and the equations employed for our code "SUGAR" are given as follows:

II-1-1. Analytical Model

Fig. II-1 illustrates the analytical model of UO_2-Na interaction in the fuel assembly.

The major hypotheses used for this analysis are listed as follows:

(1) The released molten fuel in the form of spherical particles homogenizes with sodium in the discharged region.

(2) The temperature distribution the fuel particles in a transient period is obtained by a heat conduction equation considering the melting latent heat and heat generation.

(3) The interacting sodium has an even temperature in both phases of gas and liquid, and Na void is in a state of constant saturation at all times.

(4) The non-condensed gas mixed in the interacting region will be subject to insulated compression variation.

(5) The interacting region is of a cylindrical form, and Na void's movement is only one dimensional in the axial direction, and no radial direction movement is considered. Consequently, any coolant outside the interacting region's cross section has no turbulent flow maintaining a nominal flow rate.

(6) Na temperature in the neighboring area of the interacting region is constant, and Na void cooling is considered. In this case, the heat transfer rate at the time of cooling is given as the function of the contact space ratio between Na voids in the interacting region and the surrounding Na.

(7) The heat transfer rate between UO_2 and Na is given as the function of the volume ratio of the gas inside the interacting region (Na void + Non-Condensed gas).

II-1-2 Theoretical Equations

The following equations were employed for the analysis.

(1) Heat transfer from fuel to sodium

The temperature distribution in the spherical fuel particle can be obtained from the following one dimensional heat conduction equation:

$$C_{PF}\,\rho_F \frac{\partial T_F}{\partial t} = \frac{1}{r^2}\frac{\partial}{\partial r}\left(K_F r \frac{\partial T_F}{\partial r}\right) + g_{FO} \qquad \text{(II-1)}$$

Here, T_F : Temperature in fuel particle

g_{FO} : Heat generation density of fuel

C_{PF} , ρ_F, K_F: Specific heat, density, and heat conductivity of fuel

The phase change from liquid to solid of the molten fuel by Na cooling has considered the melting latent heat of the fuel and the heat transfer rate from fuel to sodium is given by the following equation:

$$\frac{dQ_{FS}}{dt} = A_{FS} h_{FS} (T_{FO} - T_S) \qquad \text{(II-2)}$$

Here, Q_{FS} : Heat transfer rate from fuel to sodium

T_{FO} and T_S : Surface temperature of fuel particle and sodium temperature

A_{FS} and h_{FS} : Contact area between fuel and sodium and heat transfer rate between fuel and sodium

Here, considering the gas blanketing effect of the fuel particle surface by Na voids and non-condensed gas, it is assumed that h_{FS} is given by the following equation:

$$h_{FS} = \alpha_G h_{FSG} + (1 - \alpha_G)\, h_{FSL} \qquad \text{(II-3)}$$

Here,

$$\alpha_G = \frac{\mathbb{V}_V + \mathbb{V}_G}{\mathbb{V}_F + \mathbb{V}_S + \mathbb{V}_G} \quad : \text{ Gas volume ratio}$$

h_{FSG} : UO_2-Na heat transfer coefficient at the time of gas blanketing.

h_{FSL} : UO_2-Na (liquid) heat transfer coefficient

$\mathbb{V}_F$, $\mathbb{V}_S$, $\mathbb{V}_G$ and $\mathbb{V}_V$: Fuel in the interacting region, Na (two-phase mixture), non-condensed gas, and Na voide volume respectively.

(2) Na thermo-dynamics equation

The energy equation of sodium is given by the following equation from the first law of thermo-dynamics.

$$\frac{dH_S}{dt} = \frac{dQ_{FS}}{dt} - \frac{dQ_{SB}}{dt} + V_S \frac{dP_S}{dt} \qquad \text{(II-4)}$$

Here, H_S, V_S and P_S : Enthalpy per unit of mass of Na, specific volume and Na pressure respectively.

Q_{SB} : Heat transfer rate from the interacting area to the surrounding coolant.

From the hypothesis of Na saturation state, the equation of Na estate at the time of two-phase mixing is given as follows:

$$H_S = xH_V + (1 - x)\, H_L \qquad \text{(II-5)}$$

$$V_S = xV_V + (1 - x)\, V_L \qquad \text{(II-6)}$$

Likewise for Na void pressure:

$$P_S = P_{sat}\,(T_S) \qquad \text{(II-7)}$$

Here, H_V and H_L : Na enthalpies for saturated vapor and

saturated liquid respectively.

V_V and V_L : Na specific volumes for saturated vapor and saturated liquid respectively.

x and P_{sat}: Na void mass ratio and saturation pressure.

(3) Thermal loss at the interacting region boundary

The heat transfer rate from sodium in the interacting region to the peripheral coolant is sought from the following expression:

$$\frac{dQ_{SB}}{dt} = A_{SB}\, h_{SB}\, (T_S - T_{BN}) \qquad \text{(II-8)}$$

Here, T_{BN} : Temperature of the peripheral coolant

A_{SB} and h_{SB} : Contact area between the peripheral coolant and sodium in the interacting region, and the contact heat transfer coefficient.

A_{SB} is given by the following expression considering the non-condensed gas:

$$A_{SB} = 2\pi R\,(R + Z_U - Z_L) \cdot \frac{\mathbb{V}_S}{\mathbb{V}_G + \mathbb{V}_S + \mathbb{V}_G} \qquad \text{(II-9)}$$

Here, R: Radius of the interacting region.

h_{SB} is assumed to be given by the following expression considering the condensation heat transfer of Na void:

$$h_{SB} = \alpha_{VS}\, h_{SL} + (1 - \alpha_{VS})\, h_{LL} \qquad \text{(II-10)}$$

Here, $\alpha_{VS} + \frac{Vv}{Vs}$ (Na void ratio)

h_{SL} and h_{LL} : Condensation heat transfer coefficient between Na void in the interaction region and the peripheral coolant, and the heat transfer coefficient between the liquid

sodium in the interaction region and the peripheral coolant.

(4) Equation of state for non-condensed gas

Assuming the gas mixed into the interacting region as an insulation compression, the following equation can be formulated:

$$P_S V_G^{\,n} = P_S(0) V_G(0)^n = \text{constant} \qquad \text{(II-11)}$$

Here, V_G : Specific volume of non-condensed gas

n: Gas constant

(5) Equation of motion of interacting region

Assuming the coolant in the periphery of the interacting region as non-compressible, the moving velocity of the upper and lower boundary faces of the interacting region is given by the following expressions:

Upper direction movement;

$$\frac{d^2 Z_U}{dt^2} = \frac{P_S - P_{out}}{\rho_N (L - Z_U)} - g - \left(\frac{f_o}{2D_e} + \zeta_U\right)\left(\frac{dZ_U}{dt}\right)\left|\frac{dZ_U}{dt}\right| \qquad \text{(II-12)}$$

Lower direction movement;

$$\frac{d^2 Z_L}{dt^2} = \frac{P_{in} - P_S}{\rho_N Z_L} - g - \left(\frac{f_o}{2D_e} + \zeta_L\right)\left(\frac{dZ_L}{dt}\right)\left|\frac{dZ_L}{dt}\right| \qquad \text{(II-13)}$$

Here, Z_U and Z_L : Heights of upper and lower boundary faces of the interacting region.

P_{in} and P_{out} : Pressures at inlet and outlet of the channel

ρ_N, f_o, and De: Coolant density, friction coefficient in the sub-channel, and equivalent flow diameter inside the cooling sub-channel respectively.

ζ_U and ζ_L: Pressure loss coefficients by the structural materials of upper and lower sections.

L : Total length of the channel

g : Gravitational acceleration

Assuming that the interacting region does not move to radius direction, the total volume of the interacting region $V_{T\phi T}$ can be given by the following expressions:

$$V_{T\phi T} = \pi R^2 (Z_U - Z_L) \qquad \text{(II-14)}$$

As $V_{T\phi T}$ is the mixture of fuel, sodium and non-condensed gas, the following equation can be formulated:

$$V_{T\phi T} = V_F + V_S + V_G \qquad \text{(II-15)}$$

(6) Calculation formula for the outlet mean flow velocity

Assuming (hypothesis 5) that only the flow fluctuation of the upper coolant on the cross section of UO_2-Na interacting region affects the outlet flow rate variation, the outlet mean flow velocity v_{out} is given by the following equation of continuity.

$$A_N \bar{v}_{out} = A_O Z_U + (A_N - A_O) v_N \qquad \text{(II-16)}$$

Consequently, the fluctuation ratio $\bar{v}_{out}$ of the outlet mean flow velocity at a rated time is:

$$\Delta \bar{v}_{out} = \frac{\bar{v}_{out} - v_N}{v_N} \qquad \text{(II-17)}$$

Here, A_N and A_O: Total cross section of the cooling channel inside the fuel assembly and the interacting cross section.

v_N: Coolant flow velocity in the channel at a normal state.

(7) Calculation formula for the detected flow velocity fluctuation rate by an outlet flowmeter

Expressing the detection time-lag of the flowmeter by τ_F, the detected flow velocity fluctuation rate $\triangle\bar{V}_F$ is sought by the following expression:

$$\frac{d(\triangle\bar{V}_F)}{dt} = \frac{\triangle\bar{V}_{out} - \triangle\bar{V}_F}{\tau_F} \qquad (II\text{-}18)$$

The physical elements to evaluate the thermal mechanism of this type of small scale UO_2-Na interaction is defined as follows:

(a) The total energy $E_{FT\phi T}$ of the released molten fuel:

$$E_{FT\phi T}(t) = M_F \left\{ \int_{T_{NO}}^{T_{MELT}} C_{PF}(T)\,dT + x_F(0)\,H_{FLAT} + \frac{g_{FO}}{\rho_F}\,t \right\} \qquad (II\text{-}19)$$

(b) The heat quantity Q_{FS} released from fuel to sodium:

$$Q_{FS}(t) = \int_0^t \frac{dQ_{FS}}{dt}\,dt \qquad (II\text{-}20)$$

(c) Heat quantity Q_{SB} released outside the interacting region:

$$Q_{SB}(t) = \int_0^t \frac{dQ_{SB}}{dt}\,dt \qquad (II\text{-}21)$$

(d) Enthalpy of Na void produced by the interaction:

$$E_V = M_{NA}\,x\,Hv \qquad (II\text{-}22)$$

Here, the above state each energy represents the increased volume above the standard of the Na energy at the initial stage of interaction.

Where, M_F and M_{NA} : The masses of fuel and Na contributing to the interaction respectively.

$x_F(0)$ and H_{FLAT} : Fuel melting rate and fuel melting latent heat respectively at the initial stage of reaction

II-2. Analysis and Evaluation

II-2-1. Analytical Conditions

The design calculation conditions and the thermal-hydraulic dynamics calculation conditions necessary for this analytical work are given in Chapter II-1. Also, considering from the thermal-hydraulic state at the time of a localized molten fuel release in the fuel assembly, the following factors were analyzed and studied as parameters; Released molten fuel (= fuel contributing to interaction); fuel particle diameter; interacting channel cross section ratio in the fuel assembly; peripheral mean temperature in the interacting region; mixing ratio of non-condensed gas; UO_2-Na heat transfer rate at the time of gas blanketing; and the coolant flow fluctuation by interaction with each parameter selecting the condensation heat transfer rate of Na voids. The calculation standard values for each parameter and the extent of survey are given in Table II-2. Especially, for the heat transfer coefficient h_{FSL} between UO_2 and Na (liquid), the experimental data of UO_2-Na interaction by A.W. Cronenberg[3], and the experimental data of the sodium pool boiling in Soviet were respectively adopted. In respect of other parameter standard values, as it was the purpose of this work to make clear the detection capability of the outlet flowmeters in a fuel release accident, they were selected on the basis of such conditions which are more difficult to be detected than the actual phenomena from the safety standpoint, namely on the basis of such conditions as the flow fluctuation are smaller.

II-2-2. Analytical Results and Evaluation

The results of the analysis conducted under the calculation conditions as shown in Table II-1 and II-2 are shown in Fig. II-2 through to Fig. II-18.

(1) Effect of Released Fuel Mass

Fig. II-2 shows Na voids' axial direction movement behavior by the fuel mass when the temperature in the periphery of the interacting region is assumed to be 600 °C. When the released fuel mass is about 10g. Na void, having a low generating pressure, does not diffuse, but more riding on the coolant stream, disappears in a short while (40 msec). If the fuel mass is about 50g, Na void growes and fills the entire area of the core helped by the void generating pressure resulting from the interaction. This Na void, however, disappears in about 188 msec cooled by the surrounding coolant flow. If the released fuel mass further increases, although the cooling effect in the Na void boundary lowers the Na void pressure and Na void is once compressed by the inert force of the upper and the lower Na columns, it once again expand following the revival of the Na void pressure since the thermal energy supply from the fuel in the interacting region surpasses the heat loss from the Na void boundary. This is clearly illustrated by Fig. II-3, Fig. II-6 and Fig. II-7 respectively.

Fig. II-3 shows the time-histories of generating pressures of Na voids under the same conditions. The first pressure peak is produced by a violent transfer of thermal energy from fuel to sodium, while the second pressure peak is created by a violent compression effect of Na void by the surrounding sodium. The pressure peaks occurring time are extremely short. It is merely about several msec after UO_2-Na contact for the first peak, while for the second peak, it is determined depending on the relations between the thermal transfer rate from fuel to sodium, heat loss rate at the boundary, and the voids' space behavior. Because of

this its time-length depends on the conditions and state at the time of fuel release. However, as the result of various parameter surveys it was made known that in the case of this type of accident, the second pressure peak occurred in most cases within the range of 200 - 300 msec.

Fig. II-6 shows the mean flow velocity fluctuation rate $\triangle V_{out}$ at the outlet of the fuel assembly created as the result of the Na voids' axial direction movement as shown by Fig. II-2. The oblique lined region represents the region above the designated points assuming that these designated points for measuring flow fluctuation by outlet flowmeters have ±10%. Under this condition, the maximum value of the flow fluctuation has occurred within 20 msec after the UO_2-Na interaction. But, for the time-length for the detection designated points above ±10%, the outlet flow fluctuation had more on the negative side in most cases.

Fig. II-5 represents the fuel and Na temperature variations by interaction when the fuel mass is 100g and the peripheral temperature is 600 °C. The reason for the abrupt drop of temperature on the surface of the fuel after the fuel-sodium contact and its rise thereafter is because that immediately after the contact, Na voids are produced and UO_2-Na heat transfer rate declines. In this case, the central temperature of the fuel particle declines after 220 msec, and even when Na voids disappear, the fuel temperature still continues the level of 1500 - 2000 °C. Consequently, after the disappearance of Na void, a potentiality of recurrence of Na boil is well considerable.

Fig. II-6 and Fig. II-7 respectively indicate the energy fluctuations in various sections by interaction and the Na void energy fluctuation. The oblique lined section of Fig. II-6

represents the Na enthalpy which is determined by the heat balance of the released energy from fuel to sodium and from sodium to the surrounding coolant. Consequently, when the oblique lined section is larger, the Na void energy is also large as shown by Fig. II-7. The second peak of the void energy is equivalent to that when the voids are abruptly compressed.

(2) Effect of Peripheral Coolant Temperature

Fig. II-8 shows the direction movements of Na voids under the influence of the peripheral temperature when the fuel quantity is 50g. As is evident from this diagram, the temperature in the fuel assembly at the time of a fuel release accident greatly affects the space transfer behavior of Na void. That is, while the localized accident in the fuel assembly remains without propagating wider, the produced Na void disappears early. But when the accident has propagated considerably wider and the temperature of the coolant in the fuel assembly as well as the temperature of the structural materials have risen higher, Na voids remain without disappearing for a long time (200 msec or longer). Consequently, detection of flow fluctuation is easier when an accident has propagated to certain degree than its initial stage.

(3) Effect of Released Fuel Particle Size

Fig. II-9 and Fig. II-10 respectively show the Na voids' space movements and the mean flow rate fluctuation ratio at the outlet at the time when the fuel particle diameters were parametered. In this case, as the fuel quantity was 50g and the peripheral temperature was 400 °C, there was no vibration of Na voids. But since the smaller is the particle diameter, the larger is the contact area with the voids, and thus the greater becomes the heat transfer energy from fuel to sodium, and the voids grow and expand further.

On the contrary, when the particle size is large, as the fuel temperature will not decline so much after disappearance of voids, recurrence of sodium boil is feared.

Judging from the outlet mean flow velocity fluctuation ratio as shown by Fig. II-10, it is evident that the smaller is the particle size, the more violent is the flow fluctuation, and that much is easier for flow fluctuation measurement.

(4) Effect of UO_2-Na Heat Transfer Rate at Gas Blanketing

Fig. II-11 shows the Na void space movement in the case when UO_2-Na (vapor) heat transfer coefficient is parametered. Under this condition, there is observed no appreciable void behavior affected by this heat transfer coefficient, and the void disappearance time lag resulted in 80 msec maximum.

(5) Effect of Na Void Condensation Heat Transfer Coefficient

Fig. II-12 represents the Na void space movement at the time when the condensation heat transfer rate is parametered. The same as in the case of Fig. II-11, the Na void movement pattern showed no much difference except in the case of making the condensation effect a zero.

(6) Effect of Interacting Cross Section Ratio

The above described interacting cross section ratio is in such a case where interactions have taken place in an area representing a 20% of the total flow channel cross section of the fuel assembly. The outlet mean flow velocity fluctuation rate in the case of having enlarged this cross section ratio is given in Fig. II-13. When the interacting region is enlarged in the radius direction, as the turbulence of coolant flow in the fuel assembly widens that much, the outlet mean flow velocity fluctuation becomes naturally larger. However, the axial direction

displacement rate of Na void is reduced in proportion to the size of the void cross section, and in this analytical model, they result in disappearing quickly. For the convenience of easier detection, naturally, it is better with wider interacting regions.

(7) Effect of Non-Condensed Gas Mixing Rate

In an actual case of accident of molten fuel release in a fuel assembly, it is expected there will be remaining some FP gas and Na voids in the vicinity of the molten fuel released region. Consequently, UO_2-Na interaction in this case is thought to present considerably a different thermohydraulic dynamic picture when compared with the state where there is no presence of mixed gas. Fig. II-14 and Fig. II-15 illustrate respectively the produced pressure change and the outlet mean flow velocity fluctuation rate in the case of parametering the mixed gas volume ratio at the initial stage of interaction. As is evident from Fig. II-14, when the mixed gas volume is large, the Na void pressure produced by the interaction substantially declines affected by the pressure absorption by the mixed gas. Consequently, the growth rate of Na voids is considerably moderated as is evident from Fig. II-15.

(8) Na Void Characteristics toward Fuel Quantity Which Contributes to Interaction

Fig. II-16 and Fig. II-17 represent the pressure peak against fuel quantity and the relation of Na voids with their disappearing time in the case where adopted some changed factors such as the peripheral temperatures of 600 ℃ and 400 ℃, UO_2-Na (vapor) heat transfer rate at 6.279W/cm^2 ℃, and the condensation heat transfer rate at 0.1W/cm^2 ℃, and the parametered standard values of other condition.

From Fig. II-16, the first pressure peak value and the fuel

quantity are approximately in a good proportional relation. But the second pressure peak value is larger when the fuel quantity is smaller so long as Na voids are remaining. In either case, impulsewise it is lower comparing with the first pressure peak. For this reason, for the pressure effect to the structural materials inside the fuel assembly, the produced pressure itself by UO_2-Na interaction remains without change as the main pressure. From Fig. II-17, it is known that the void existing time is greatly influenced by not only the fuel quantity but also the peripheral boundary conditions and the effect of various kinds of heat transfer rates. The fact that the void existing time under the peripheral temperature of 600 °C shows an abrupt rise in the vicinity of 60g of fuel quantity well indicates that the released energy in the vicinity of this quantity of fuel is giving a critical value whether to make disappear Na voids after they have once been produced or have them revived once again to continue vibrating in the space.

II-2-3. Evaluation of Respondency of Outlet Flowmeters

The space movements of Na voids by a localized UO_2-Na interaction following a localized molten fuel release in the fuel assembly have been analyzed and evaluated as described under previous chapters by survey calculations on the basis of various parameters. In this chapter, the outlet flowmeter's respondency shall be evaluated by use of the analysis results of outlet flow rate fluctuation respondence. Fig. II-17 illustrates the respondency performance of the flowmeters in the case that the flowmeter's time constant τ_F against the outlet mean flow velocity fluctuation rate under 100g of released fuel quantity and 600 ℃ of the peripheral temperature is parametered. Under

this condition, the space movements of Na voids by the UO_2-Na interaction are fairly large and continue for a long time (~ 400 msec). Because of this, with a flowmeter of time constant from 25 msec to 100 msec, it is possible to detect them since the present flowmeters designed to reach the detection designated point ±10%. Even so, however, it seems hardly expectable to detect Na void space vibration behavior in this case.

Consequently, in the event of trying to detect an accident of a localized UO_2-Na interaction, it becomes essential to detect the flow fluctuation immediately after the occurrence of an interaction. Considering this matter from the standpoint of detecting such flow rate fluctuation, the time lapse T_{FD} exceeding the detection designated point +10% to measure the outlet mean flow rate variation ratio is considered to be an important factor for judging the easiness of detection. On this basis, Fig. II-18 shows the relation between the value of T_{FD} and the released fuel as the result of various parameter surveys.

With the increase of fuel quantity, the space movements of Na voids become stronger in proportion to the fuel increase amount, and it is clear as from the diagram that T_{FD} also grows larger. Likewise, as shown by said diagram, since Na voids' growth lasts for a longer time as higher is peripheral temperature, greater is UO_2-Na (vapor) heat transfer rate and smaller is the condensation heat transfer coefficient, T_{FD} also becomes larger.

Now, considering from the time constant of the present designed flowmeter, if the safe-side $T_{FD} \geqq 50$ msec is assumed as a detection feasible region, it may be safe to consider as detection feasible in the case of an accident involving more than at least 100g molten fuel release as indicated by the diagram.

Since the maximum pressure producing value of UO_2-Na interaction with about 100g of molten fuel is at the level of 50 atm, it is hardly conceivable that there is any possibility of damage on the wall of the wrapper tube.

Table II-1. Calculation Conditions for Analysis of Flow Fluctuation of Coolant by Localized UO_2-Na Interaction

Input Calculation Condition	Symbol	Value	Unit
Total flow channel cross section in a Fuel Assembly	A_N	38.69	cm^2
Total flow channel length	L	280	cm
Axial central position of interaction region	H_{CENT}	83	cm
Channel outlet pressure	P_{out}	1.5	atm
Steady state flow velocity in flow channel	v_N	600	cm/sec
Initial flow velocity at UO_2-Na interaction	$\dot{Z}_V(0), \dot{Z}_V(0)$	600	cm/sec
Initial fuel temperature at UO_2-Na interaction	T_{FO}	2700	℃
Initial fuel melting rate	x_{FO}	1.0	—
Initial Na Temperature at UO_2-Na interaction	T_{NO}	881.3	℃
Na Quantity Contributing the interaction	M_{NA}	10	g
UO_2-Na (Liquid) heat transfer coefficient	h_{TCL}	6.279	W/cm^2 ℃
Heat transfer coefficient betweeen Liquid Na.	h_{TCL}	10.0	W/cm^2 ℃
Axial central position of initial interaction region.	H_{CENT}	83	cm

Table II-2. Parameter Range for Analysis of Coolant Flow Behavior by Local UO_2-Na Interaction

Parameter	Symbol	Standard Value	Survey Extent	Unit
Molten fuel quantity contributing to the interaction (UO_2/Na mixing weight ratio)	M_F	50	10 - 200	g
Fuel particle diameter	D_{FO}	1.0	2.0 - 2.5	mm^{ϕ}
Cross section ratio of the interaction region to total flow channel	A_O/A_N	0.20	0.2 - 0.81	—
Peripheral temperature of the interaction region	T_{BN}	400/600	400 - 800	℃
Initial voluminal mixing ratio of non-condensed gas	$V_G/V_{T\phi T}$	0	0. - 0.99	—
UO_2-Na Heat transfer coefficient at gas blanketing	h_{TCG}	0.1	0. - 6.279	W/cm^2 ℃
Heat transfer coefficient of Na void condensation	h_{SL}	0.580	0. - 1.0	W/cm^2 ℃

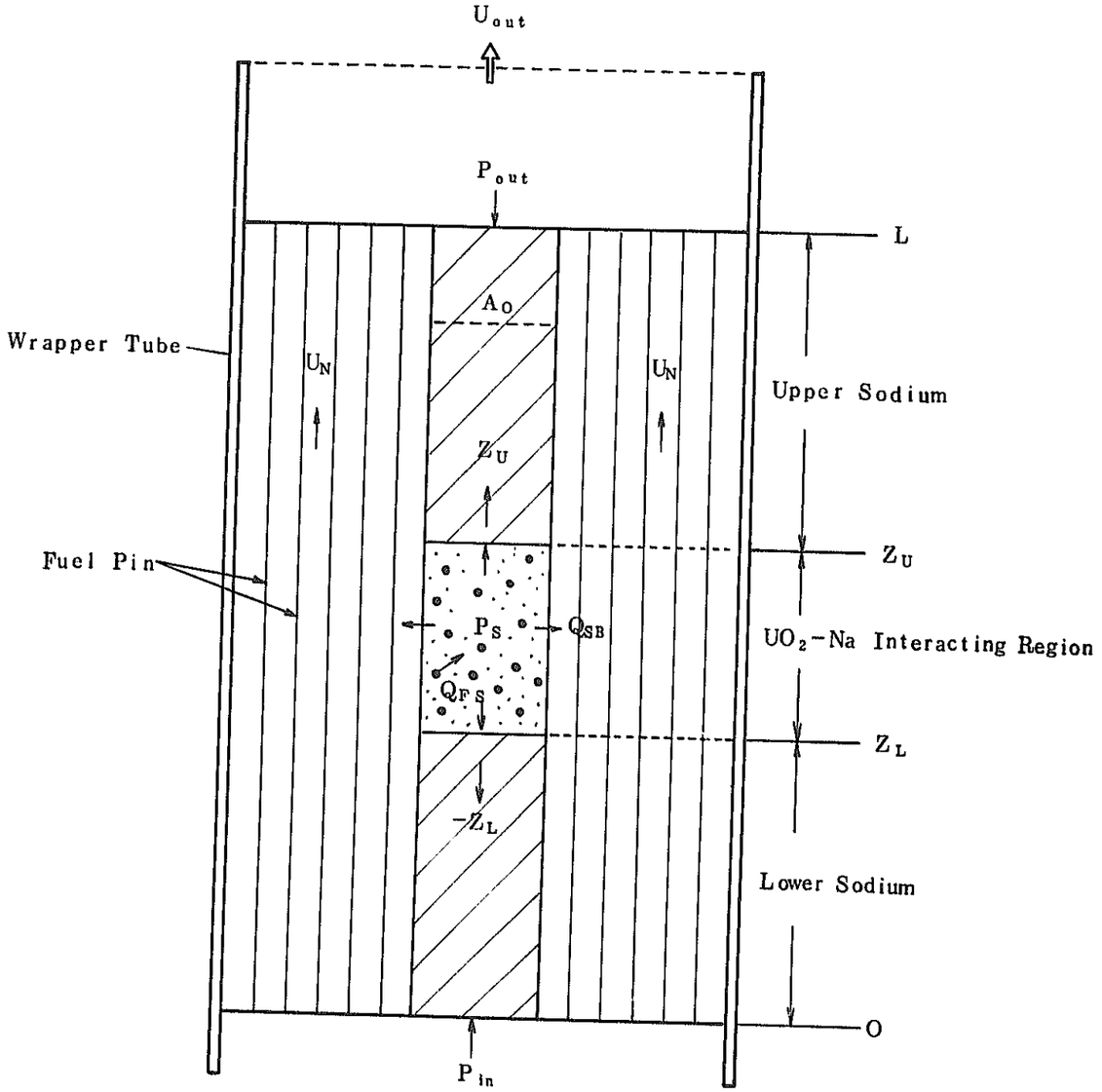

Fig. II-1. Analytical Model of Coolant Flow Behavior by Local UO_2-Na Interaction

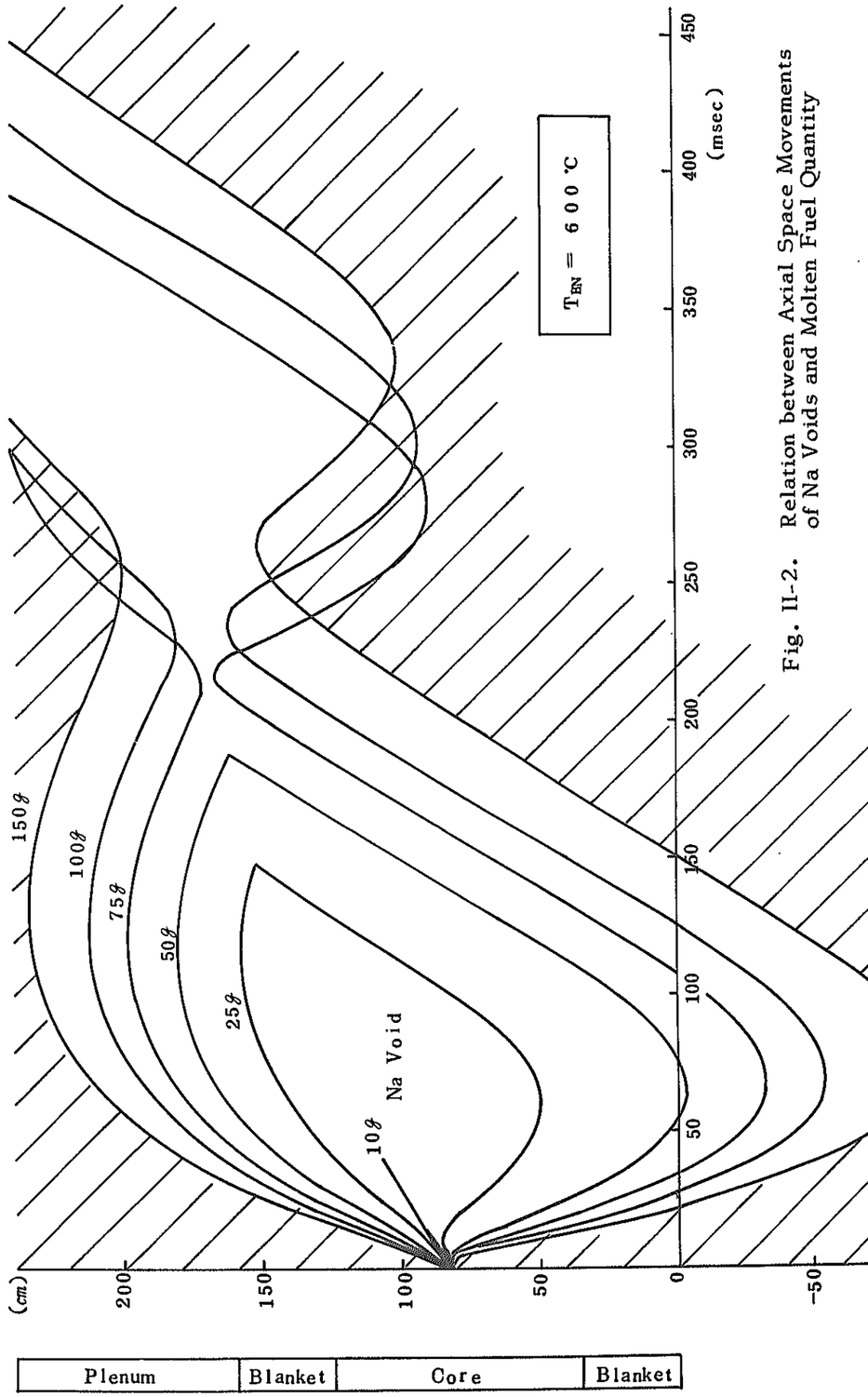

Fig. II-2. Relation between Axial Space Movements of Na Voids and Molten Fuel Quantity

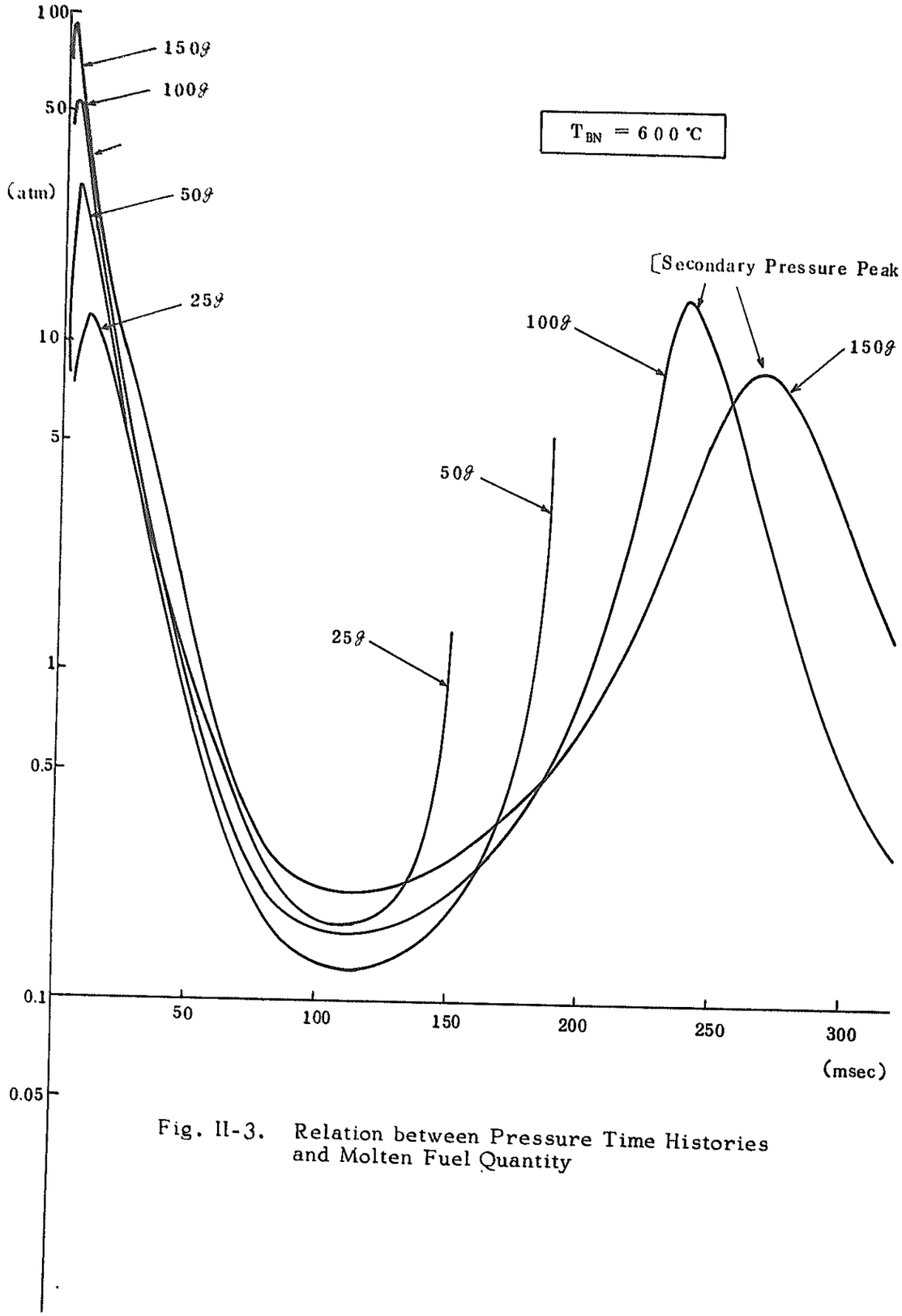

Fig. II-3. Relation between Pressure Time Histories and Molten Fuel Quantity

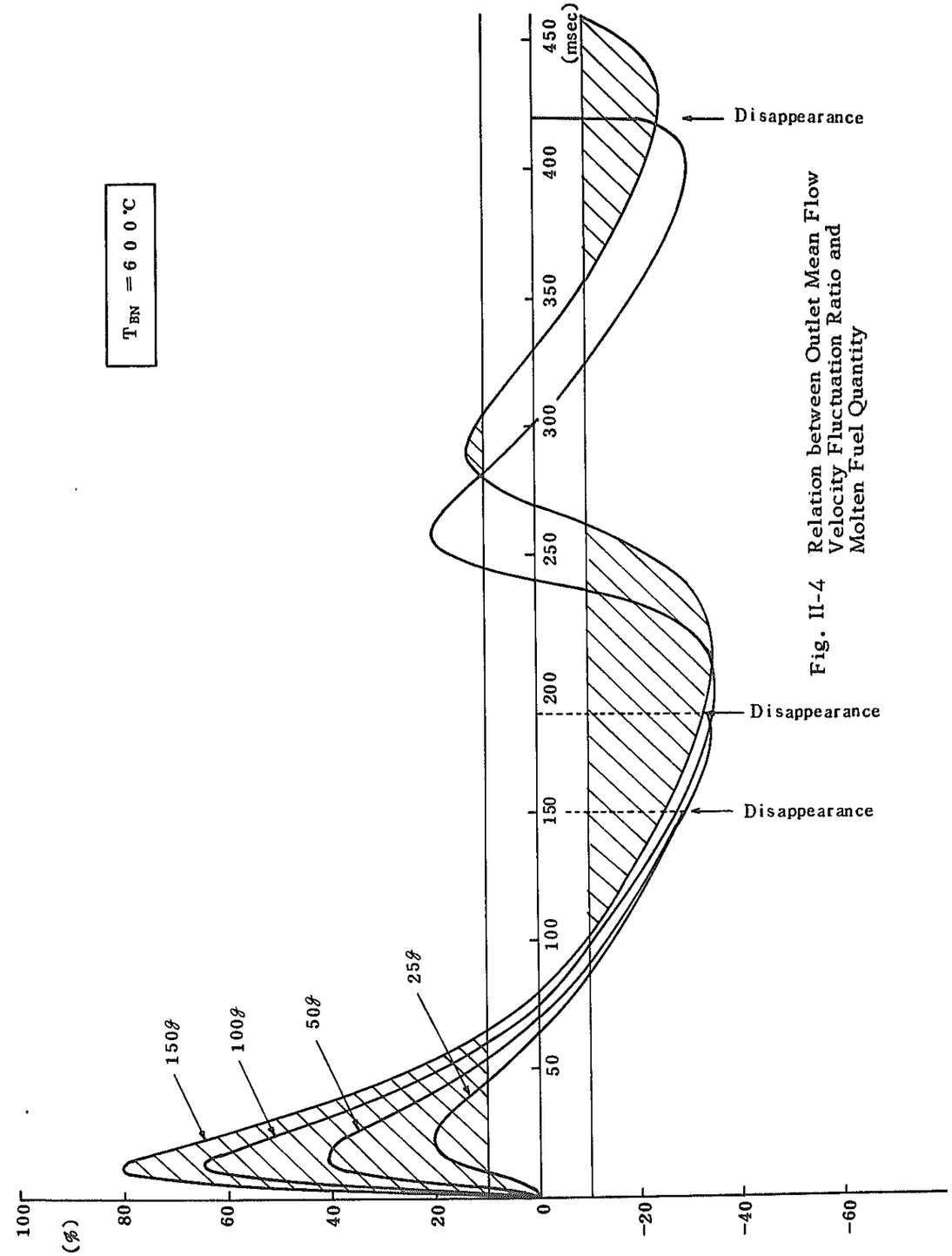

Fig. II-4 Relation between Outlet Mean Flow Velocity Fluctuation Ratio and Molten Fuel Quantity

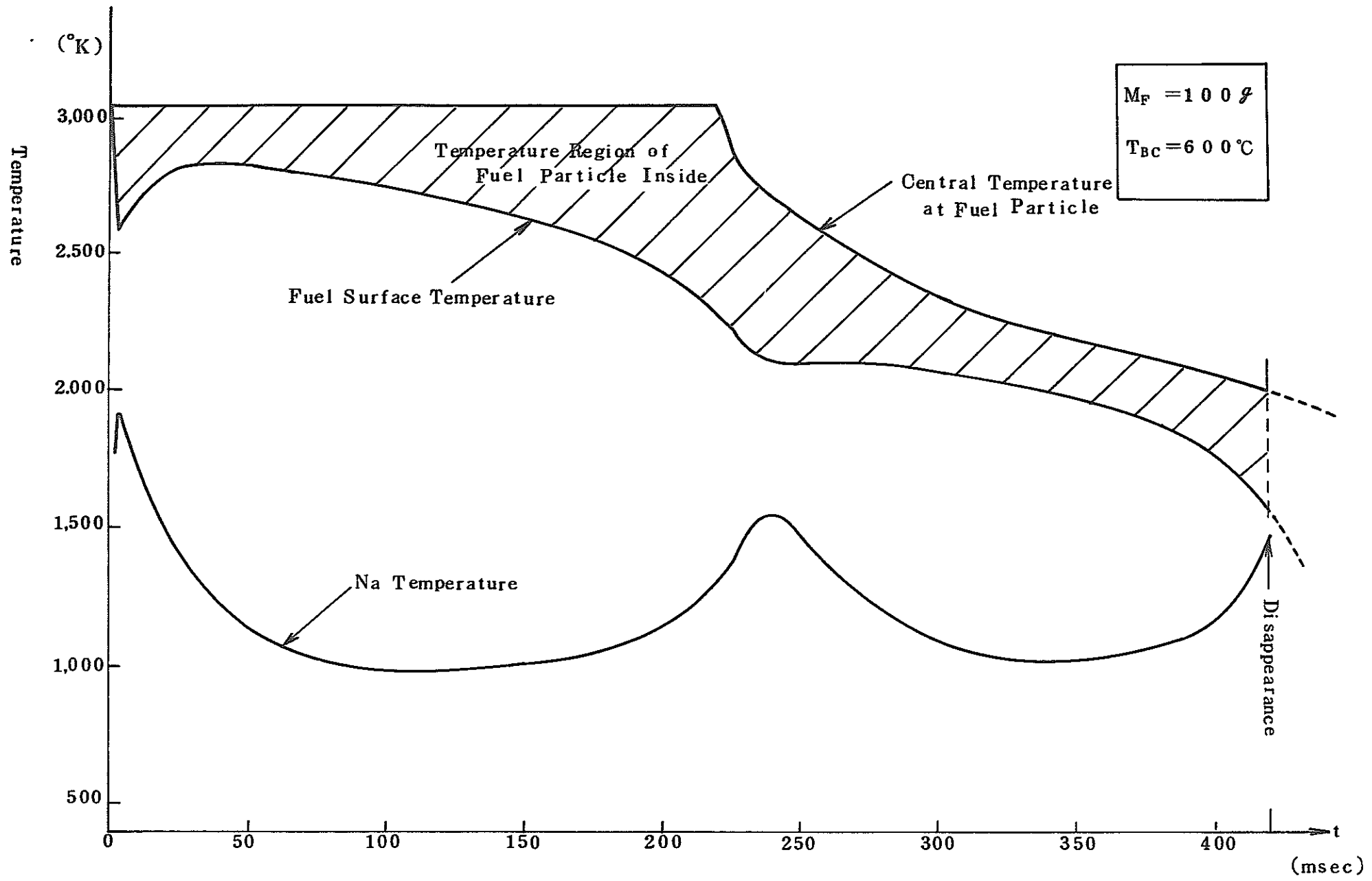

Fig. II-5. Temperature changes of fuel and Na during UO_2-Na interaction

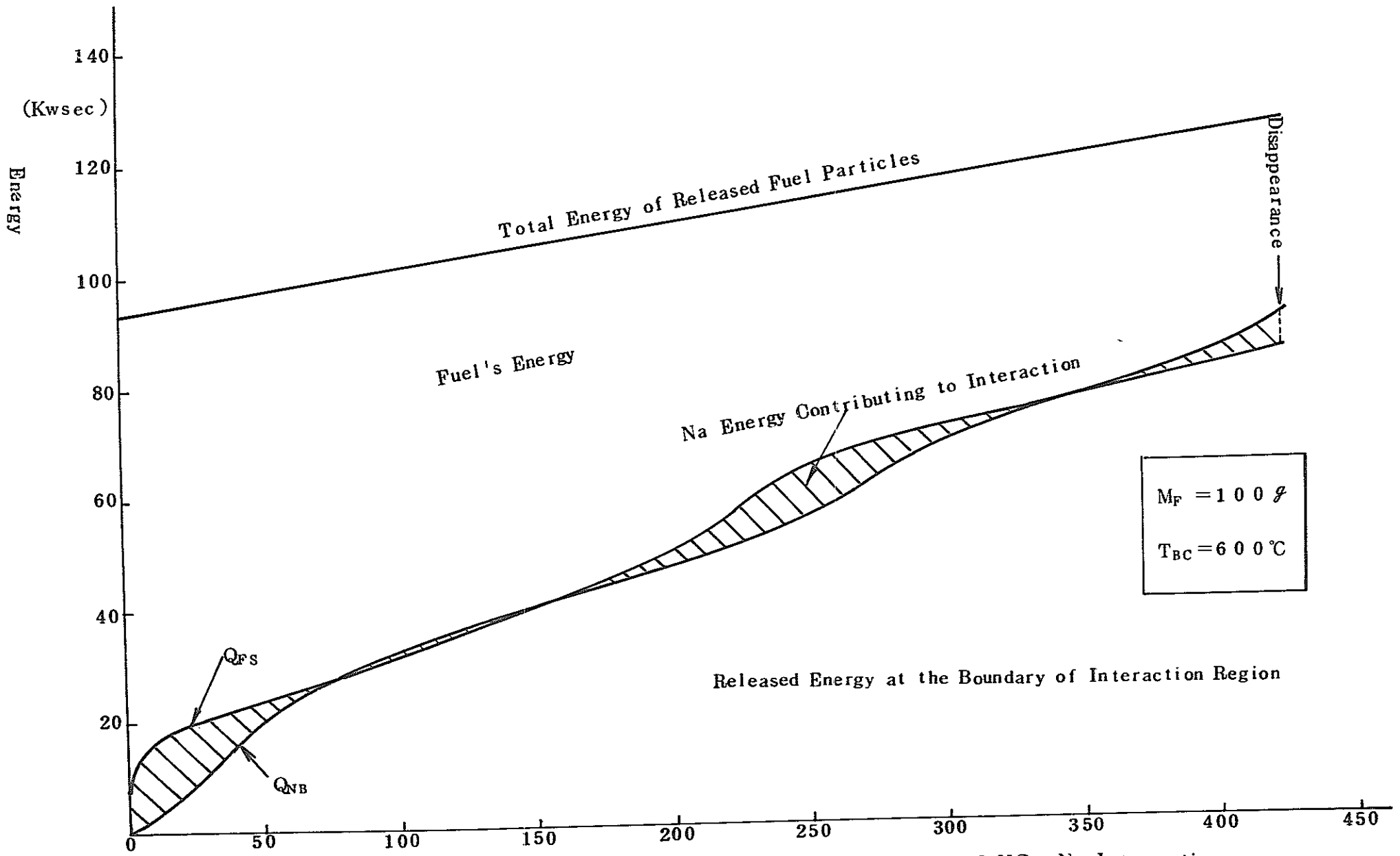

Fig. II-6. Energy Variation at Each Section by Local UO_2-Na Interaction

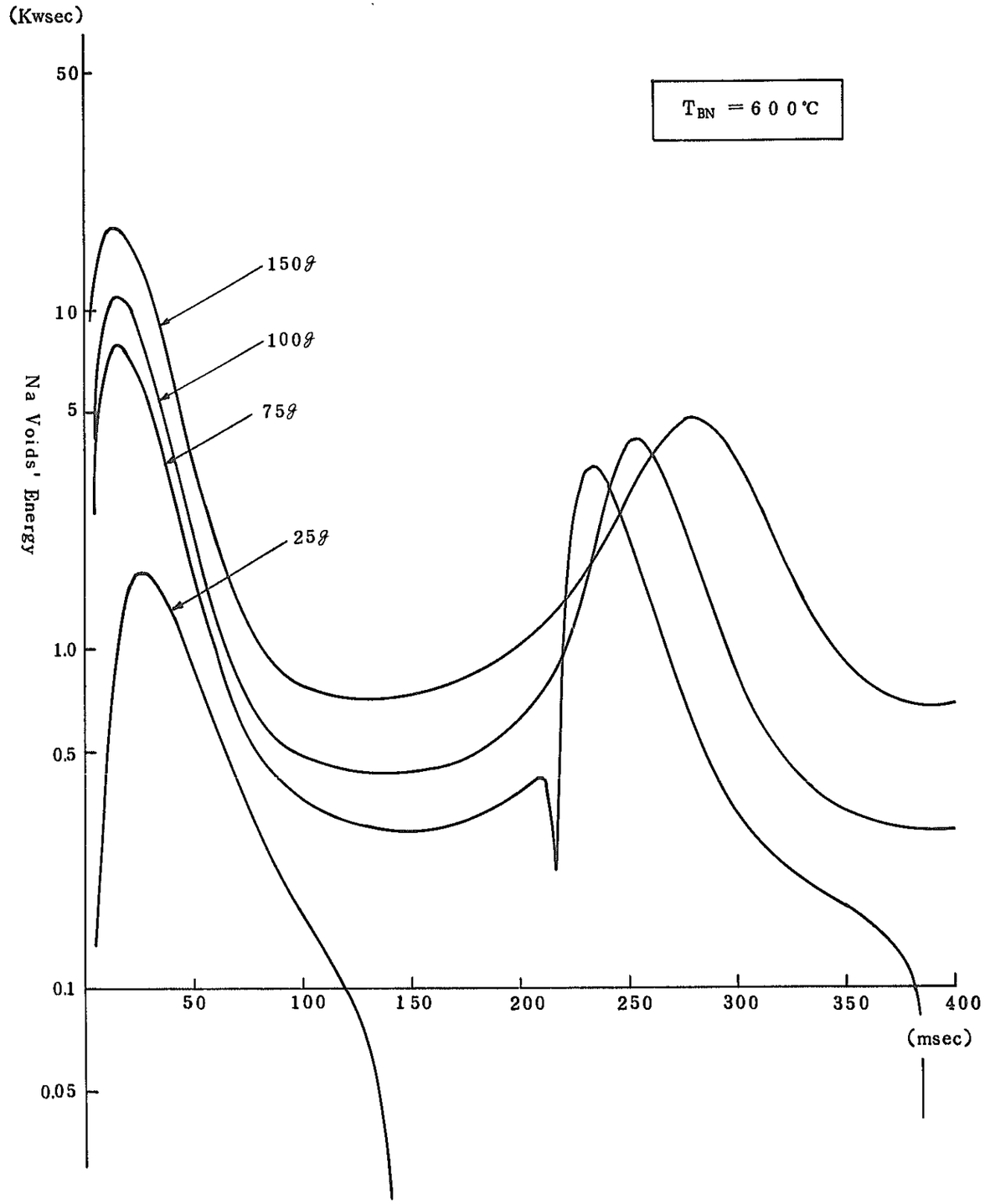

Fig. II-7. Relation between Na Voids' Energy Fluctuation and Molten Fuel Quantity

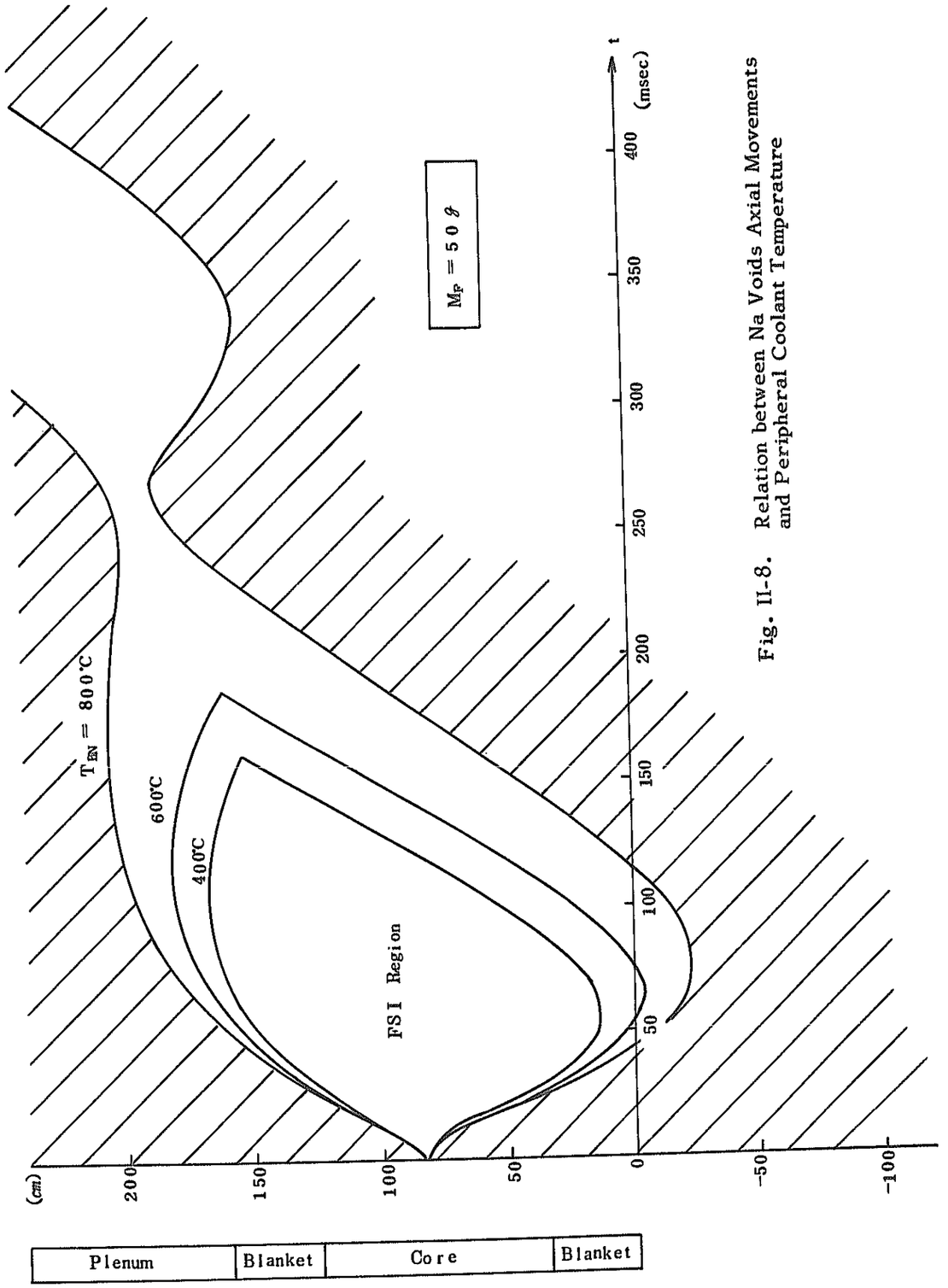

Fig. II-8. Relation between Na Voids Axial Movements and Peripheral Coolant Temperature

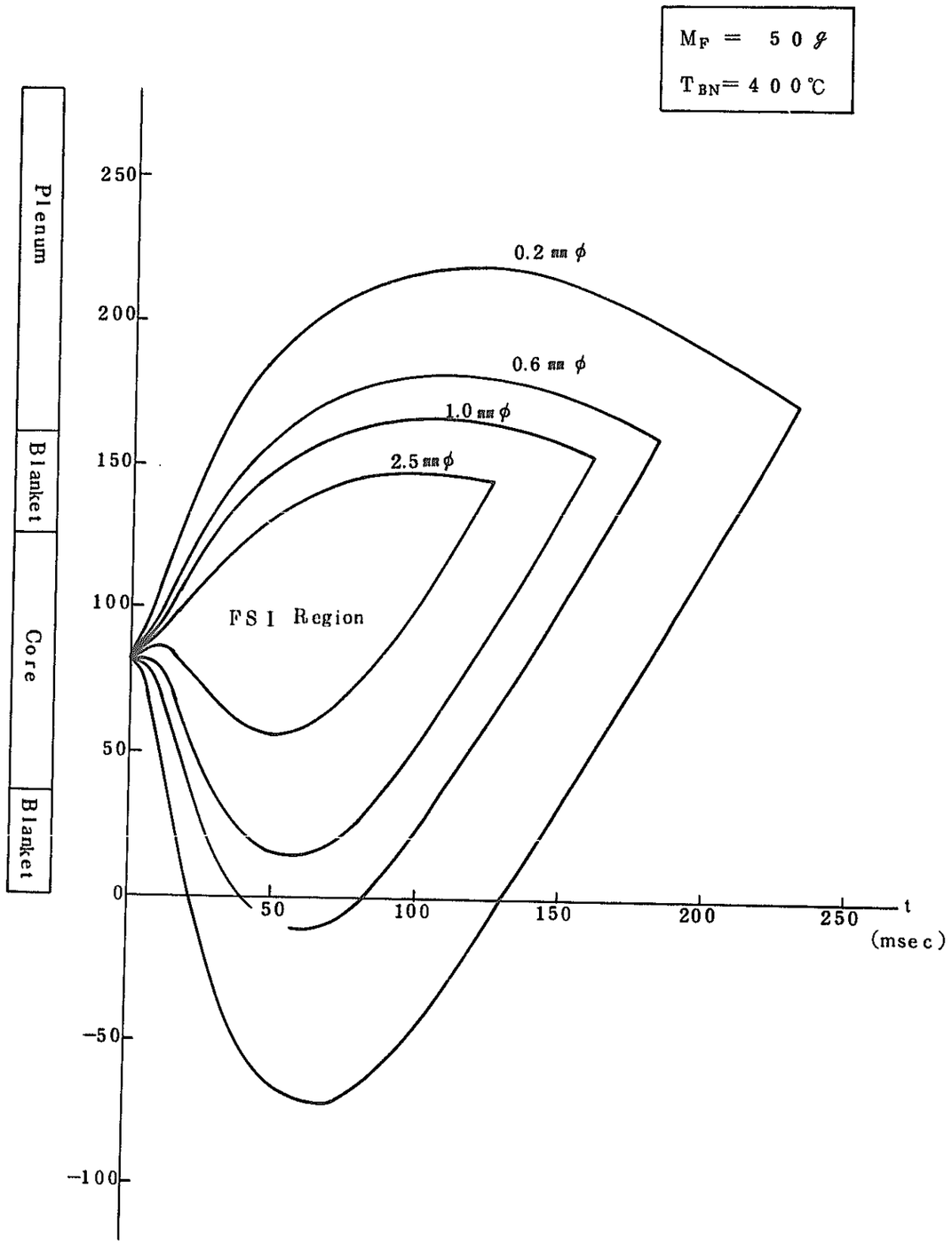

Fig. II-9. Relation between Na Void Space Movement and Fuel Particle Diameter

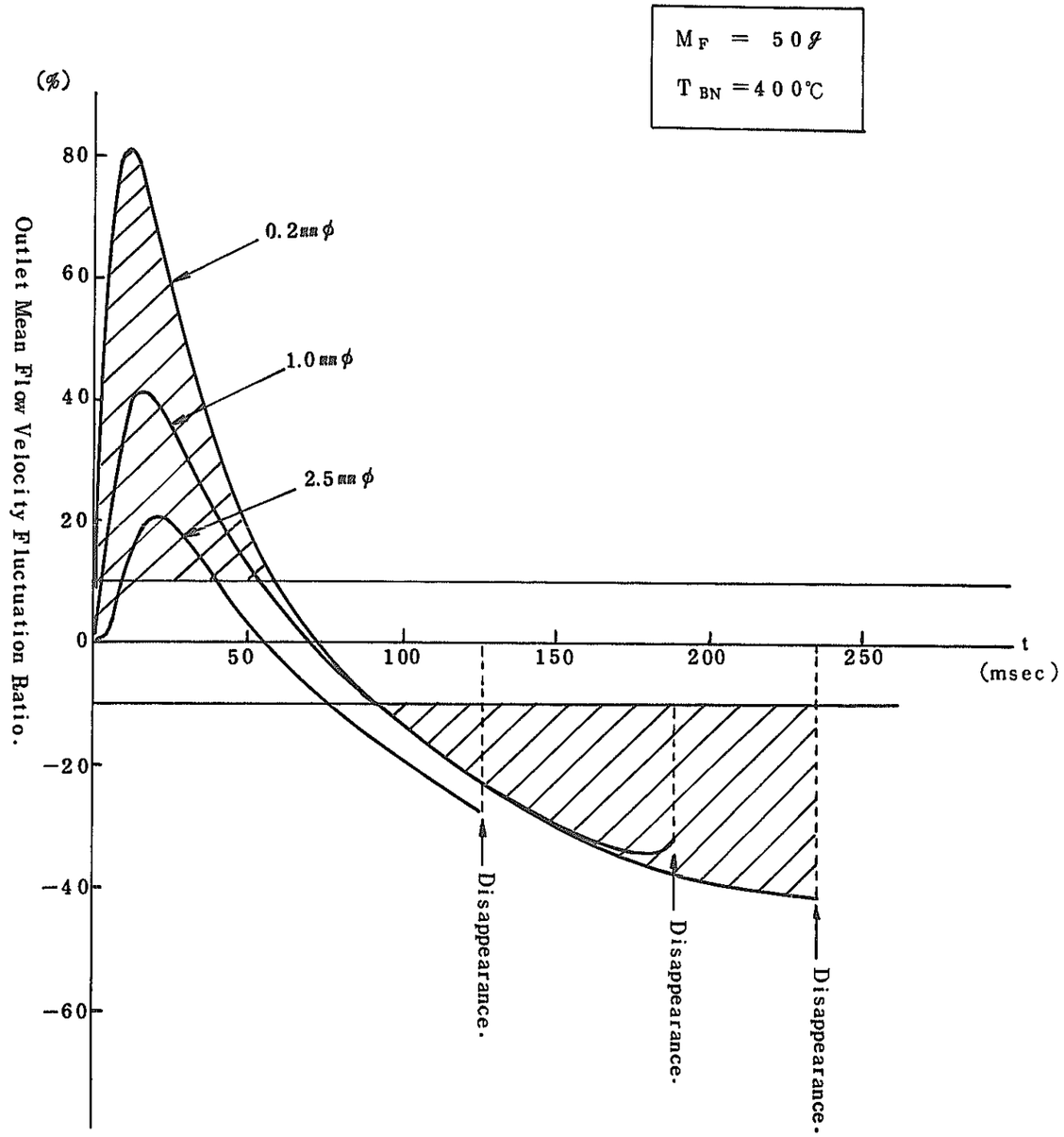

Fig. II-10. Outlet Mean Flow Velocity Fluctuation Ratio by Fuel Particle Diameter

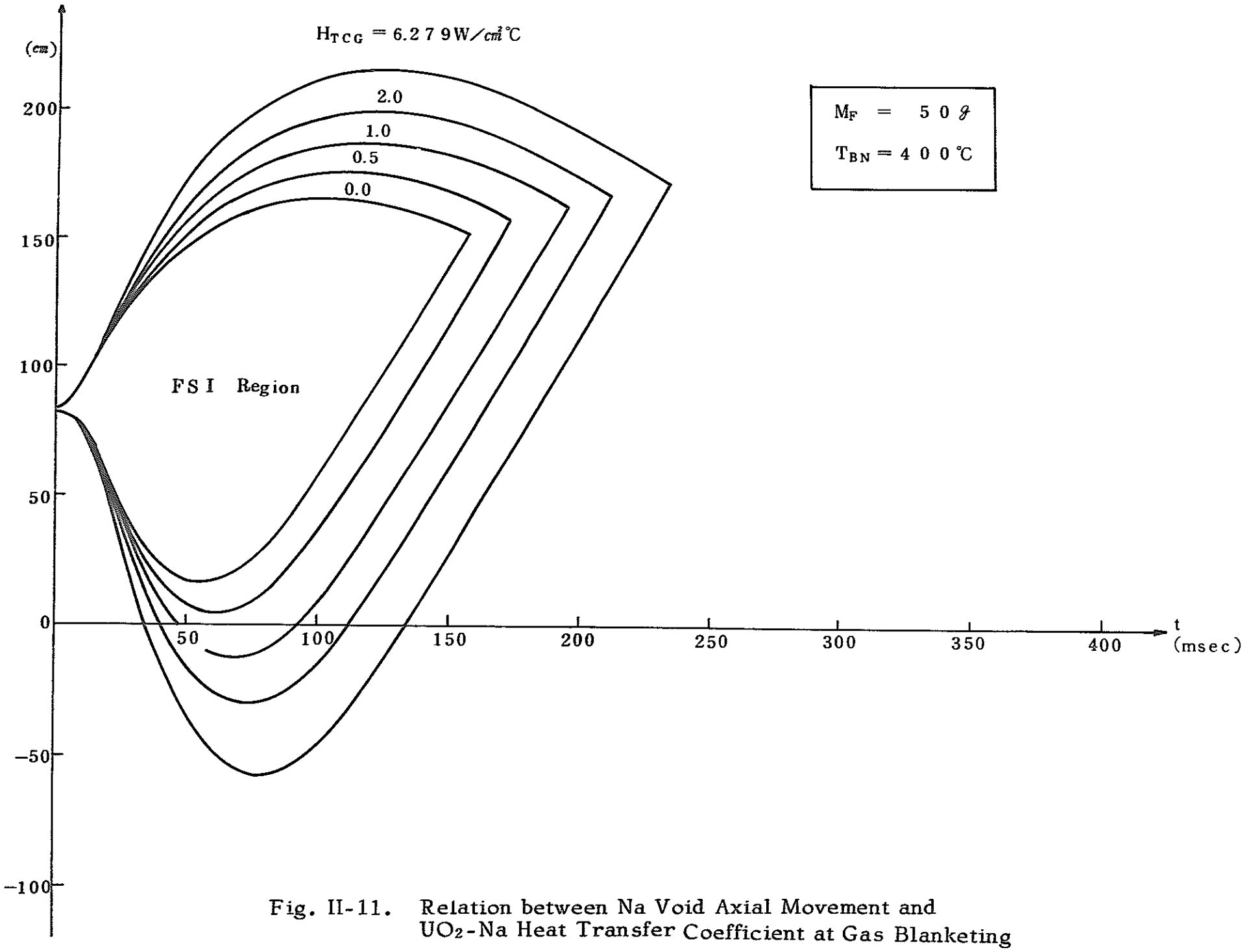

Fig. II-11. Relation between Na Void Axial Movement and UO_2-Na Heat Transfer Coefficient at Gas Blanketing

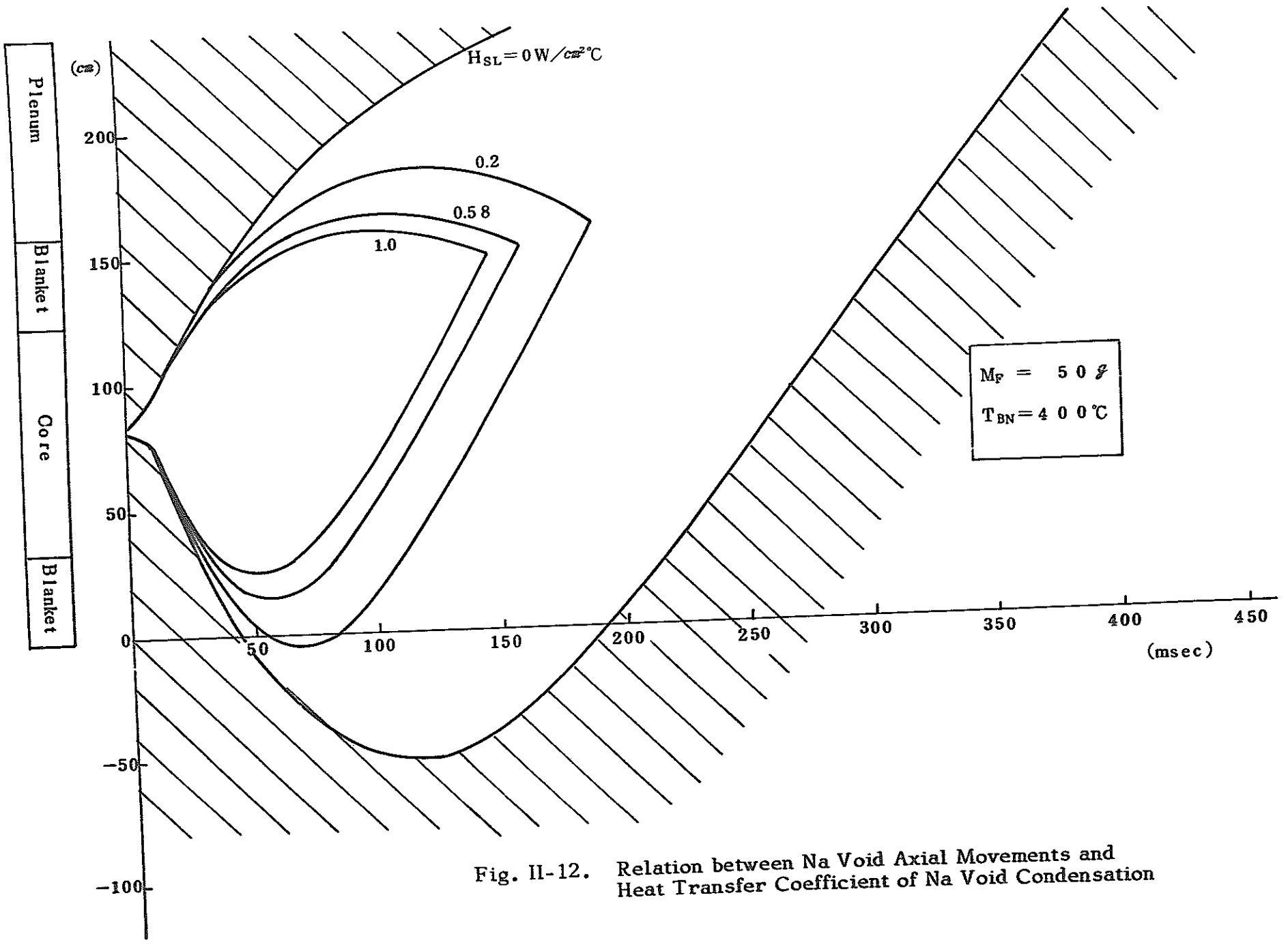

Fig. II-12. Relation between Na Void Axial Movements and Heat Transfer Coefficient of Na Void Condensation

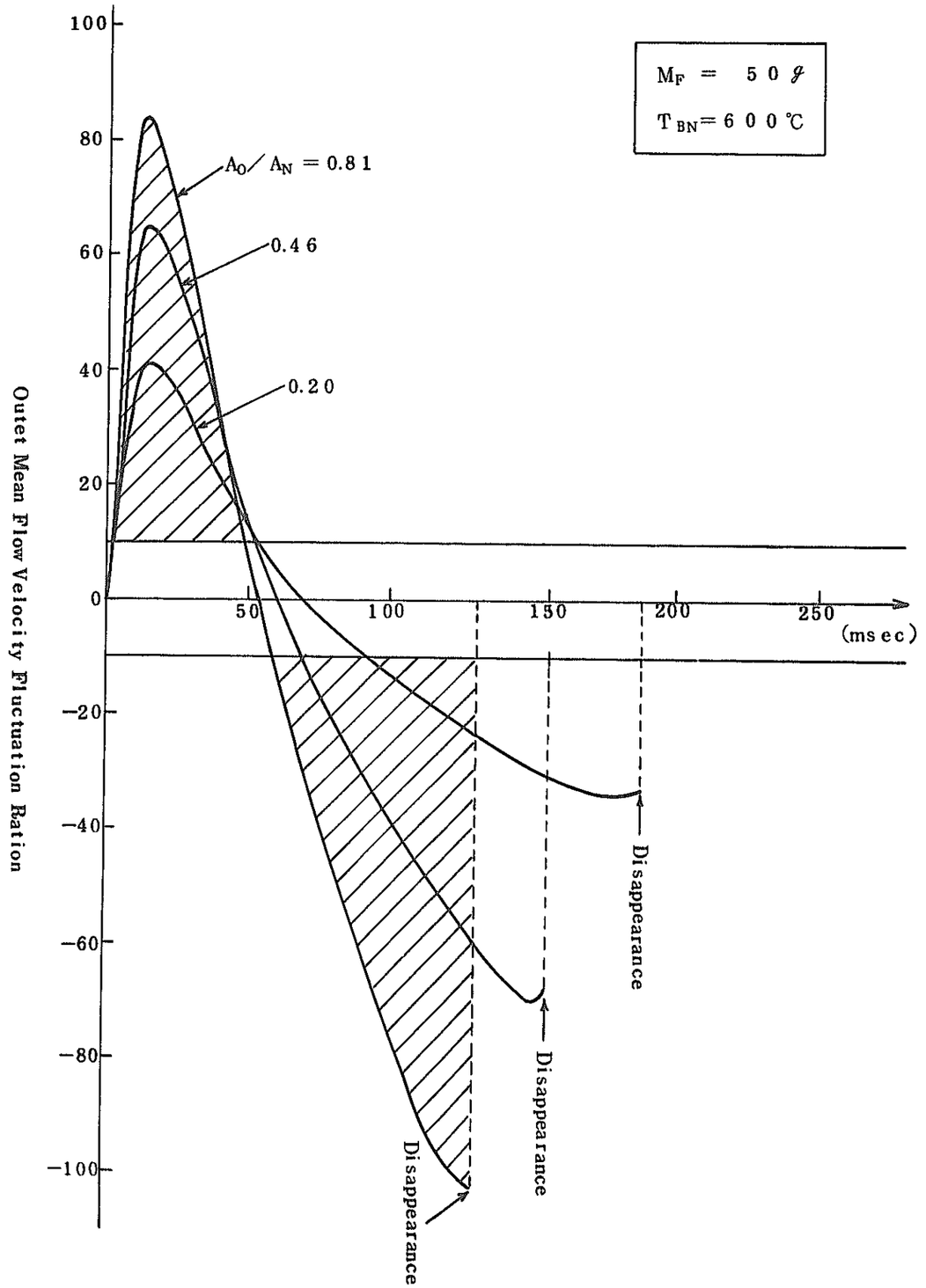

Fig. II-13. Relation between Outlet Mean Flow Velocity Fluctuation Ratio and Interacting Cross Section Ratio

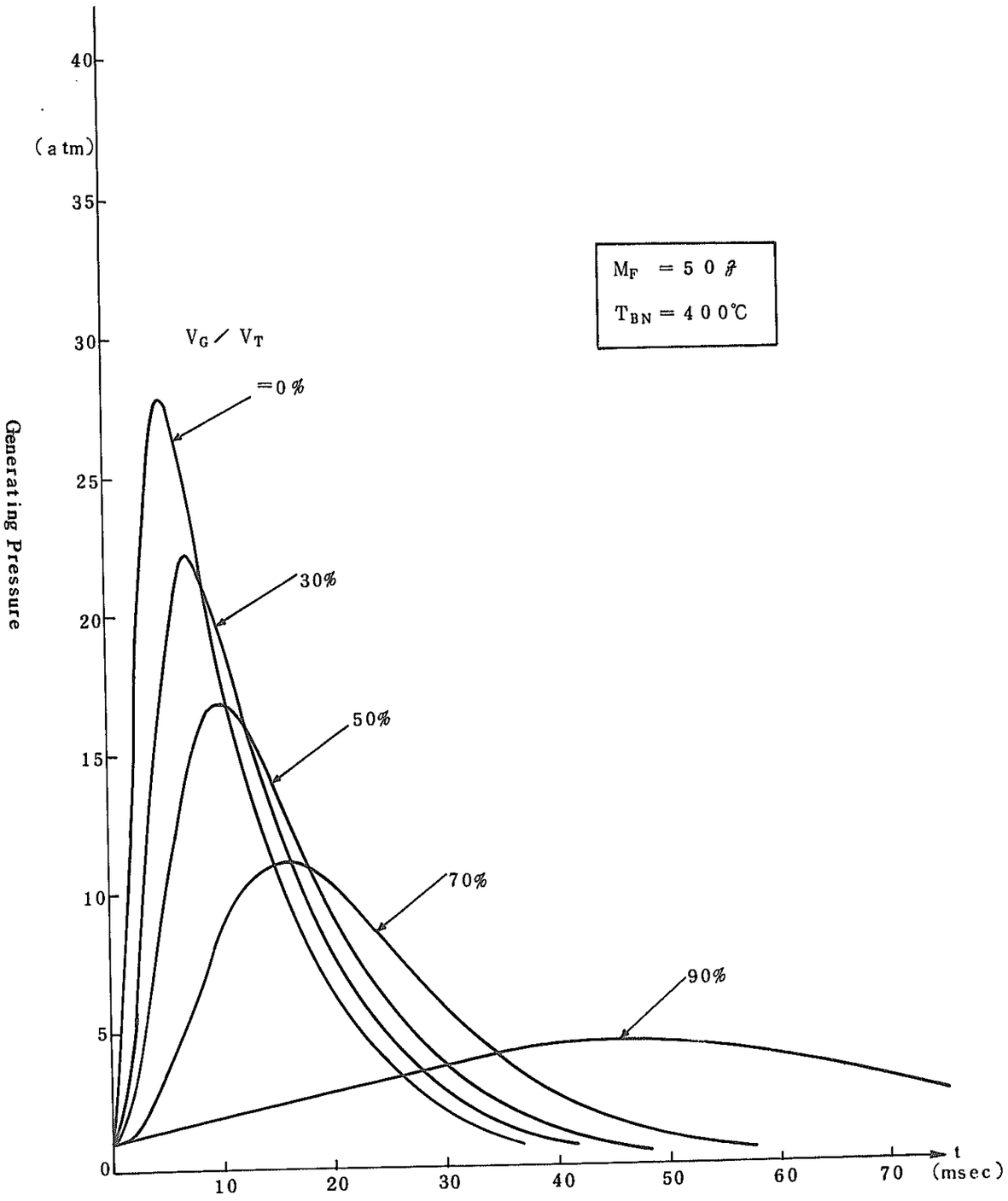

Fig. II-14. Relation between Interaction Produced Pressure Change and Non-Condensed Gas Mixing Ratio

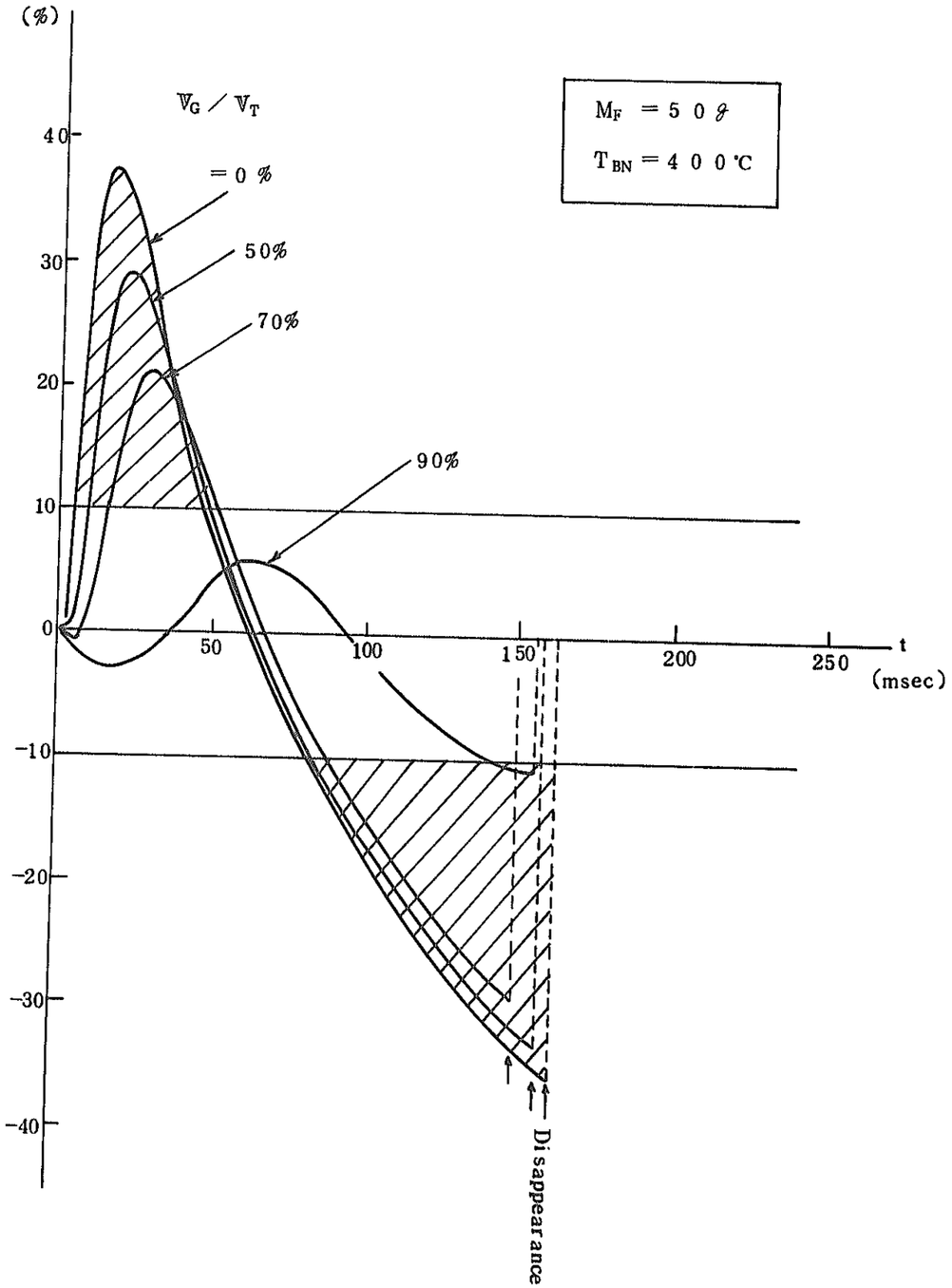

Fig. II-15. Relation between Outlet Mean Flow Velocity Fluctuation Ratio and Non-Condensed Gas Mixing Ratio

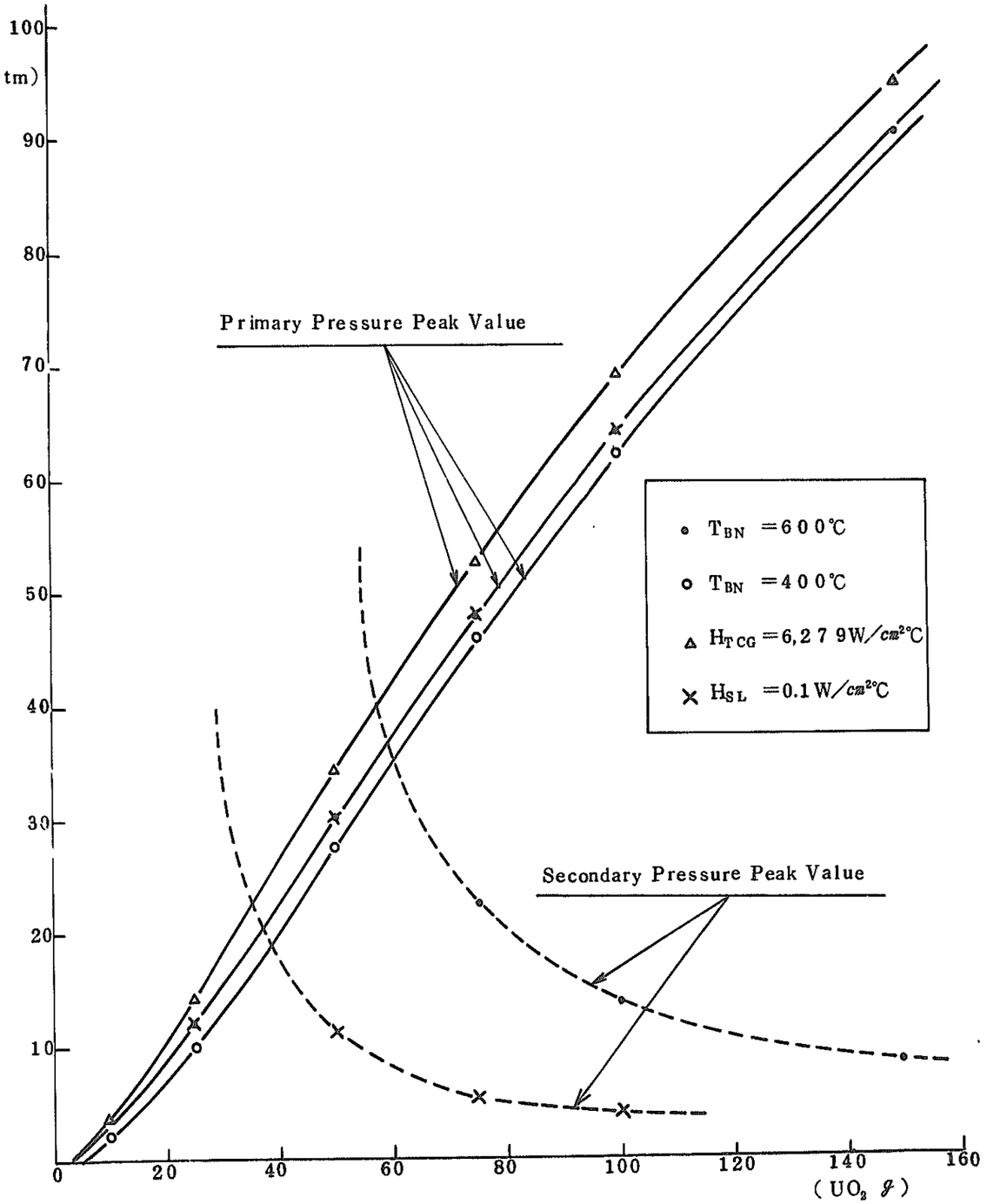

Fig. II-16. Relation of Generating Pressure Peak with Molten Fuel Quantity Contributing to Interaction

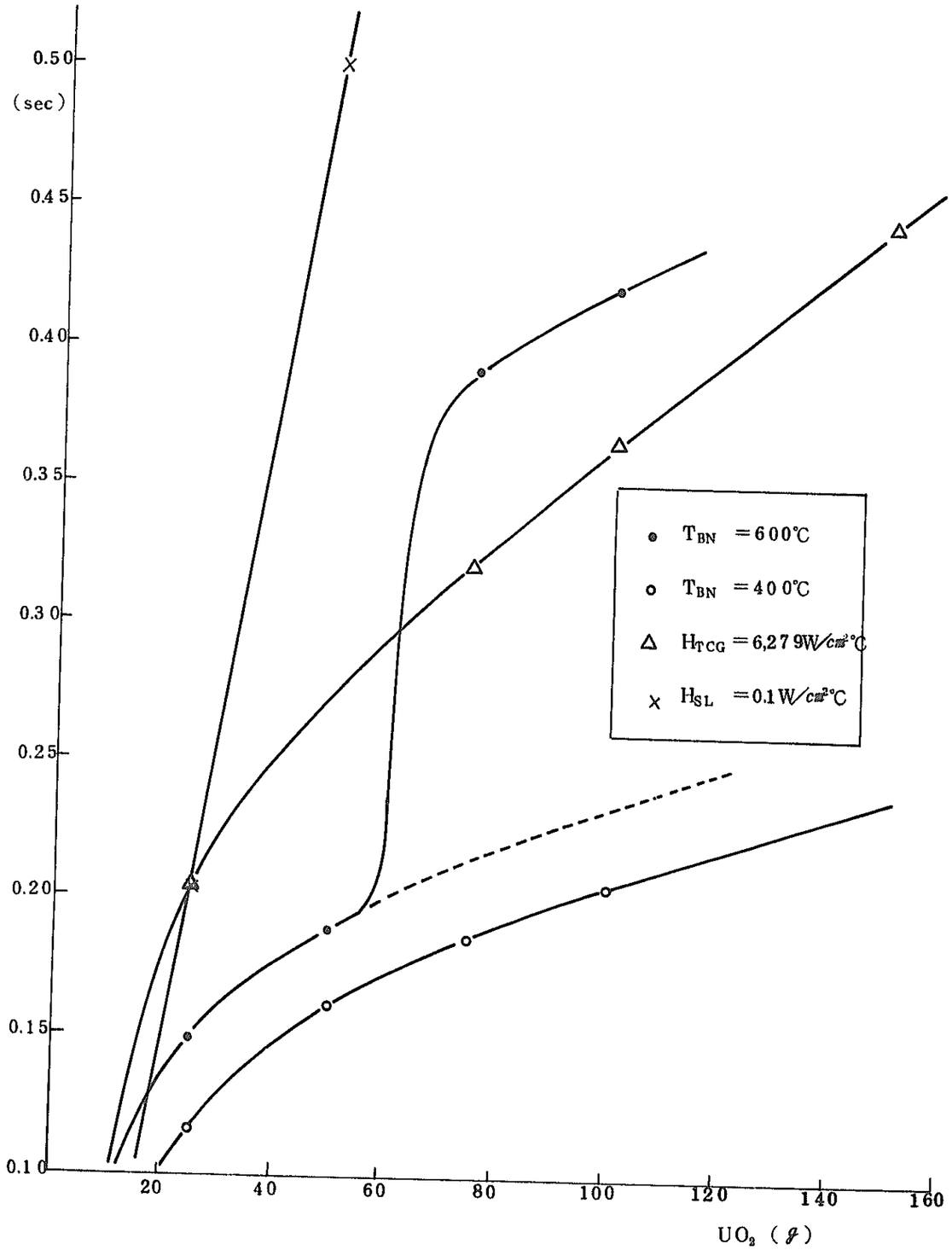

Fig. II-17. Relation of Na Voids Disappearing Time with Molten Fuel Quantity Contributing to Interaction

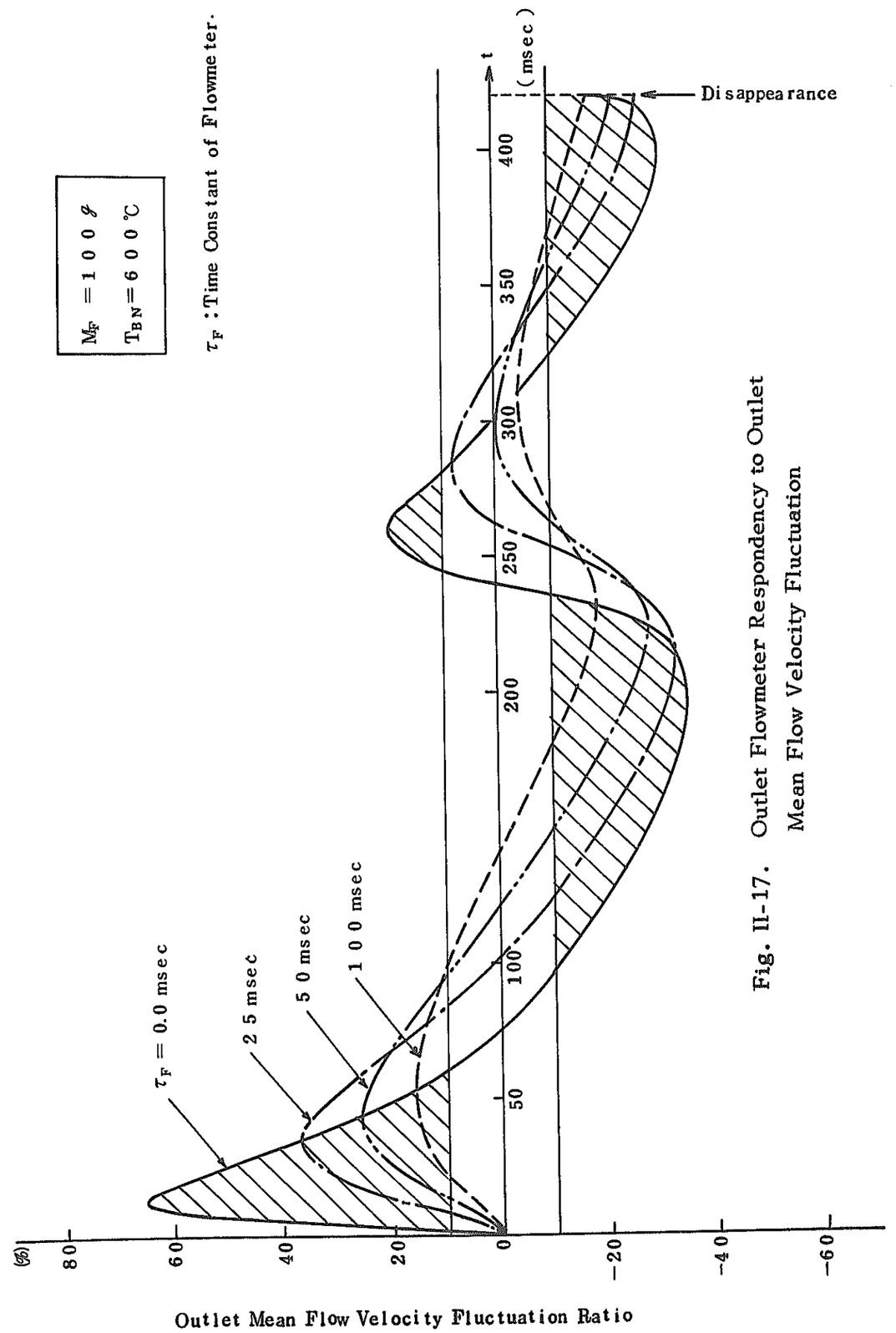

Fig. II-17. Outlet Flowmeter Respondency to Outlet Mean Flow Velocity Fluctuation

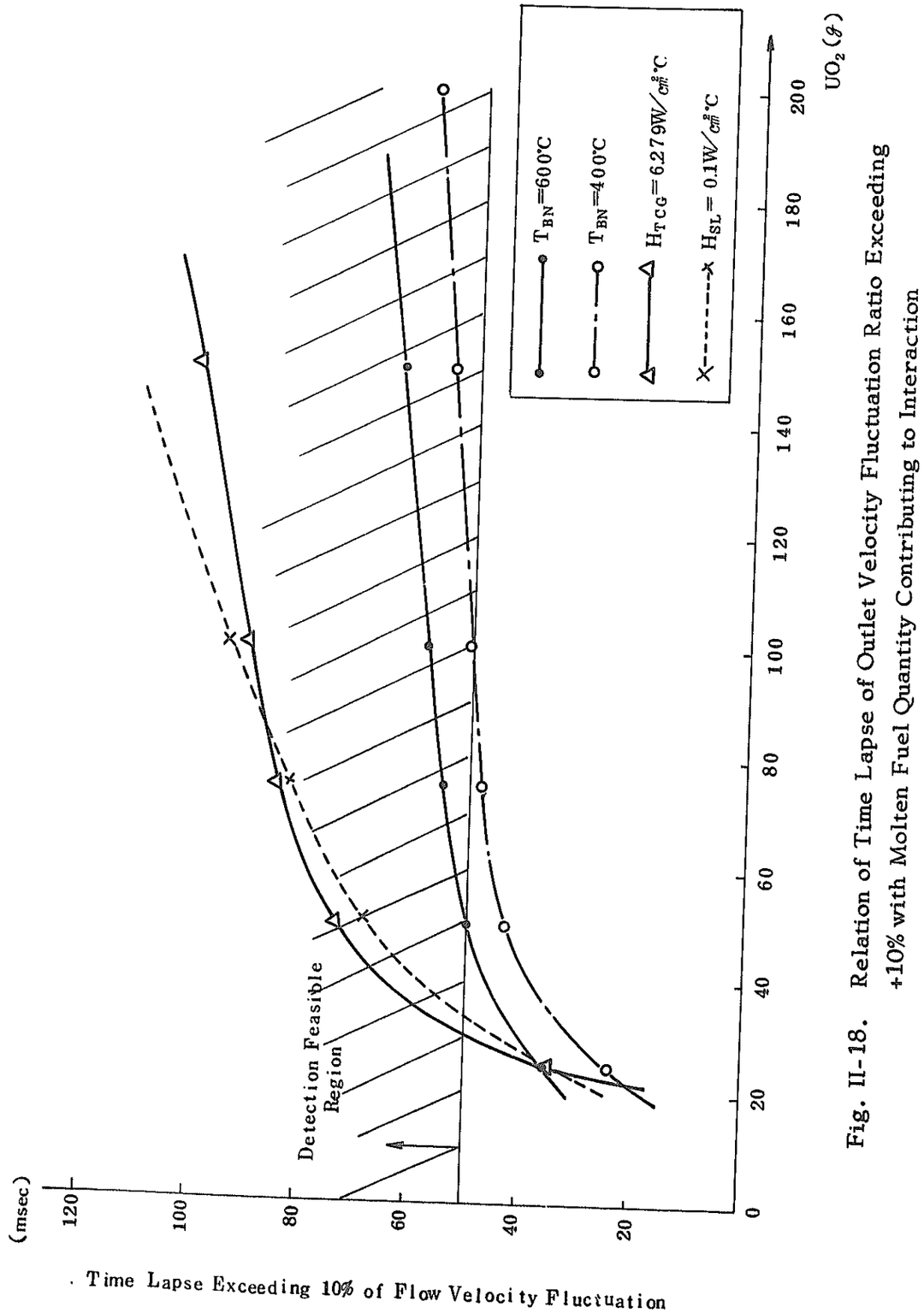

Fig. II-18. Relation of Time Lapse of Outlet Velocity Fluctuation Ratio Exceeding +10% with Molten Fuel Quantity Contributing to Interaction

· Time Lapse Exceeding 10% of Flow Velocity Fluctuation

III. Analysis of Thermal Propagation Behavior In Fuel Assembly Following Localized Molten Fuel Release

The high temperature fuel, which is locally overheated by a localized channel blockage in the fuel assembly or the molten fuel which is released in sodium, releases a large quantity of heat energy in the surrounding sodium and the adjacent fuel pins. But before it reaches to the outlet of the fuel assembly following the coolant flow, its heat is absorbed by the heat mixing effect with sodium which flows in other sub-channel in the fuel assembly and by the fuel pins (especially at the upper plenum section). Because of this, the temperature rise ratio at the outlet is considerably moderated, and the outlet temperature responding time is supposed to also delay.

Therefore, in order to thermally detect such a localized accident in the fuel assembly by an outlet thermometer, the following analytical work has been undertaken to study what amount of accidental release energy is generated when converted into a release molten fuel quantity.

III-1. Analytical Method

For the analysis of thermal propagation behavior in the fuel assembly by a localized fuel release, a calculation code "DETECT" which was developed as an analytical code for multi-channel coolant mixing calculation at a transient period was employed.

III-1-1. Analytical Model

Fig. III-1 illustrates the analytical model of a molten fuel release accident in the center of the fuel assembly, and Fig. III-2 shows the case of a fuel release near the wrapper tube. In this case, for the purpose of thermal calculation of each fuel pin, each single pin is divided into sections as shown by the diagram, and each divided section of a

fuel pin contacting the same coolant channel is handled as the same pin.

The major hypotheses employed in the analysis are listed as follows:

(1) Each sub-channel flow is one dimensional flow and the normal flow rate is maintained constant at all time.

(2) The cross section of each channel inside the fuel released region is reduced by the same proportion equivalent to the released fuel volume.

(3) The following two items are employed for the handling of the coolant flow rate in the fuel released region.

  (a) The sodium flow velocity in the fuel released region is counted as the same flow velocity as that of outside of said region.

  (b) The sodium mass flow rate in each channel in the fuel released region is taken as the same flow mass rate as in each channel outside of said region.

(4) The released fuel particle are spherical and evenly diffuse inside the released region.

(5) No consideration is given to Na void generation by the released fuel.

(6) For the calculation of the intra-subchannel coolant mixing effect, the experimental equations (5) of thermal conduction under normal condition, turbulent flow mixing, and forced mixture effect by spacers are employed.

(7) As to the released fuel heat generation, two cases are studied, where it is taken into consideration and not taken into consideration.

III-1-2. Theoretical Expressions

The following equations were used for the analysis:

(1) Thermal conduction equation inside fuel rods

$$C_{PF}\rho_F\frac{\partial T_F^i}{\partial t}=\frac{1}{r}\frac{\partial}{\partial r}\left(K_F r\frac{\partial T_F^i}{\partial r}\right)+g_{FO} \qquad \text{(III-1)}$$

(2) Thermal conduction equation inside clad tubing.

$$C_{PC}\rho_C\frac{\partial T_C^i}{\partial t}=\frac{1}{r}\frac{\partial}{\partial r}\left(K_C r\frac{\partial T_C^i}{\partial r}\right) \qquad \text{(III-2)}$$

(3) Equation of the coolant energy.

$$C_{PN\ N}\frac{\partial T_N^i}{\partial t}+v_N^i C_{PN}\rho_N\frac{\partial T_N^i}{\partial Z}=r_{CN}^i\phi_{CN}^i+r_{MN}^i\phi_{MN}^i-r_{NW}^i\phi_{NW}^i+\sum_j^{N_i}r_{NN}^{ij}\phi_{NN}^{ij} \qquad \text{(III-3)}$$

(4) Thermal conduction equation inside the released fuel particle

$$C_{PM}\rho_M\frac{\partial T_M^i}{\partial t}=\frac{1}{r^2}\frac{\partial}{\partial t}\left(K_H r\frac{\partial T_M^i}{\partial r}\right)+g_{FD} \qquad \text{(III-4)}$$

(5) Heat calculation equation for wrapper tube.

$$C_{PW}\rho_W\frac{\partial T_W^i}{\partial t}=r_{NW}^i\phi_{NW}^i-r_{W\bar{O}}^i\phi_{W\bar{O}}^i \qquad \text{(III-5)}$$

(Note: for the calculation of the wall temperature of the wrapper tube, it was sought at one point radial direction)

(6) Equation of coolant energy in-between the fuel assembly tube walls.

$$C_{PN}\rho_N\frac{\partial T_O^i}{\partial t}+v_O C_{PN}\rho_N\frac{\partial T_O^i}{\partial Z}=r_{WO}^i\phi_{WO}^i-r_{OW'}^i, \qquad \text{(III-6)}$$

(7) Calculation equations of various kinds of thermal flux.

$$\phi_{CN}^i\equiv\phi_{CN}^i(Z,t)=h_{CN}\{T_{CS}^i(Z,t)-T_N^i(Z,t)\} \qquad \text{(III-7)}$$

$$\phi_{NM}^i\equiv\phi_{NM}^i(Z,t)$$

$$= \begin{cases} h_{NM}\{T_M^i(Z,t) - T_N^i(Z,t)\} & ; \text{ Fuel released region} \\ 0 & ; \text{ Non-fuel released region} \end{cases} \quad \text{(III-8)}$$

$$\phi_{NW}^i \equiv \phi_{NW}^i(Z,t)$$

$$= \begin{cases} h_{NW}\{T_N^i(Z,t) - T_W^i(Z,t)\}; & \text{Wrapper tube contact region} \\ 0 & ; \text{ Wrapper tube non-contacting region} \end{cases} \quad \text{(III-9)}$$

$$\phi_{NN}^i \equiv \phi_{NN}^i(Z,t)$$

$$= h_{NN}\{T_N^j(Z,t) - T_N^i(Z,t)\} \quad \text{(III-10)}$$

$$\phi_{WO}^i \equiv \phi_{WO}^i(Z,t)$$

$$= h_{WO}\{T_W^i(Z,t) - T_O^i(Z,t)\} \quad \text{(III-11)}$$

$$\phi_{OW'}^i \equiv \phi_{OW'}^i(Z,t)$$

$$= h_{OW'}\{T_O(Z,t) - T_{W'}(Z,t)\} \quad \text{(III-12)}$$

(8) Equation of the coolant mixture effect. (From JAERI-memo 4422)

In the case of a turbulent flow, the heat transfer rate φ_τ is given by the following expression:

$$\varphi_\tau = C_{PN}\rho_N\left(\frac{\nu_N}{P_\tau} + E_H\right)\frac{b'}{\delta'_{ji}}(T_N - T_N^i) \quad \text{(III-13)}$$

The relation between the general eddy temperature conductive rate E_H and the general vortex viscosity coefficient is as follows:

$$E_H = 0 \cdot 6\, E_M \quad \text{(III-14)}$$

As E_M is expressed by the sum of the natural mixture effect $\varepsilon_①$ and the forced mixture effect $\varepsilon_②$, it is:

$$\frac{E_M}{\nu_N} = \frac{\varepsilon_①}{\nu_N} + \frac{\varepsilon_②}{\nu_N} \quad \text{(III-15)}$$

As the result of the analysis of JOYO's characteristics, the following equations have been introduced:

$$\frac{\varepsilon_①}{\nu_N} = 0.0038 \quad \frac{\delta_{ji}}{b'}\,Re^{0.9} \quad \text{(III-16)}$$

$$\frac{\varepsilon_②}{\nu_N} = \left\{\frac{0.158}{Km}\cdot\frac{(D+h)}{De_i}\theta_{ji}\right\}^{\frac{1}{3}} Re^{\frac{11}{12}} \quad \text{(III-17)}$$

$$; Km = 4.1\left(\frac{P_S}{D}\right)^{1.7}$$

Consequently, the appearent heat transfer coefficient by the mixing of turbulent flows in various sub-channels is given by the following equation:

$$h_{NN}^{ij} = \left\{K_N + 0.6\, C_{PN}\rho_N\nu_N\left(\frac{E_M}{\nu_N}\right)\right\}\frac{b'}{\delta_{ji}} \quad \text{(III-18)}$$

(9) The calculation equation of the detected temperature of the outlet thermo-electric couple.

$$M_T C_T \frac{\partial T_T}{\partial t} = A_T h_{NT}(T_{out} - T_T)$$

Thermo-electric couple constant is placed;

$$\tau_T = \frac{M_T C_T}{A_T H_{NT}}$$

Then,

$$\frac{dT_T}{dt} = (T_{out} - T_T)/\tau_T \quad \text{(III-19)}$$

The fuel assembly's outlet mean temperature is sought by the following equation.

$$T_{out} = \sum_i^{N_T} A_N^i T_N^i(Z_{out}) \Big/ \sum_i^{N_T} A_N^i \quad \text{(III-20)}$$

The symbols used in the above equation have the following each meaning:

F.C.N.M.W.O.W'.T ..... Fuel, cladding tube, molten fuel, wrapper tube, Na outside of wrapper tube, adjacent wrapper tube, and thermo-electric couple.

C_{pm}, ρ_m, K_m, ν_m ..... Specific heat of material m, density, heat conductivity, and kinematic viscosity.

T_m^i ..... Temperature at channel i of material m.

g_{FO} ..... Fuel heat generation density.

V_N^i ..... Na flow velocity at channel i .

$\gamma_m^i{}_{,n}$ ..... Contact ratio of material m and n.

$\phi_m^i{}_{,n}$ ..... Thermal flux transfered from material m to n in sub-channel i .

$h_{m,n}$ ..... Heat transfer coefficient between material m and n.

b' ..... Gap between fuel pins

δ_{ij} ..... Effective gap between the sub-channels of j and i

D ..... Fuel pin radius

h ..... Spacer thickness

θ_{ji} ..... Central angle of j and i sub-channel centroid

De_i ..... Equivalent diameter of sub-channel i

P_S ..... Spacer pitch

M_T ..... Thermoelectric couple mass

A_N, A_T ..... Na flow channel cross section and Na-thermoelectric couple contacting area.

Z_{out} ..... Height of channel outlet

t, r, Z ..... Time, radial length, and axial length.

Re, P_r ..... Reynolds' number and Prandtl's number.

Lastly, in order to perform evaluation of the thermal energy produced by a fuel release accident, the following physical quantities are defined as follows:

(a) The released energy from fuel to coolant: E_A and the energy velocity: Q_A.

$$E_A(t) = \int_0^t Q_A(t')\,dt' \qquad \text{(III-21)}$$

$$Q_A(t) = \sum_i^{N_A} \int_{Z_{AL}}^{Z_{AU}} A_{MN}\, h_{MN} \{T_M^i(Z,t) - T_N^i(Z,t)\}\,dZ \qquad \text{(III-22)}$$

Here, NA indicates the total number of cells in the fuel released region, and Z_{AU} and Z_{AL}, the upper and lower positions in the axial direction of the released region.

(b) The outflowing energy from the fuel assembly's outlet: E_{out}, and the outflowing energy velocity: Q_{out}.

$$E_{out}(t) = \int_0^t Q_{out}(t)\,dt \qquad \text{(III-23)}$$

$$Q_{out}(t) = \sum_i^{N_T} A_N^i\, C_{PN}\, \rho_N\, V_N^i \{T_{out}(t) - T_{out}(0)\} \qquad \text{(III-24)}$$

Here, $T_{out}(0)$ indicates the outlet mean temperature at a normal state.

(c) The released energy from the wrapper tube wall to the outside of the fuel assembly: E_W, and the energy velocity: Q_W.

$$E_W(t) = \int_0^t Q_W(t)\, dt \qquad \text{(III-25)}$$

$$Q_W(t) = \sum_i^{N_W} \int_0^L \ell_W^i h_{WO} \{ T_W^i(Z,t) - T_O^i(Z,t) \} dZ \qquad \text{(III-26)}$$

Here, N_W is the total number of cells in the wrapper tube, and ℓ_W is the width of the contact cross section of the wrapper tube with sodium outside of the fuel assembly. Therefore, in case of an occurrence of a local accident inside the fuel assembly by a local fuel release, the total energy E_{av} to be absorbed inside the fuel assembly may be obtained by the following energy preservation equation:

$$E_{av} = E_A - E_{out} - E_W \qquad \text{(III-27)}$$

More precisely, it is that whether a fuel release accident will invite a propagation of the accident inside the fuel assembly depends on E_{av}, that whether any thermal damage propagation is extended to the adjacent fuel assembly is dependent upon E_W, and that whether the outlet thermometer is able to detect such accident propagation depends on E_{out} respectively.

III-2. Analysis and Evaluation

III-2-1. Calculation Conditions

The design calculation conditions and the thermo-hydraulic dynamic calculation conditions necessary for this analysis are given in Table III-1. Considering the accident phenomena, the following

factors have been selected for parameters: the release cross section position in the fuel assembly, the released fuel mass, the fuel particle diameter, number of fuel released sub-channels, the UO_2/Na mixture ratio inside the fuel released flow sub-channels, the UO_2-Na heat transfer rate, and the coolant mixing coefficient between the sub-channels. Further, from the fact that the total heat generation volume in the fuel assembly remains constant so long as the fuel particle remain there without flowing outside, when the entire energy balance in the fuel assembly is handled, the heat generation of the released fuel is not considered. While, in conducting a thermal evaluation in the vicinity of the fuel released region, the thermal generation is taken into consideration during the analysis. Table III-2 represents the calculation conditions of various parameter surveys.

The analysis covered a total of 12 cases of which 10 were for the fuel release in the vicinity of the S/A center, while the remaining 2 were in the case of fuel release in the vicinity of the wrapper tube. For the parameter standard values, the conditions of Case 1 were mainly followed.

Also, as the handling method of the coolant flow behaviors in the released region, as given by Hypothesis (3), from Case 1 to Case 6, the flow velocity was set constant, while from Case 7 to Case 12, the mass flow rate was set constant. In the case of the former, the mass flow rate inside the fuel released region drops stepwise by the channel blockage as the result of the fuel release, but the channel in the down stream from such fuel released region is equivalent to the case where the divergence cross flow among the sub-channels is extremely good. In the case of the latter, it is equivalent to the case where the flow resistance by the blockage does not at all affect the flow rate fluctuation. As the real flow behavior, it is assumed that it will take the

middle of these conditions.

As to the UO_2-Na heat transfer coefficient, considering the effect of gas blanketing by Na voids, the standard value was taken one figure below the UO_2-Na (liquid) heat transfer coefficient of 6.279 $W/cm^2\,℃$[3].

III-2-2. Analytical Result and Evaluation

The results of analyses performed under the analytical conditions shown by Table III-1 and Table III-2 are given in Fig. III-3 through to Fig. III-23.

(A) In Case of Fuel Release in the Vicinity of S/A Center.

(1) Heat Propagation Behavior in Fuel Assembly

Fig. III-3 and Fig. III-4 respectively show the contour line charts taken stepwise at certain time intervals of the coolant temperatures in the vicinity of the fuel released region in the cases of Case 1 and Case 7. In both cases, it is known that, with the lapse of time, the high temperature coolant in the vicinity of the released region diffuses in the axial and radial direction. But, in the same 1 Kg of molten fuel release, the thermal propagation behaviors in Case 1 and Case 7 differ from each other considerably. Namely, in Case 1, on the basis of the consideration of the heat generation of the fuel, the flow rate in the released channel has declined in proportion to the reduced flow channel by blockage, and because of this, the coolant temperature in the vicinity of the fuel released region has ascended extremely, and there is no great heat propagation in the outside of the fuel released region (especially in the down stream from the affected region).

On the other part, in Case 7, which hypothetically has ignored fuel heat generation, and set the mass flow rate in the fuel released channel the same as the mass flow rates in other channels, the temperature in the vicinity of the fuel released region shows no much rise comparing with that of Case 1 because of the larger rate of heat transfer due to the flow of coolant, and thus, the heat propagation in the fuel assembly is made smoothly.
The coolant mixture effect as used in this analysis is known to have little effect to the radial propagation of heat to any other area except to the adjacent cells of the fuel released cell. But this fact is based on a hypothesis that the coolant flow rate in each cooling flow channel except the fuel released region is maintained constantly at a nominal flow rate. But in the actual reality, it is conceivable that there would naturally take place a sodium boil and the peripheral coolant flow would be disturbed as the actual phenomena. Because of this, a thermal propagation in the radial direction will develop more strongly than in the case of the above results.
However, in the case that the released fuel is in smaller quantity and the fuel released region is wider, then, it is assumed also from the analytical results under Chapter II that the void effect by Na boil will influence little to the coolant mixture effect since the so produced voids will disappear quickly. Under such a fuel release condition, this analytical model can be said relatively a good approximation.
Fig. III-5 shows the temperature variation inside the fuel particle of the released fuel in the case of Case 7. As the release location is at the highest temperature of the coolant in the fuel released region, it is equivalent to such a location where is the

slowest in cooling the fuel. In this case, the fuel particle diameter is assumed as 2.5 mm$^{\phi}$ which is the largest spherical particle in any of the flow channels. Considering the effect of gas blanketing, the UO_2-Na heat transfer rate has employed the value one figure below the actual value, and after 3 sec from the release, it is thermally in almost the equivalent state with the surrounding coolant.

Fig. III-6 and Fig. III-7 show respectively the time change of axial coolant temperature distribution in the central cells in the fuel released region in both cases of Case 1 and Case 7. As previously described, the axial thermal propagation rate of the coolant is known from these diagram larger in Case 7 than in Case 1. Likewise, the reason for the thermal equilibrium of the coolant in a state of high temperature in the vicinity of the fuel released region as shown by Fig. III-6 is because of the heat generation effect of the released fuel. Further, although the thermal energy from the released fuel moves toward downstream following the coolant flow upto the time 0.5 sec after the fuel release, after 1.0 sec from the fuel release, the released energy from the fuel declines, and by contrast, it is learned from the diagram that the thermal energy which the upper plenum has absorbed from the high temperature coolant is, in turn, returned to the coolant. In short, the fuel plenum section plays a role of heat moderation against an accident where heat release is violent.

Fig. III-8 shows the heat absorption effect inside the fuel pins at the upper plenum section. This diagram indicates the temperature variation inside each fuel pin near the fuel released region in the lowest end of the upper plenum in Case 1. From this

diagram, it is learned that although the thermal response of the cladding tube to the coolant temperature change is quick, inside the plenum, the thermal response delays 2 or 3 sec because of its poor heat transfer rate. Consequently, it is assumed that even though the thermal release from the released fuel to sodium is completed within 1 sec., the thermal release from the plenum may continue for 2 or 3 sec thereafter.

(2) Thermal Energy Evaluation

The energy and the energy velocity variation defined (equations III-21 - III-24) under the preceding Chapter are shown respectively in Fig. III-9 through to Fig. III-11. Fig. III-9 gives the comparison of Case 1 and Case 7 for the energy velocity released from fuel to sodium; $Q_A(t)$, and the energy velocity flowing out from the fuel outlet; $Q_{out}(t)$. It is known from these diagrams that in Case 1, as the fuel heat generation is considered, both Q_A and Q_{out} have settled down with the equivalent values to that of the fuel heat generation velocity. The reason for the higher peak of the outlet flow energy velocity in Case 7 than that of Case 1 is because in Case 7 the coolant heat transport inside the released region is better than that of Case 1, and for this, the outlet thermal respondency is shown larger.

Fig. III-10 and Fig. III-11 show the energy variations in the respective cases of Case 1 and Case 7. As it is a fuel release in the S/A center, the released energy E_W from the wrapper tube is ignored. For this, from the relation of the equation III-27, the oblique lined area in the diagram corresponds to the absorbed energy E_{av} in the fuel assembly.

The value obtained by deducting E_A from the total energy of the released fuel is the residual energy held by the released fuel.

The fuel assembly absorbed energy E_{av} grows to the maximum after 1 sec from the fuel release under this condition (In Case 1, 0.84 MW_{sec} . and in Case 7, 0.72 MW_{sec} .) and thereafter, in 5 sec, it declines by the energy discharge from the outlet down to 0.63 MW_{sec} in Case 1 and 0.17 MW_{sec} in Case 7. Consequently, unless any new fuel failure or fuel melting is provoked inside the fuel assembly by the fuel assembly absorbed energy during this short period, it may be said that there will be no danger of any successive accident taking place within a short time (several seconds) under the released energy equivalent to 1 Kg fuel.

(3) Response of Outlet Mean Temperature

The respondency of the outlet mean temperature by each parameter in the case of considering the flow velocity constant in the fuel released region and the heat generation of the released fuel was analyzed and evaluated from Case 1 through to Case 6. The results are shown by Fig. III-12.

As is evident from this diagram, the parameter which most greatly affects to the outlet temperature is also the released fuel mass. The maximum increase of the outlet mean temperature in the case of the fuel release of 100g (Case 2) is 2.2 ℃, and in the case of the fuel of 2 Kg (Case 3) is 30.8 ℃.

In the case where the fuel grain diameter is small as 0.5 mm^{ϕ} (Case 3), and where the UO_2-Na heat transfer coefficient is large as 6.279 W/cm^2 ℃ (Case 5), the outlet temperature response is quick by about 0.2 sec comparing with the standard condition of Case 1, and the maximum temperature increase is about 20.8 ℃ which is about 2.2 ℃ higher comparing with Case 1. But thereafter, it has declined more rapidly. In other words,

the conditions of Case 3 and Case 5 are both corresponding to the enlarged rate of UO_2-Na heat transfer. So much so, as the released energy velocity from fuel to sodium is so large that the outlet temperature response also becomes quick. However, comparing with the severeness of the accident in the fuel released region, the response of the outlet temperature is not as quick as expected. This, as previously described, evidently tells the fact that it has received a considerable amount of thermal moderation before it reaches the outlet by the coolant mixture effect and the plenum heat absorption effect.

In the case that even with an equivalent UO_2/Na mixture ratio in the fuel released channel, if the space is large as to afford a number of released cells as many as 96 (Case 4), the outlet mean temperature increase rate is lower comparing with Case 1 because of the increase of heat absorption effect by the coolant in the fuel assembly and the fuel pins as shown by the diagram.

On the other part, the outlet mean temperature response by various parameters considering the mass flow rate constant in the fuel released channel and no heat generation of the released fuel is given in Fig. III-13, which lists the results of analyses from Case 7 through to Case 10.

Although the heat generation of the released fuel is not considered, as the total heat generation rate in the fuel assembly is constant, the outlet mean temperature settles down after little longer than 5 sec to the temperature before the fuel release accident.

When UO_2-Na heat transfer coefficient is lowered to 0.1 W/cm^2℃ (Case 8), the fuel released energy's velocity substantially slows down, and for this reason, the responding time of the outlet temperature delays by 0.5 sec comparing with Case 7, and the

maximum mean outlet temperature's increase rate also declines substantially to 10.4 °C.

When UO_2/Na mixture ratio in the fuel released region is lowered to 2.0 (Case 9), the heat absorption of the coolant increases in proportion to the decline of the mixture ratio, and that much amount of heat is transfered to the fuel plenum, and thus the outlet temperature response is somewhat reduced comparing with Case 7.

Likewise, when the intra-sub-channel coolant mixture coefficient is set to 1/6 of the standard value (Case 10), the outlet temperature response becomes slightly quicker, but not distinctively different from Case 7. Because of this, the outlet mean temperature response by the coolant mixture effect does not give any appreciable variation comparing with other parameters.

(B) Fuel Release Close to Wrapper Tube

(1) Thermal Propagation Behavior in Periphery of Wrapper Tube

Fig. III-14 shows the process of thermal propagation in the coolant flow channel in the vicinity of a fuel released region in the event of an accident of molten fuel release of 1 Kg amount in No. 14 cell of thecoolant channel close to the walls of the wrapper tube (Case 11). In this case, no consideration is given to heat generation of the released fuel, and the flow rate in the fuel released region is assumed as equivalent to the flow rate in other channels. The reason for the higher coolant temperature in the fuel released region as evidenced by this temperature contour chart comparing with the case of S/A central release as indicated by Fig. III-4 is because that there are few released cells and the fuel's axial release extends excessively long. Also, for the

reason of the extremely low temperature in the channel close to the wrapper tube comparing the coolant temperature between the fuel pins, it is assumed that the flow rate in the channel is 1.8 times as large as the flow rate inside the fuel assembly, and also that the thermal discharge to the outside of the walls of the wrapper tube is considerably great. But after more than 2 sec from the release, it declines to the original, pre-release level by the effect of the coolant.

Fig. III-15 and Fig. III-16 represent the time variation of axial direction temperature distribution of each coolant respectively in the case that the fuel released cells are the cell adjacent to the wrapper tube (No. 1 cell) and the release central cell (No. 3 cell). Assuming that the number of fuel released cells is 8, and the fuel released channel cross section is reduced to 58.3% (UO_2/Na mixture ratio in the channel : 5) of the normal case by the fuel release, the coolant temperature throughout the entire length of the core including the upper and lower blanket sections goes up since the released region's axial length extends as long as 129.8cm against 1 Kg of the released fuel. As previously described, the coolant temperature nearby the wrapper tube does not reach higher than 881 ℃ maximum comparing with that inside the fuel assembly because of heat absorption by the wrapper tube itself and the cooling effect by the 1.8 times larger coolant flow rate. Because of this, no Na boil will take place in this channel. On the other part, in the released central section, there will take place naturally a sodium boil since the maximum temperature there exceeds 1100 ℃ .

Fig. III-17 shows the time change of radial direction temperature distribution of the coolant in the periphery of the fuel released

region at the lower end of the upper blanket in the axial direction. In this case, as the temperature at the wrapper tube's wall in the adjacent fuel assembly is assumed as constant, it is somewhat overly estimated than the actual heat outflow outside the wrapper tube's wall. Under this condition, the coolant between the wrapper tube walls does not boil, and after 4 seconds from the fuel release, it settles down to the pre-release state.

(2) Energy Evaluation

Fig. III-18 and Fig. III-19 show respectively the energy velocity and the energy change at various sections in Case 11. From these diagrams, it is known that, since a massive thermal energy is discharged outside of the wrapper tube walls immediately after the fuel release, and this discharged energy amounts to in 4 seconds as much as more than 50% of the entire energy from fuel to sodium, the outflow energy from the fuel assembly outlet has declined conspicuously comparing with the case of the S/A central release in Case 7. Similarly, the thermal absorption energy inside the fuel assembly also considerably declines by the heat release through the wrapper tube wall, which provides less possibility of fuel failure propagation in the fuel assembly comparing with the case of S/A central release.

(3) Outlet Temperature Response

Fig. III-20 represents the time respondency of radial distribution of temperature at the fuel assembly outlet in Case 11. The reason for the quicker higher temperature response at the fuel released cell No. 7 than the cell No.3 comparing with Fig. III-17 is that there worked a mixture effect which has stronger effect by virtue of the cooling effect nearby the wrapper tube.

Fig. III-21 shows the respondency of the outlet mean increased

temperature in Case 11 and Case 12 in comparison with Case 7 at the time of S/A central release. As previously described by the heat discharge effect outside the wrapper tube wall, the mean increase rate of the outlet temperature barely reaches 50% of that of the S/A central release. When the fuel released cell is No. 8 cell nearby the wrapper tube and has the same release length and the same ratio of channel cross section in the fuel released region as in the case of Case 11 (Case 12), the released fuel rate is equivalent to 662g. But as the mean increase rate of the outlet temperature does not reach even 5 ℃ maximum, it may be almost hopeless to monitor it by the outlet thermometer.

III-2-3. Respondency Evaluation of Outlet Thermometer

The thermal propagation behaviors in the fuel assembly at the time of a localized molten fuel release in the fuel assembly have been analyzed and evaluated by parameter surveys upto the foregoing chapters. In this chapter, the respondency of outlet thermometers to this kind of accident shall be evaluated utilizing the results of the respondency analysis of the outlet mean temperature of the fuel assembly.

The detection performance characteristics of the outlet thermometers with the parametered time constant of a thermoelectric couple to the outlet mean temperature respondency at the time of a molten fuel release accident in the case of Case 7 are given in Fig. III-22, and in the case of Case 11 in Fig. III-23 respectively.

Viewing from the present day reactor design, it is feasible to maintain the outlet mean temperature fluctuation under a normal operation within ±5 ℃ . Therefore, when the abnormality monitoring point against this kind of reactor accident is set as outlet mean temperature

increase of +5 ℃ , and if 1 Kg of molten fuel is released at the S/A center, it may be possible to detect the accident by the outlet thermometer within the time constant of 4 sec. However, in the case of a fuel release in the equivalent fuel amount nearby the wrapper tube, it may be possible to detect it by only such a thermometer which has a time constant of not longer than one second.

This fact indicates that, with the currently designed outlet thermometers of 2 - 3 sec time constant, it is impossible to detect the fuel release near the wrapper tube even though it may possible to detect the fuel release in the center of a fuel assembly at the time of 1 Kg of molten fuel release.

Judging from the analytical results given in Fig. III-12 and Fig. III-13, the parameters of the released fuel particle size, UO_2-Na heat transfer coefficient, coolant mixture ratio between the sub-channels, and the UO_2/Na mixture ratio in the fuel released region may be said to effectuate no great influence upon the outlet mean temperature response except in the case where the thermal transfer rate is extremely aggravated by gas blanketing effect in the periphery of the released fuel.

Consequently, summarizing the above analysis and evaluation, the outlet thermometers which are the subject of the current design will have sufficient performance to detect thermal energy release only when about 2 Kg of molten fuel is released in the channel in a fuel assembly.

Table III-1 Analytical Conditions for Thermal Propagation Behavior In Fuel Assembly Following Localized Molten Fuel Release

Calculation Conditions	Symbol	Value	Unit
No. of Fuel Pins in One Fuel Assembly	N_T	169	piece
Fuel Pin Arrangement Pitch	P_F	7.9	mm
Fuel Pellet Diameter	D_F	5.4	mm
Cladding Tube External Diameter	D_C	6.5	mm
Cladding Tube External Wall Thickness	R_C	0.45	mm
Reactor Core Length	L_C	90	cm
Lower Blanket Length	L_{BL}	35	cm
Upper Blanket Length	L_{BU}	35	cm
Upper Plenum Length	L_P	113	cm
Fuel Pin Total Length	L	280	cm
Wrapper Tube Thickness	R_W	3.0	mm
Adjacent Wrapper Tube Gap	R_W'	5.0	mm
Fuel Assembly Inlet Temperature	T_{IN}	400	℃
Coolant Flow Velocity In Fuel Assembly	V_N	560	cm/sec
Mean Linear Output of Core Section	Q_{AV}	220	w/cm
Maximum Linear Output of Core Section	Q_{MAX}	420	w/cm
Total Heat Generating Velocity in One Fuel Assembly	$Q_{T\phi}$	5.03	MW
Na Flow Velocity in Adjacent Wrapper Tube Gap	V_ϕ	50	cm/sec
Axial Central Position of Fuel Release	H_{cent}	Center of the Core	cm

Table III-2. Parameter Calculation Conditions for Analysis of Thermal Propagation Behavior in Fuel Assembly Following Localized Fuel Release

Calculation Case No.	A	B	C	D	E		F	G	H
	Fuel release S/A cross Section Position	Released Fuel Mass (Kg)	Spherical Fuel Particle Diameter (mmφ)	No. of Fuel Released Channels (cell)	UO_2/Na Mix Ratio in Released Region (%)	Fuel Released Axial Length (cm)	UO_2-Na Thermal Transfer Rate (W/cm²℃)	Subchannel Turbulent Flow Mix Ratio	Heat Generation Density of Released Fuel Particle (g_{FO})
Case -1	S/A center	1	2.5	54	10	42.6	0.6279	β^*	g_{FO}
-2	"	0.1	2.5	54	1	42.6	0.6279	"	"
-3	"	1	0.5	54	10	42.6	0.6279	"	"
-4	"	1	2.5	96	10	42.6	0.6279	"	"
-5	"	1	2.5	54	10	42.6	6.279	"	"
-6	"	2	2.5	54	20	42.6	0.6279	"	"
-7	"	1	2.5	54	10	42.6	0.6279	"	$g_{FO} = 0$
-8	"	1	2.5	54	10	42.6	0.10	"	$g_{FO} = 0$
-9	"	1	2.5	54	2	106.5	0.6279	"	$g_{FO} = 0$
-10	"	1	2.5	54	10	42.6	0.6279	$\beta/6$	$g_{FO} = 0$
-11	Near Wrapper Tube	1	2.5	14	10	129.8	0.6279	β^*	$g_{FO} = 0$
-12	"	0.662	2.5	8	10	129.8	0.6279	"	$g_{FO} = 0$

Note: β^* : JAERI memo 4422 employed turbulent mix ratio

UO_2/Na mix ratio: UO_2/Na weight ratio in the case when Na remains stationary in the fuel released region. (This proportionates to the channel blockage ratio by the released fuel.

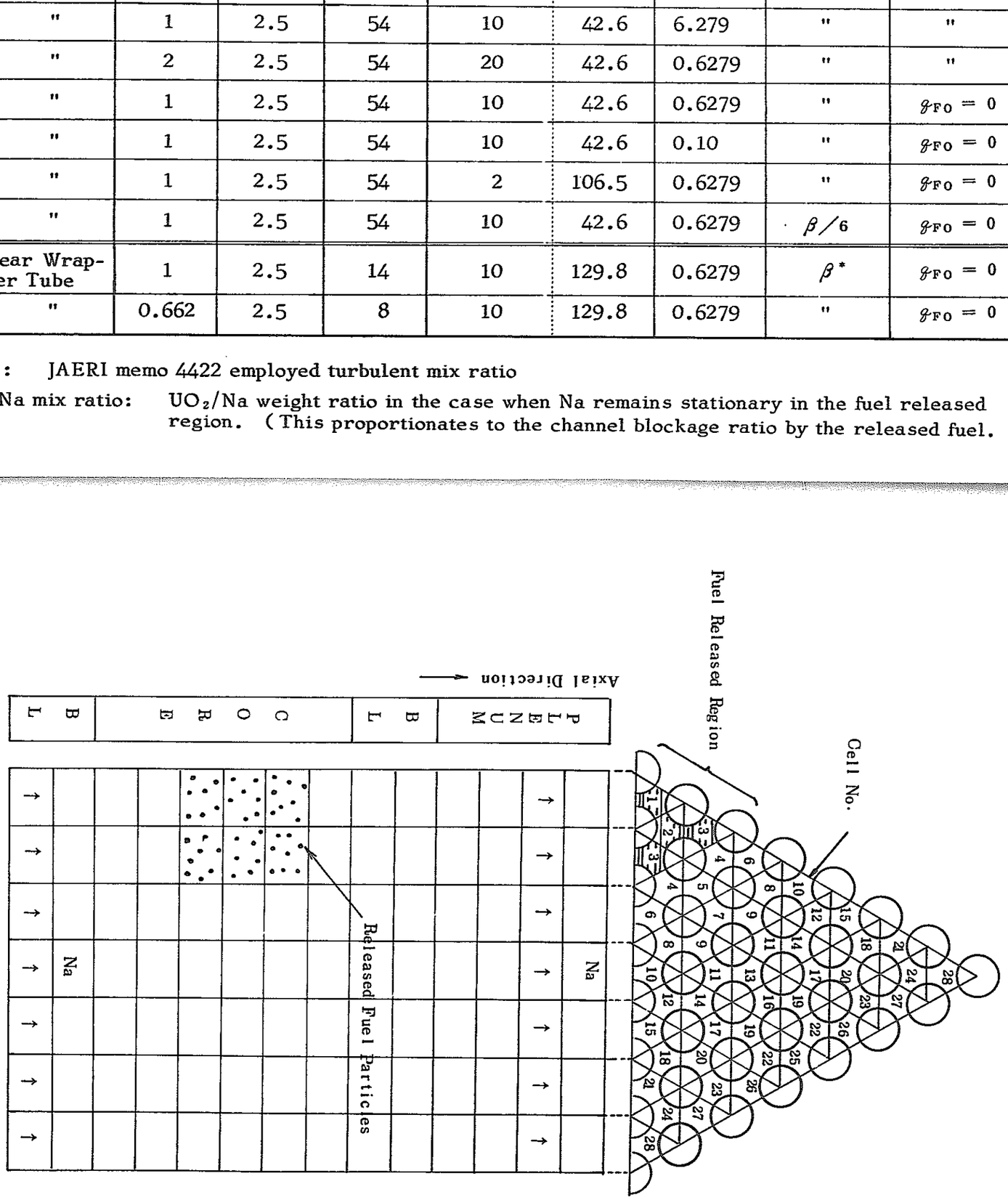

Fig. III-1. Analytical Model for Thermal Propagatin Behavior by Localized Molten Fuel Release
(In the Case of S/A Central Release)

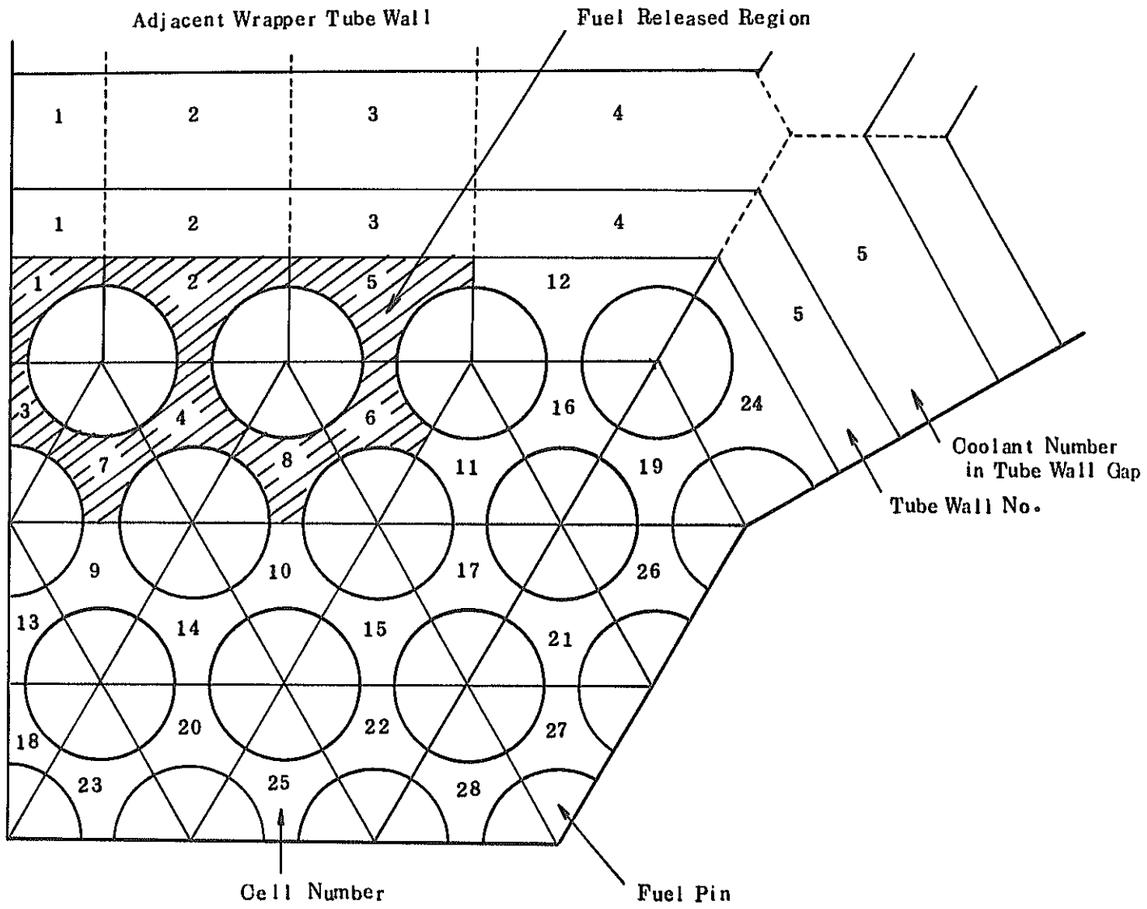

Fig. III-2. Analytical Model for Thermal Propagation Behavior by Localized Molten Fuel Release
(In the Case of Fuel Release near Wrapper Tube)

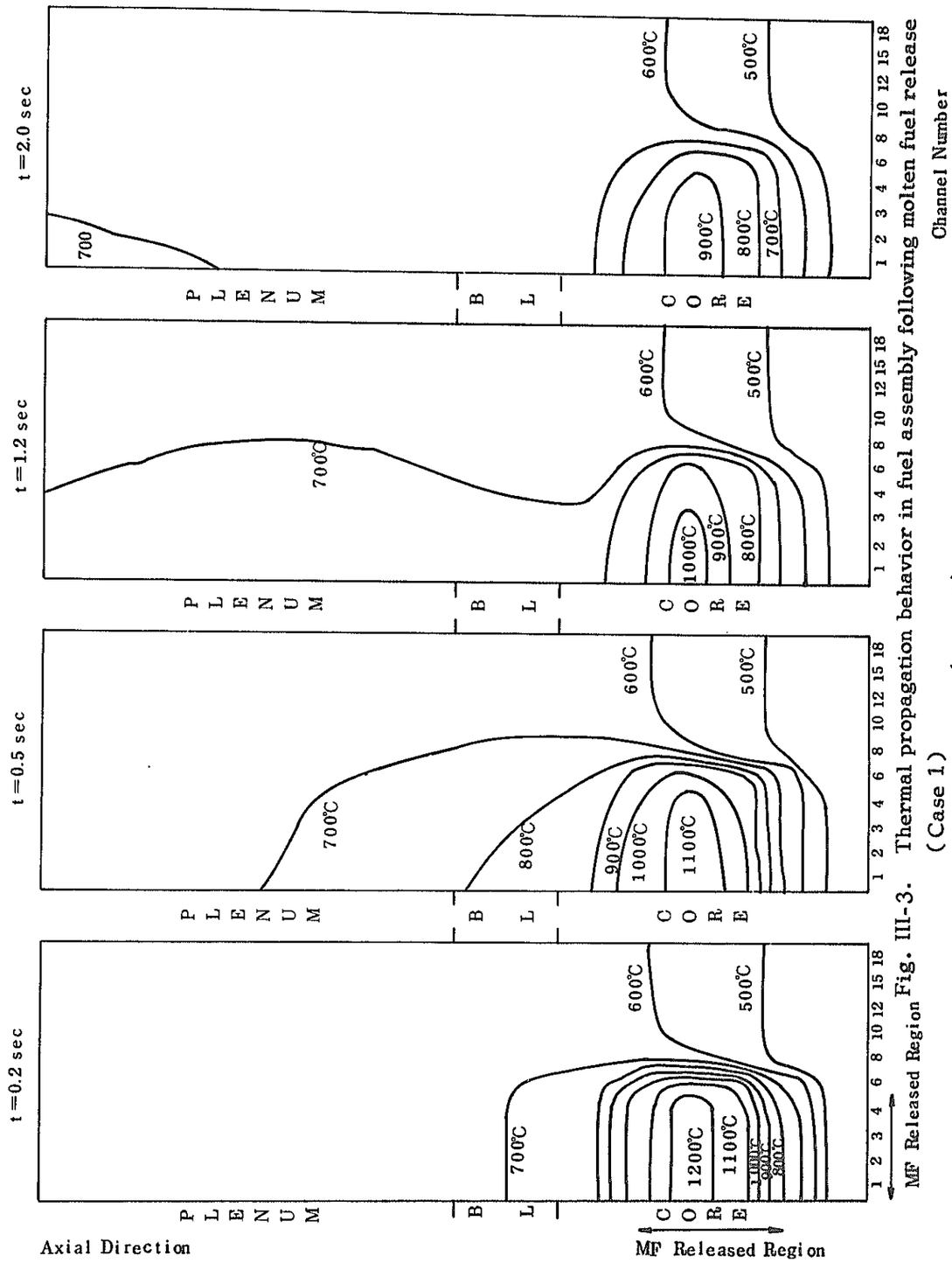

Fig. III-3. Thermal propagation behavior in fuel assembly following molten fuel release (Case-1)
(Case 1)

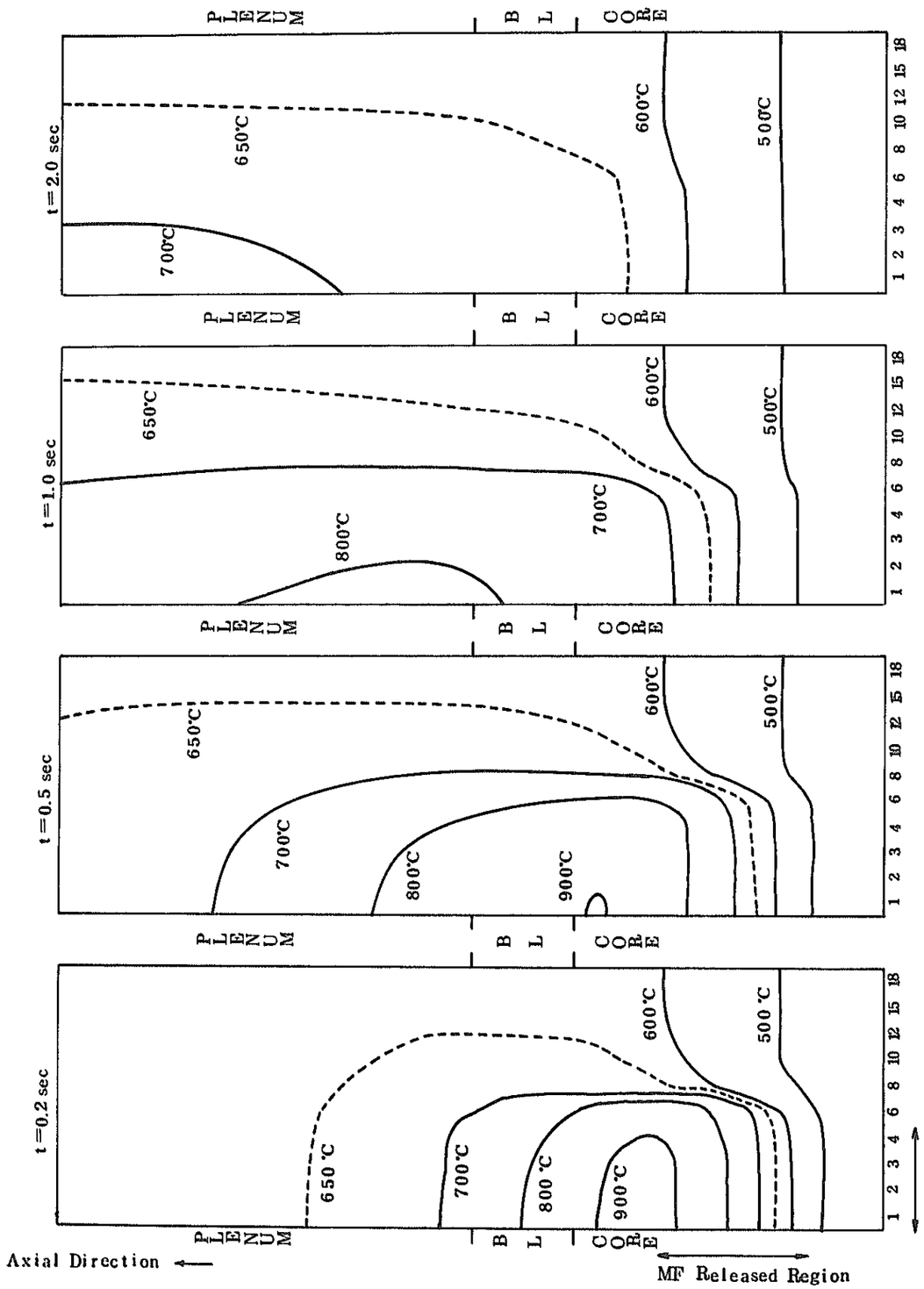

Fig. III-4. Thermal propagation behavior in fuel assembly following molten fuel release (Case 7)

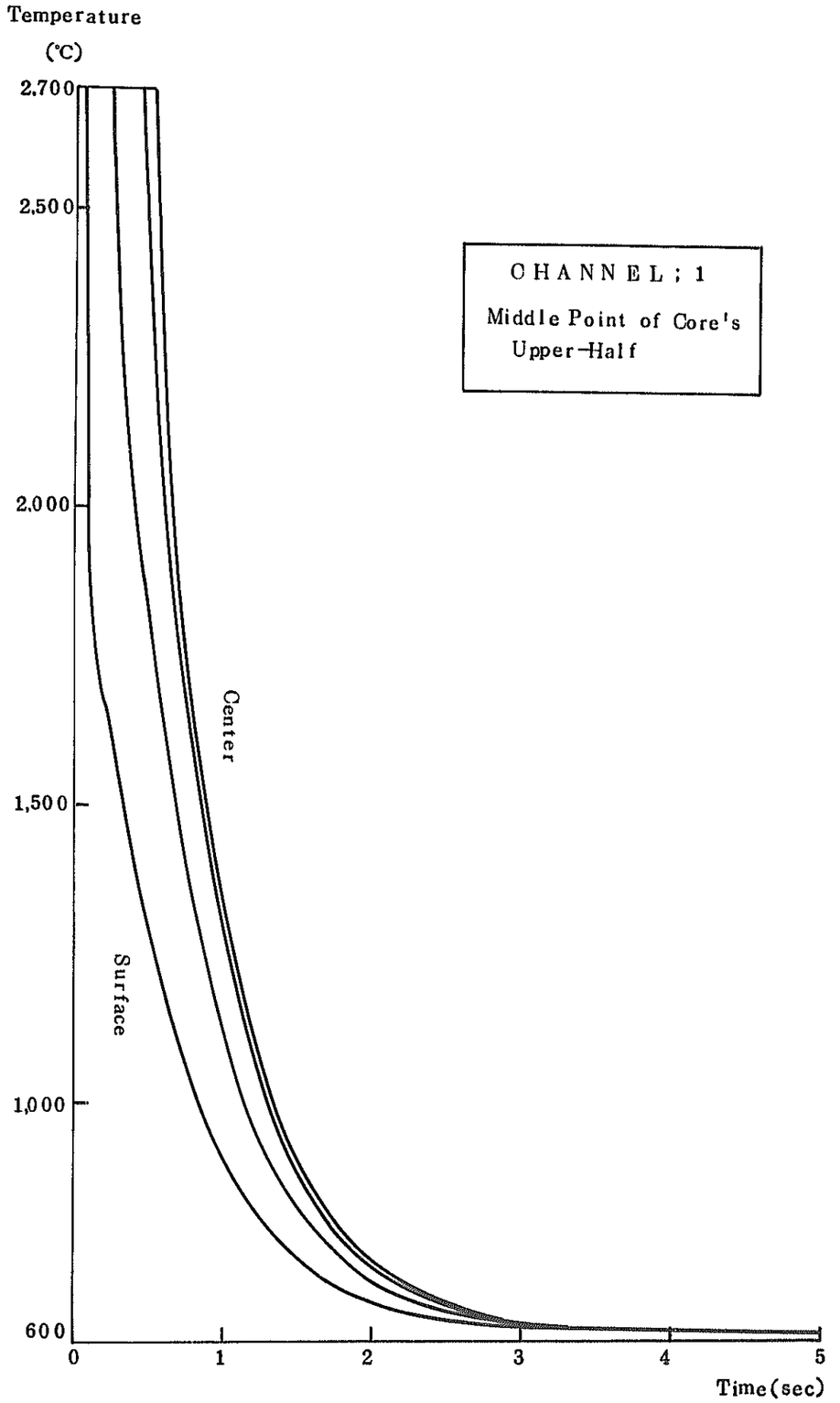

Fig. III-5. Time Change of Molten Fuel Temperature (Case 7)

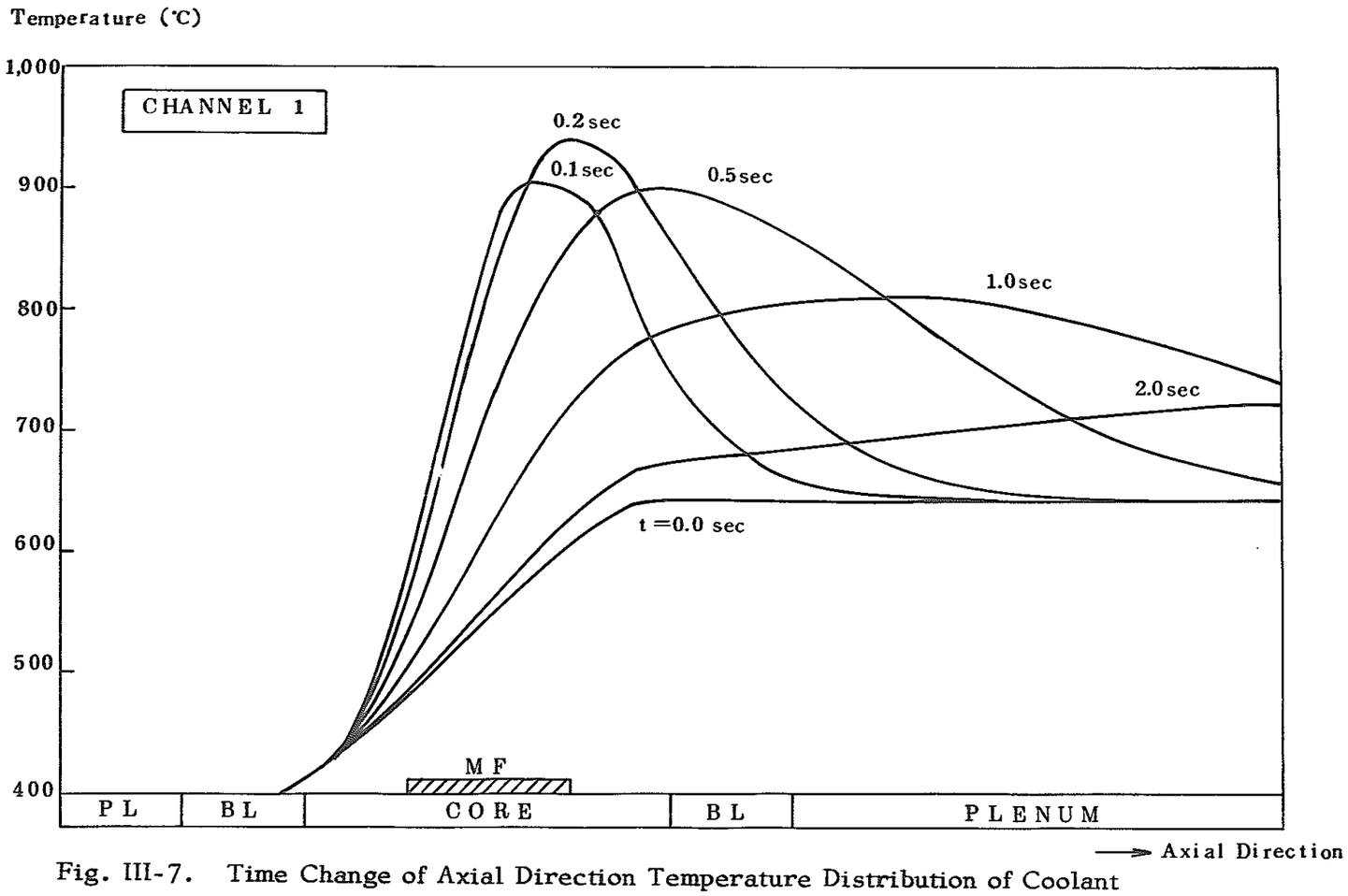

Fig. III-7. Time Change of Axial Direction Temperature Distribution of Coolant Following Molten Fuel Release. (Case 7)

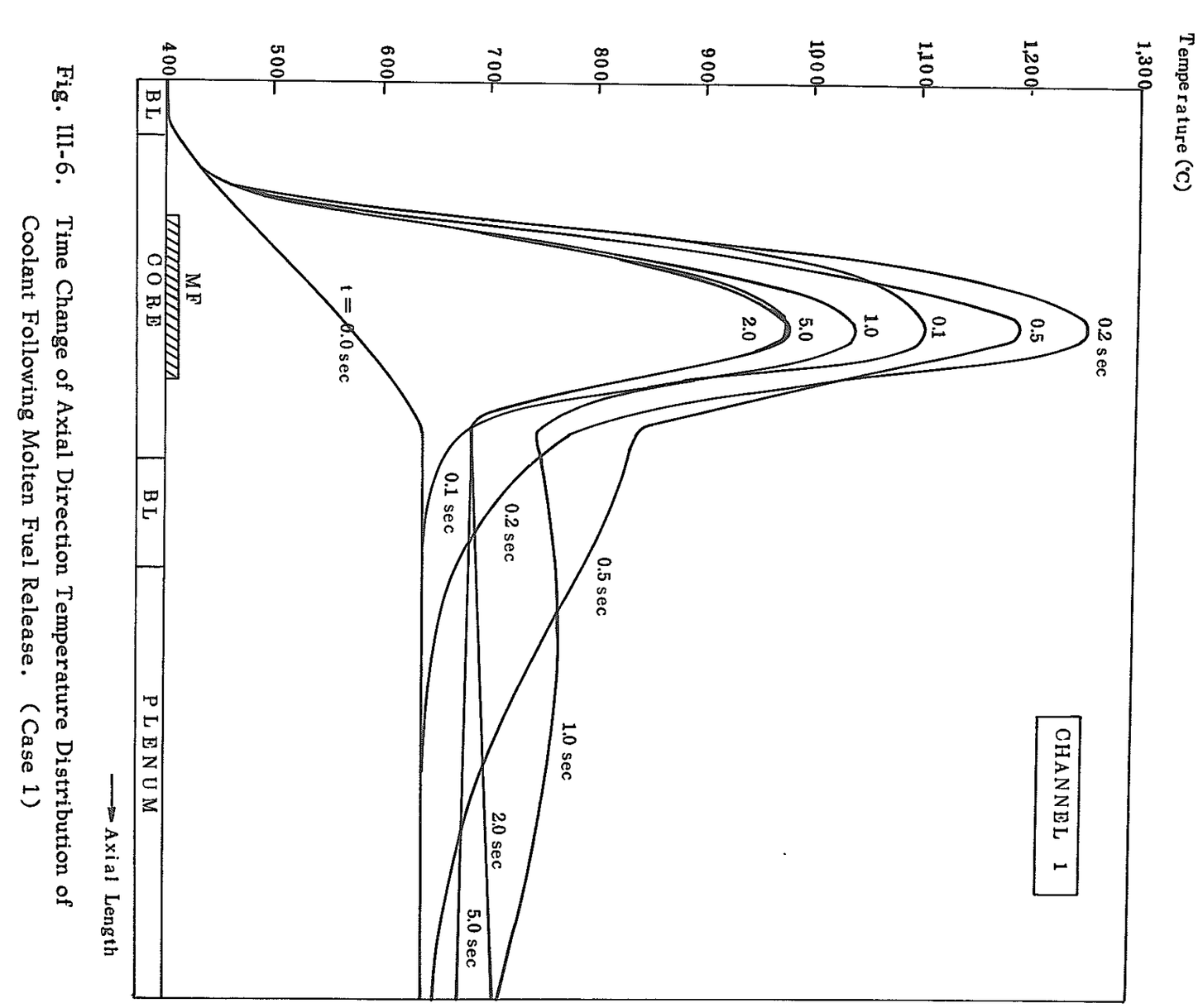

Fig. III-6. Time Change of Axial Direction Temperature Distribution of Coolant Following Molten Fuel Release. (Case 1)

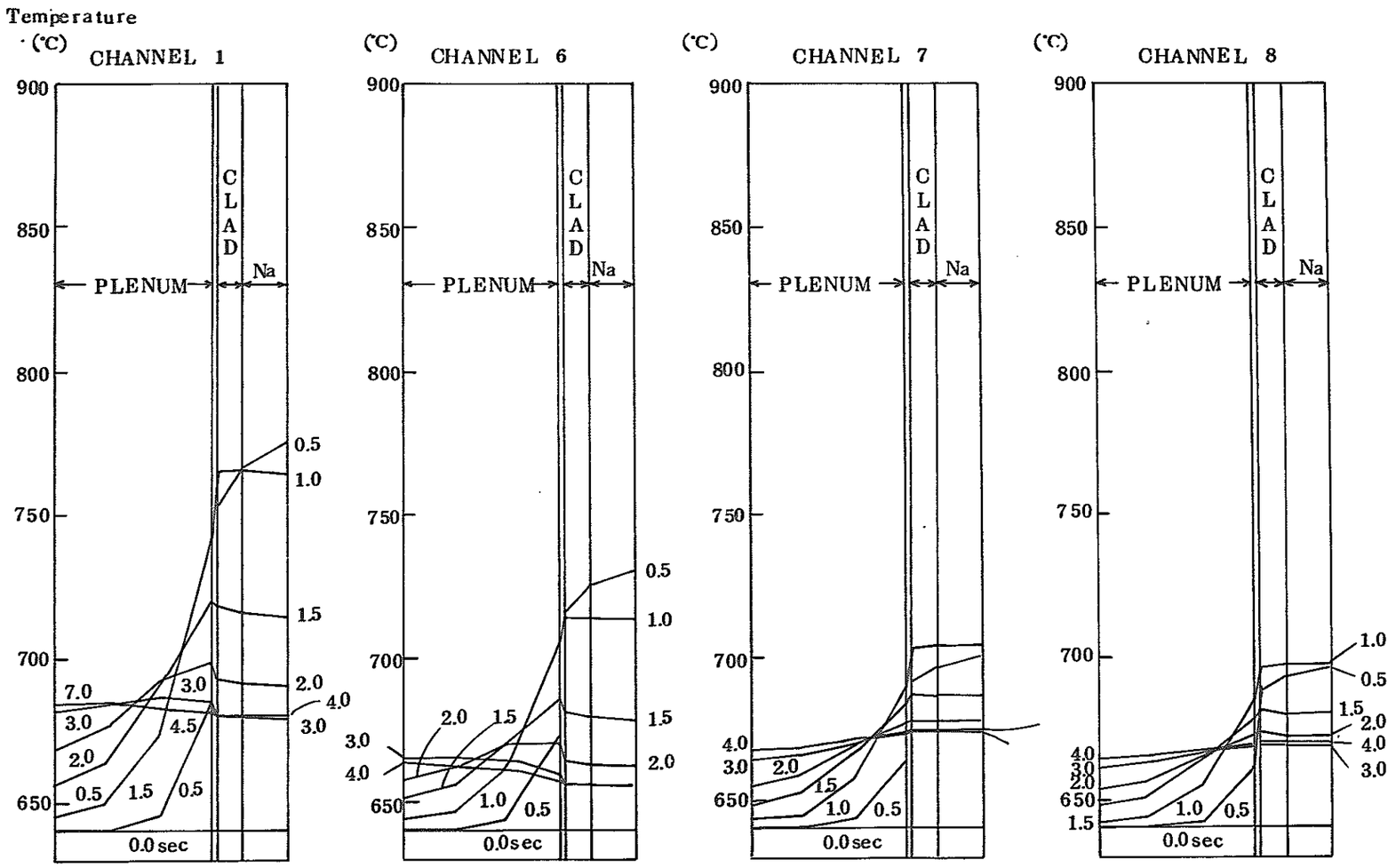

Fig. III-8. Plenum Heat Absorption Effect Following Molten Fuel Release (Lower End of Upper Plenum). (Case 1)

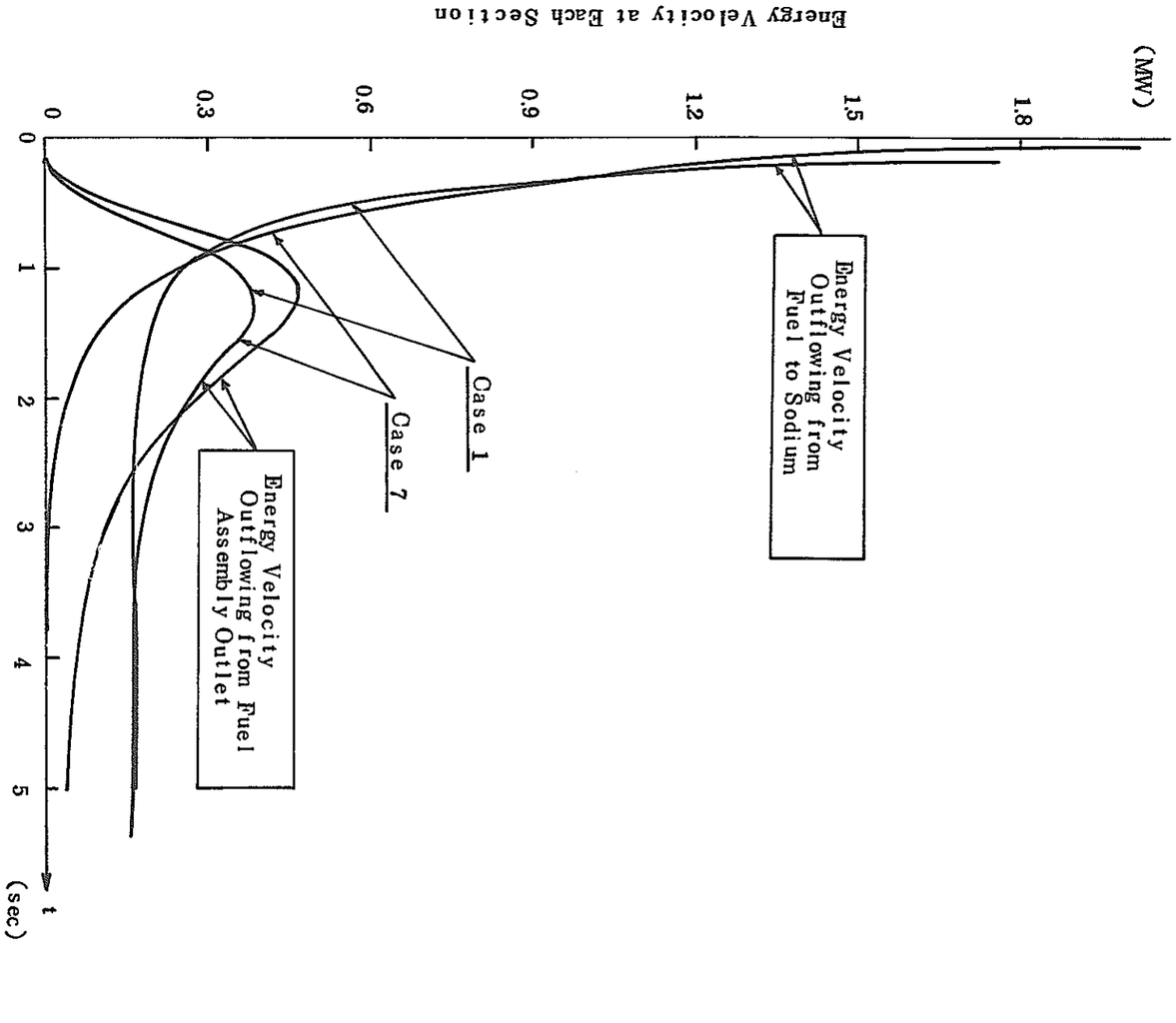

Fig. III-9. Energy Velocity at Each Section Following Molten Fuel Release. (Case 7)

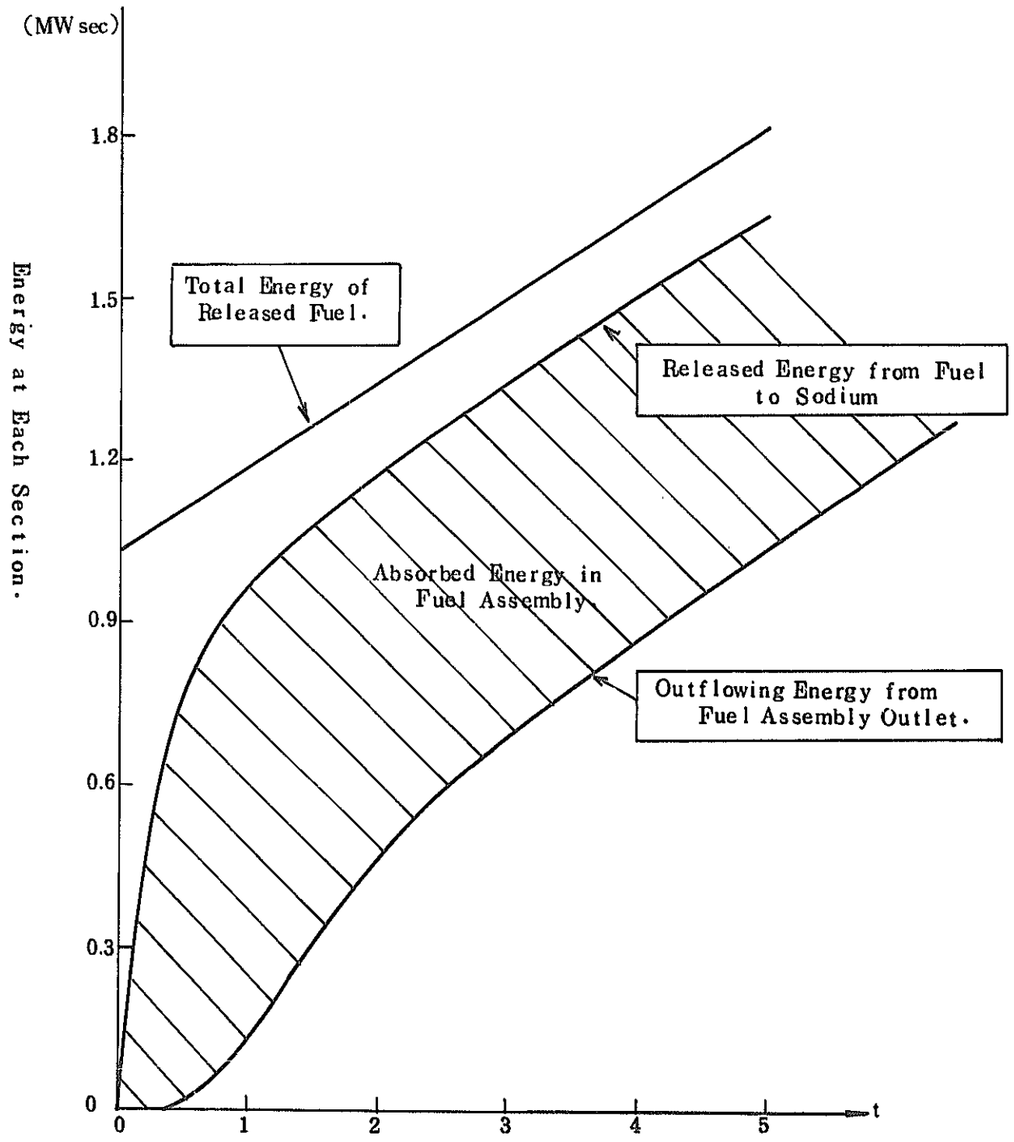

Fig. III-10. Energy Variation at Each Section Following Molten Fuel Release. (Case 1)

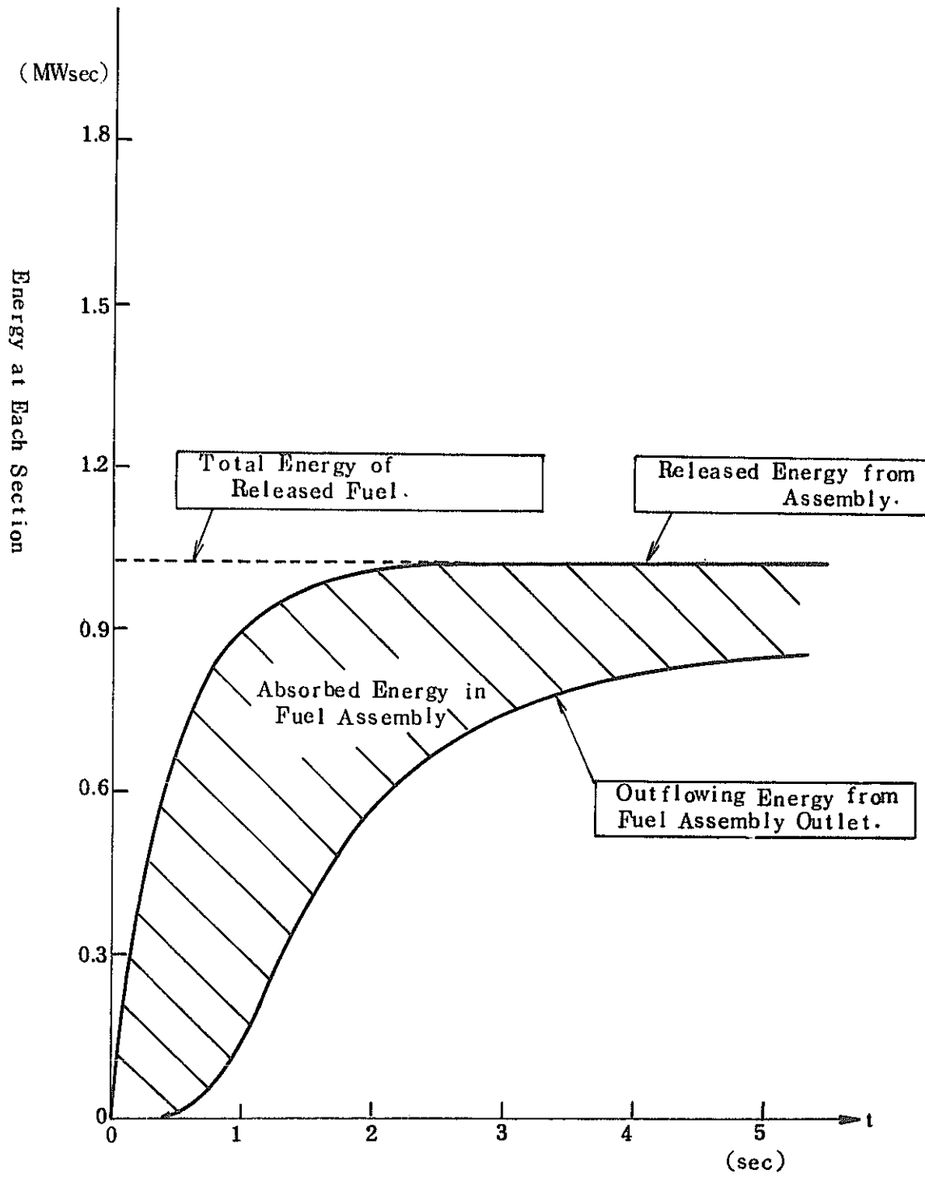

Fig. III-11. Energy Variation at Each Section Following Molten Fuel Release. (Case 7)

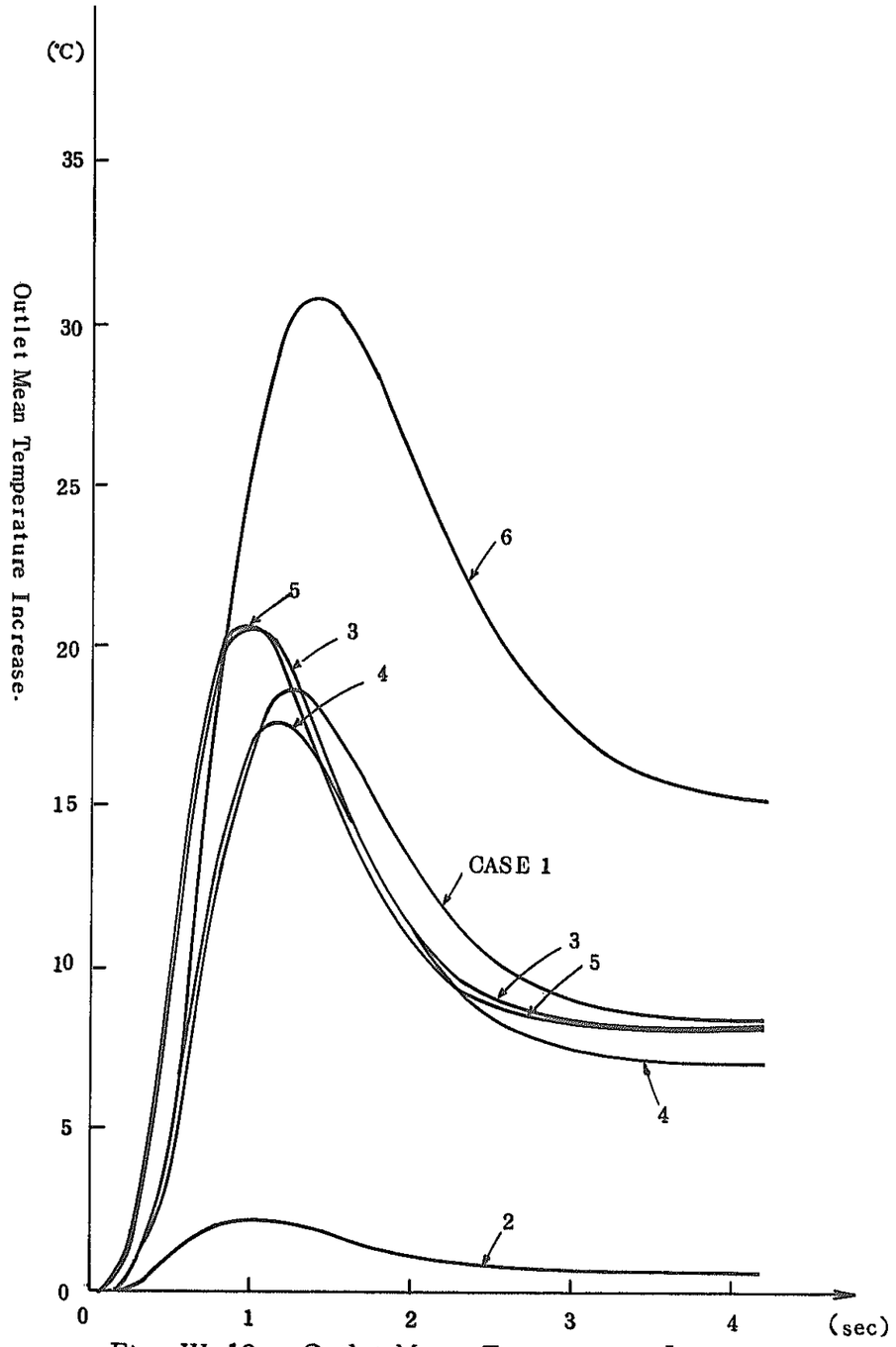

Fig. III-12. Outlet Mean Temperature Increase Following Molten Fuel Release

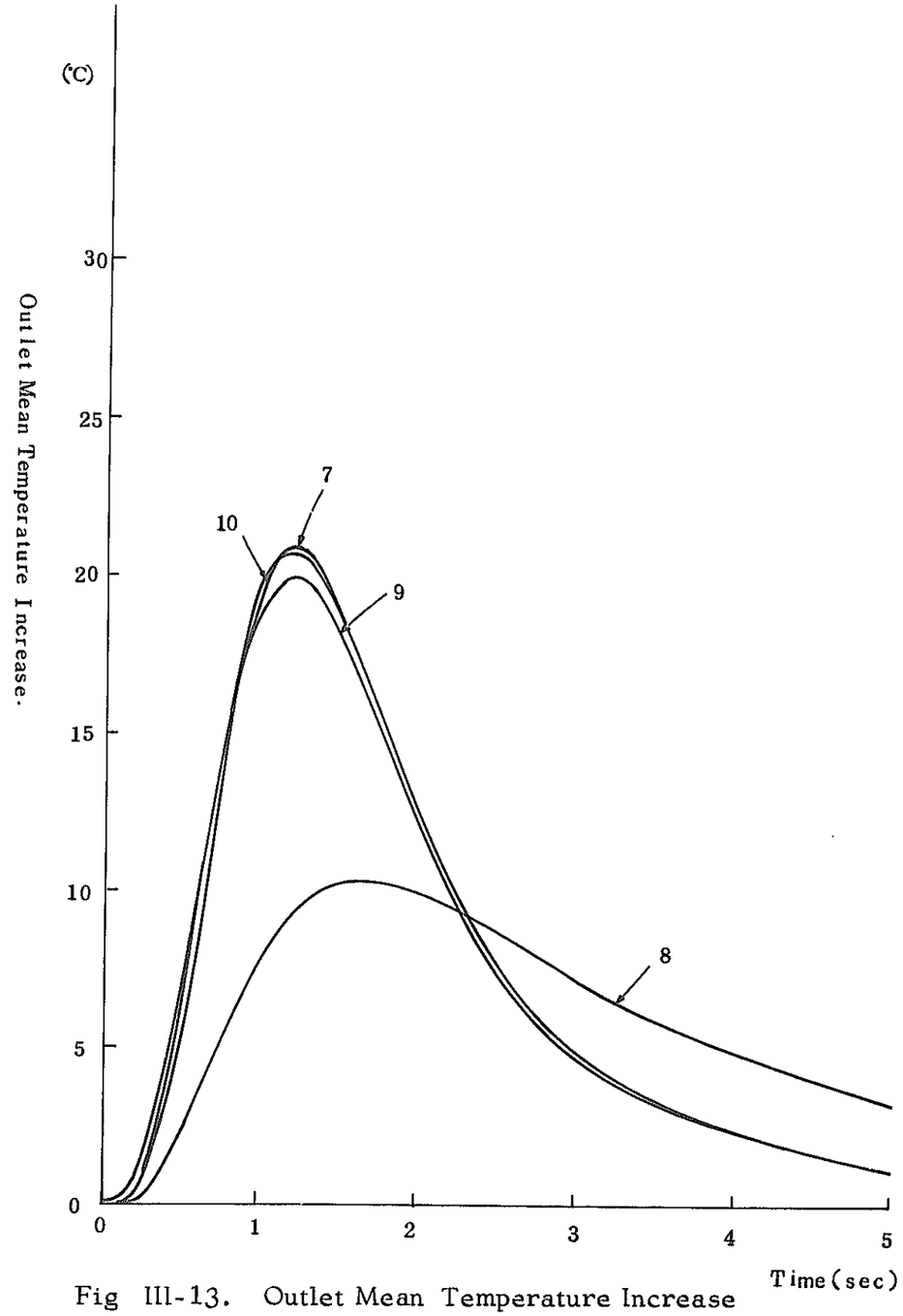

Fig III-13. Outlet Mean Temperature Increase Following Molten Fuel Resease

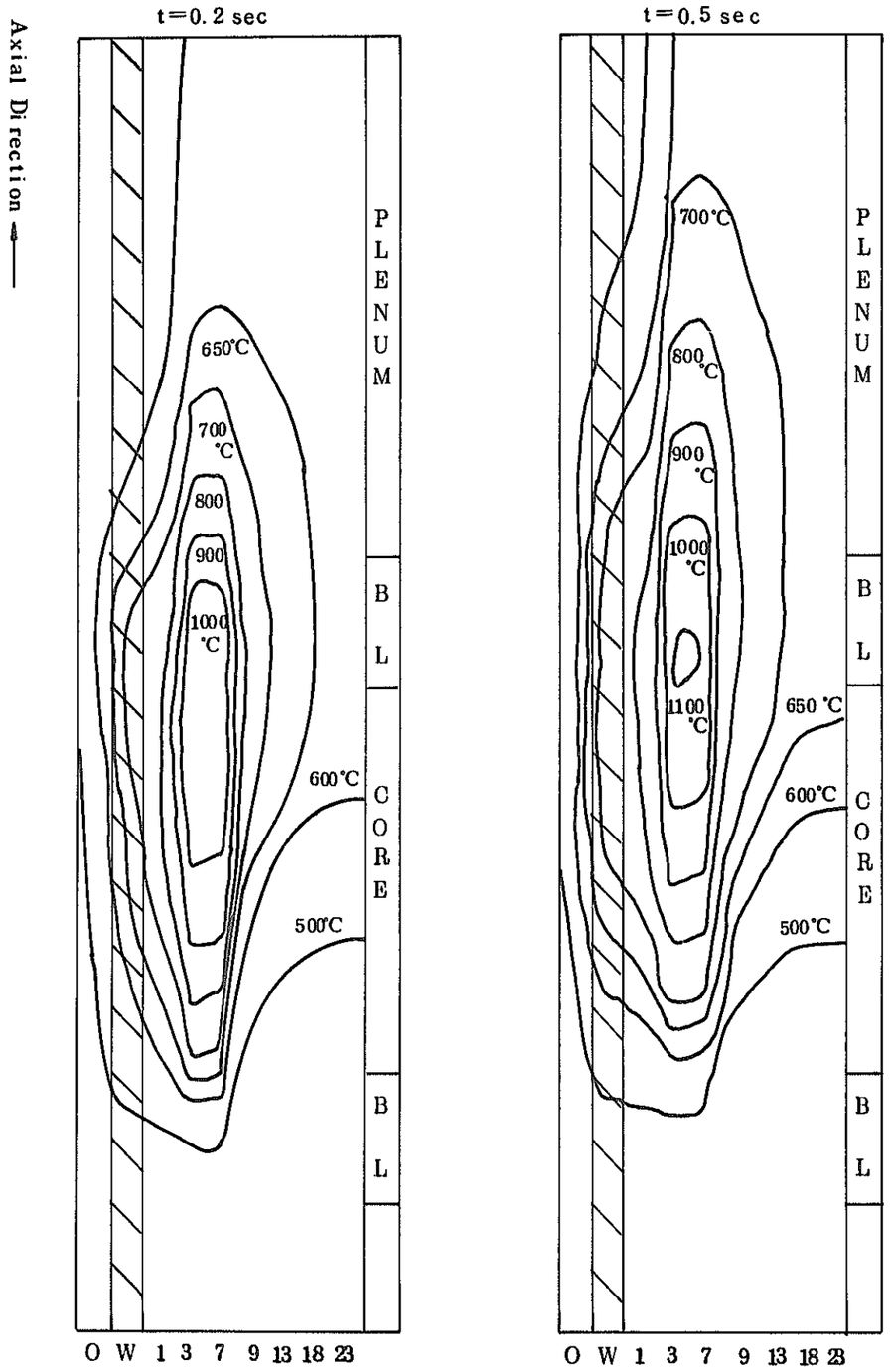

Fig. III-14 (1/2). Thermal Propagation Behavior near Wrapper Tube Following Molten Fuel Release. (Case 11)

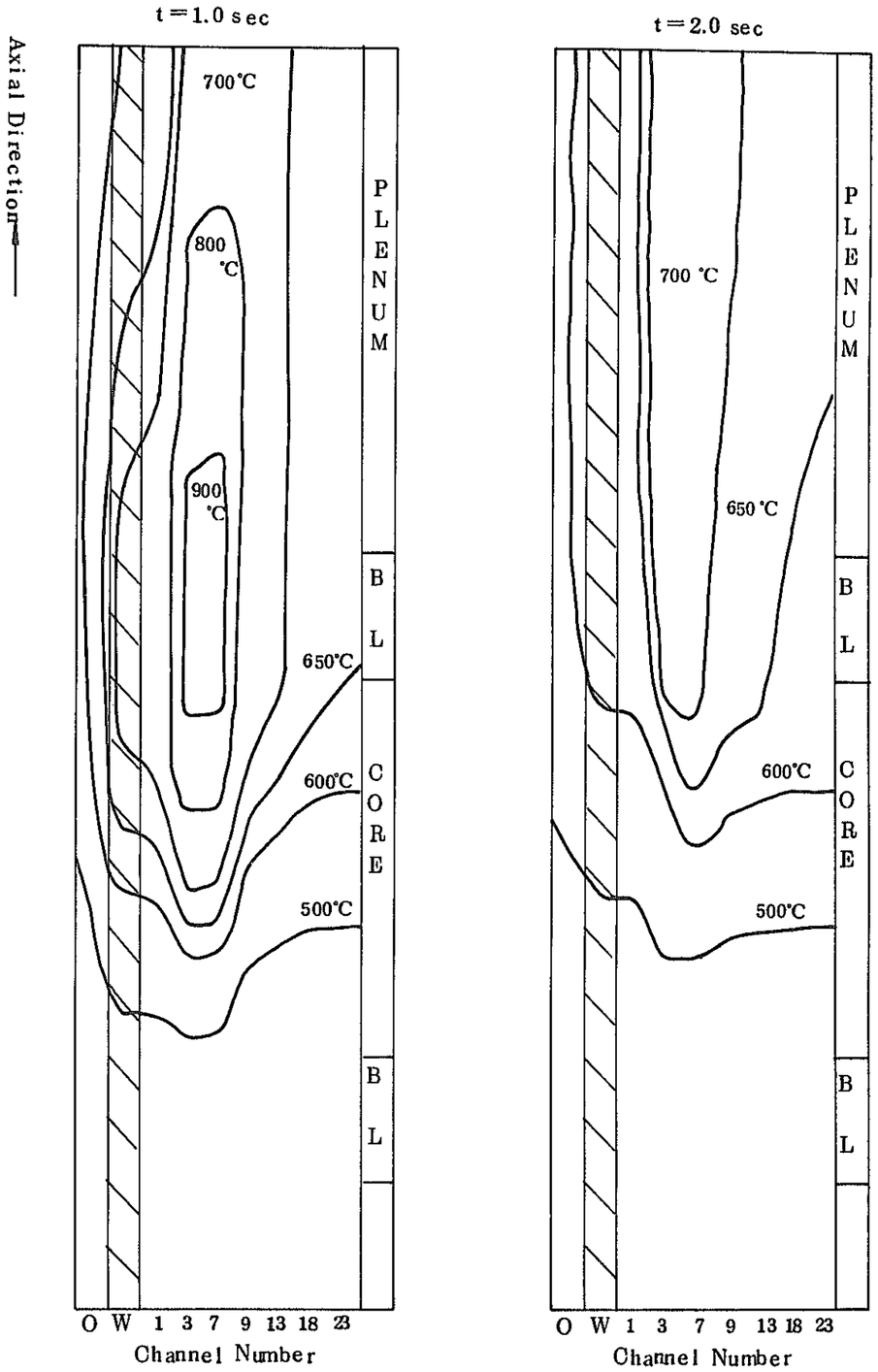

Fig. III-14 (2/2). Thermal Propagation Behavior near Wrapper Tube Following Molten Fuel Release. (Case 11)

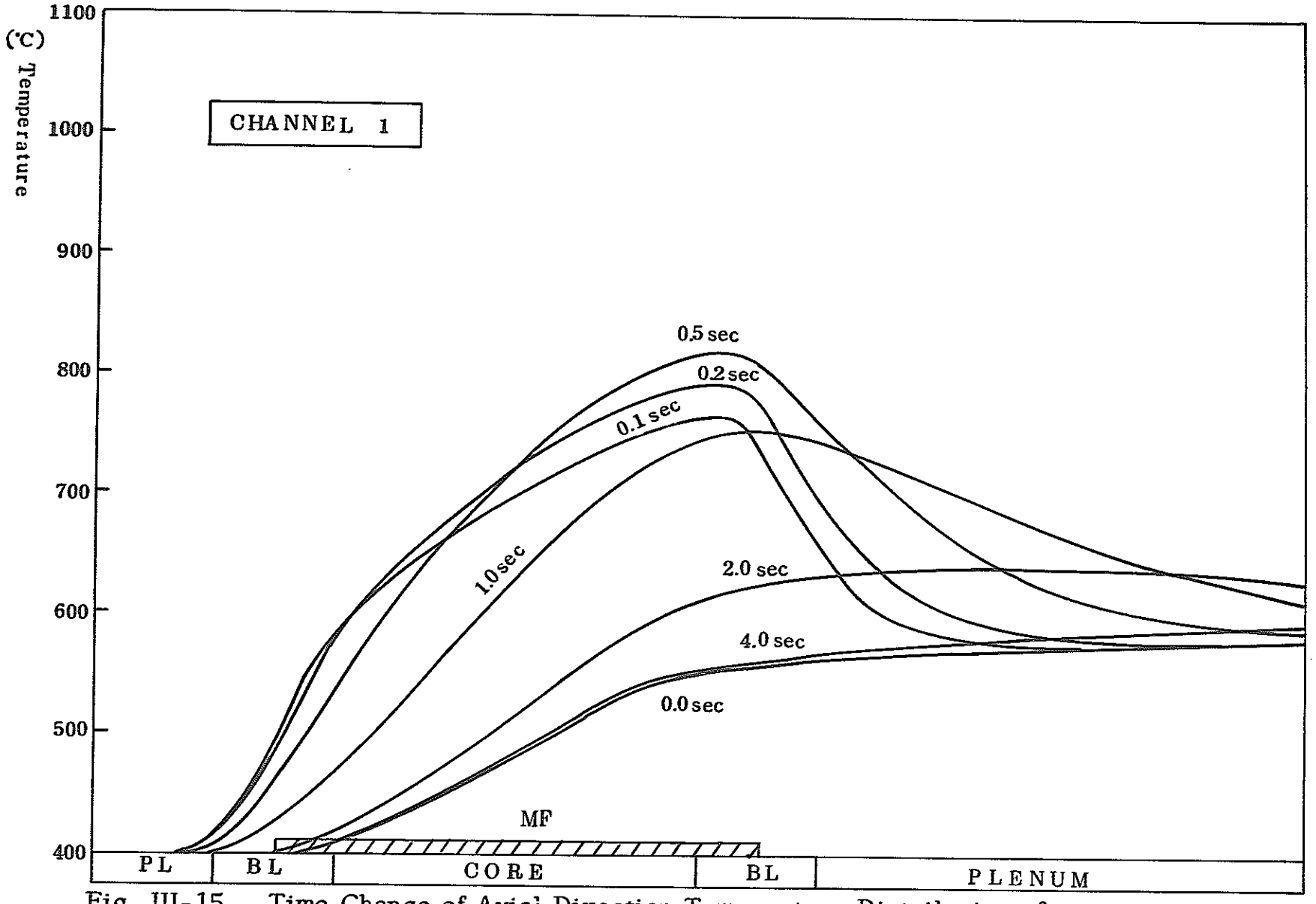

Fig. III-15. Time Change of Axial Direction Temperature Distribution of Coolant Following Molten Fuel Release. (Case 11)

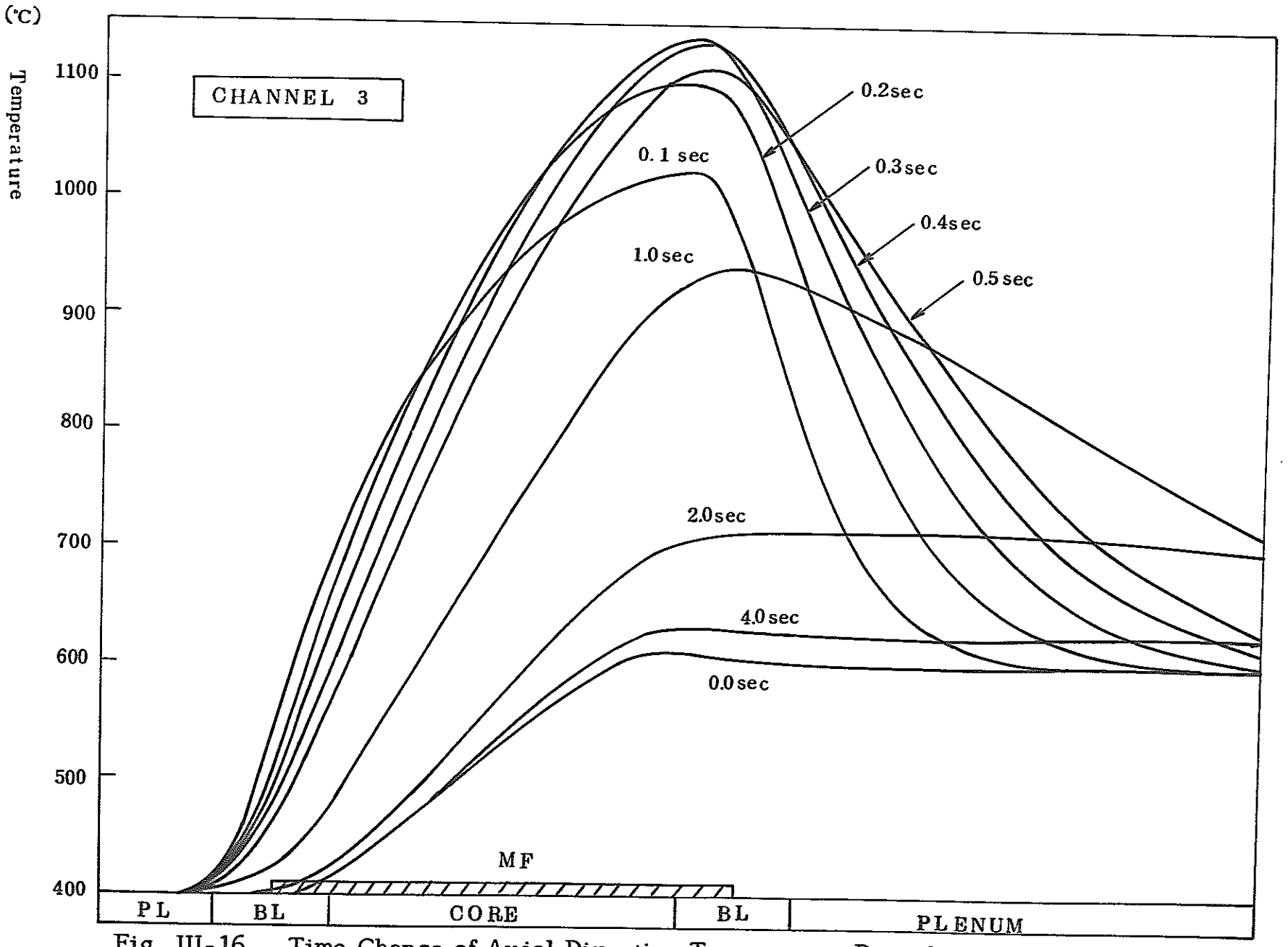

Fig. III-16. Time Change of Axial Direction Temperature Distribution of Coolant Following Molten Fuel Release. (Case 11)

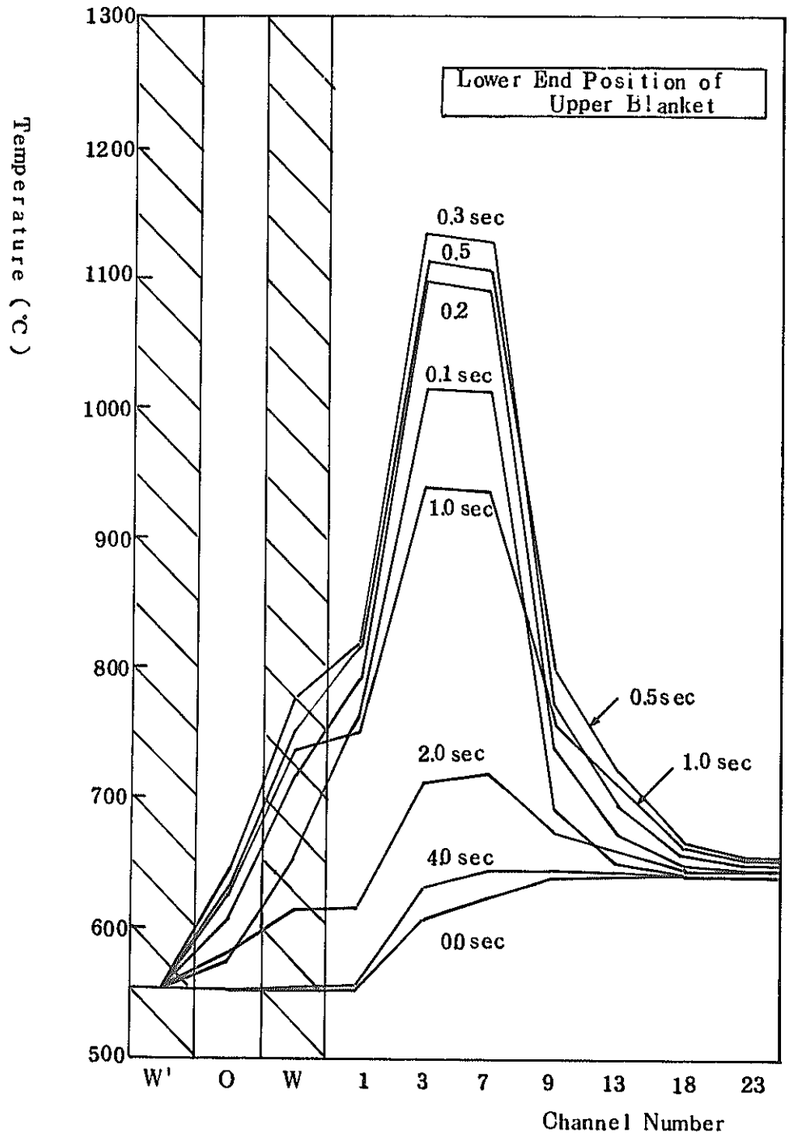

Fig. III-17. Time Change of Radial Direction Temperature Distribution of Coolant Following Molten Fuel Release.

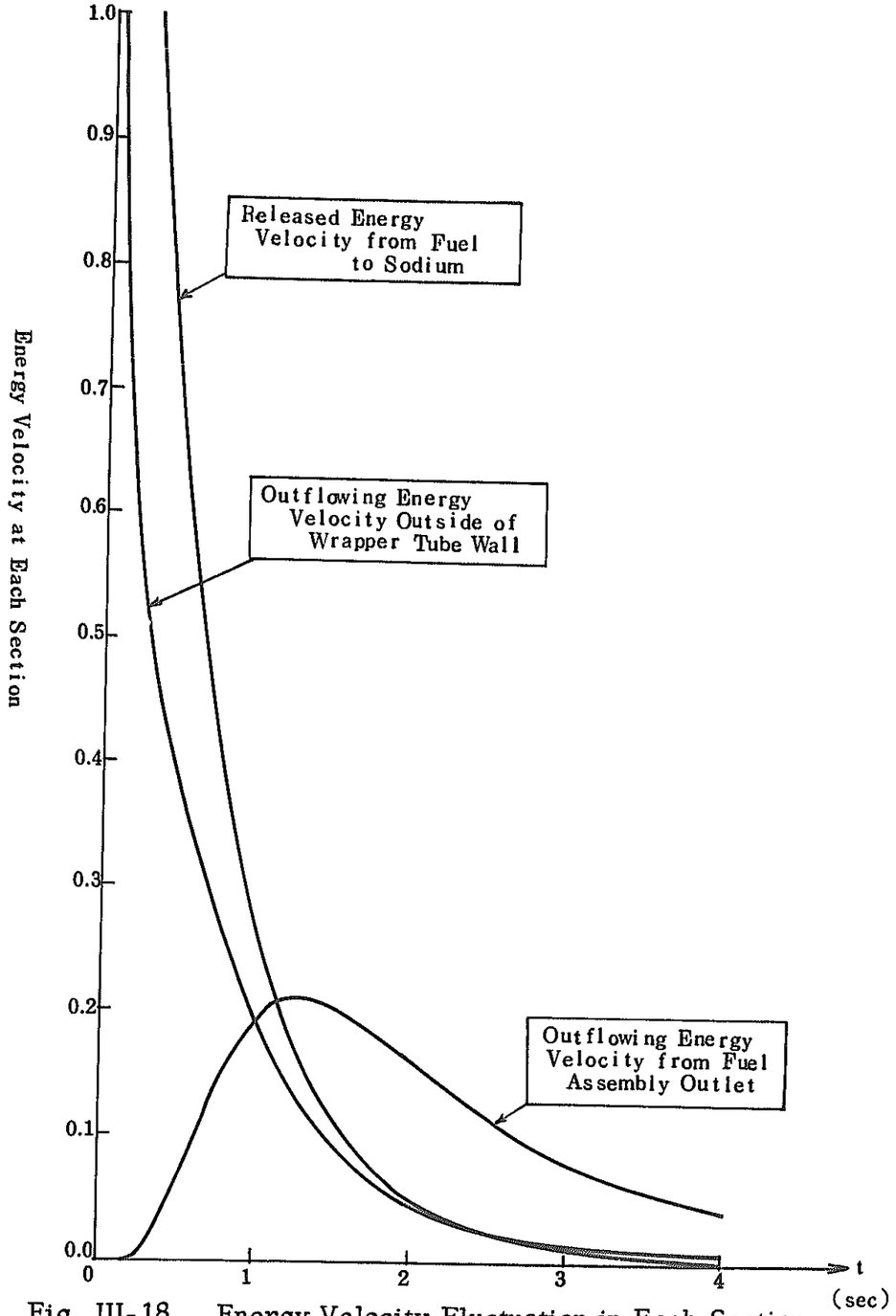

Fig. III-18. Energy Velocity Fluctuation in Each Section Following Molten Fuel Release. (Case 11)

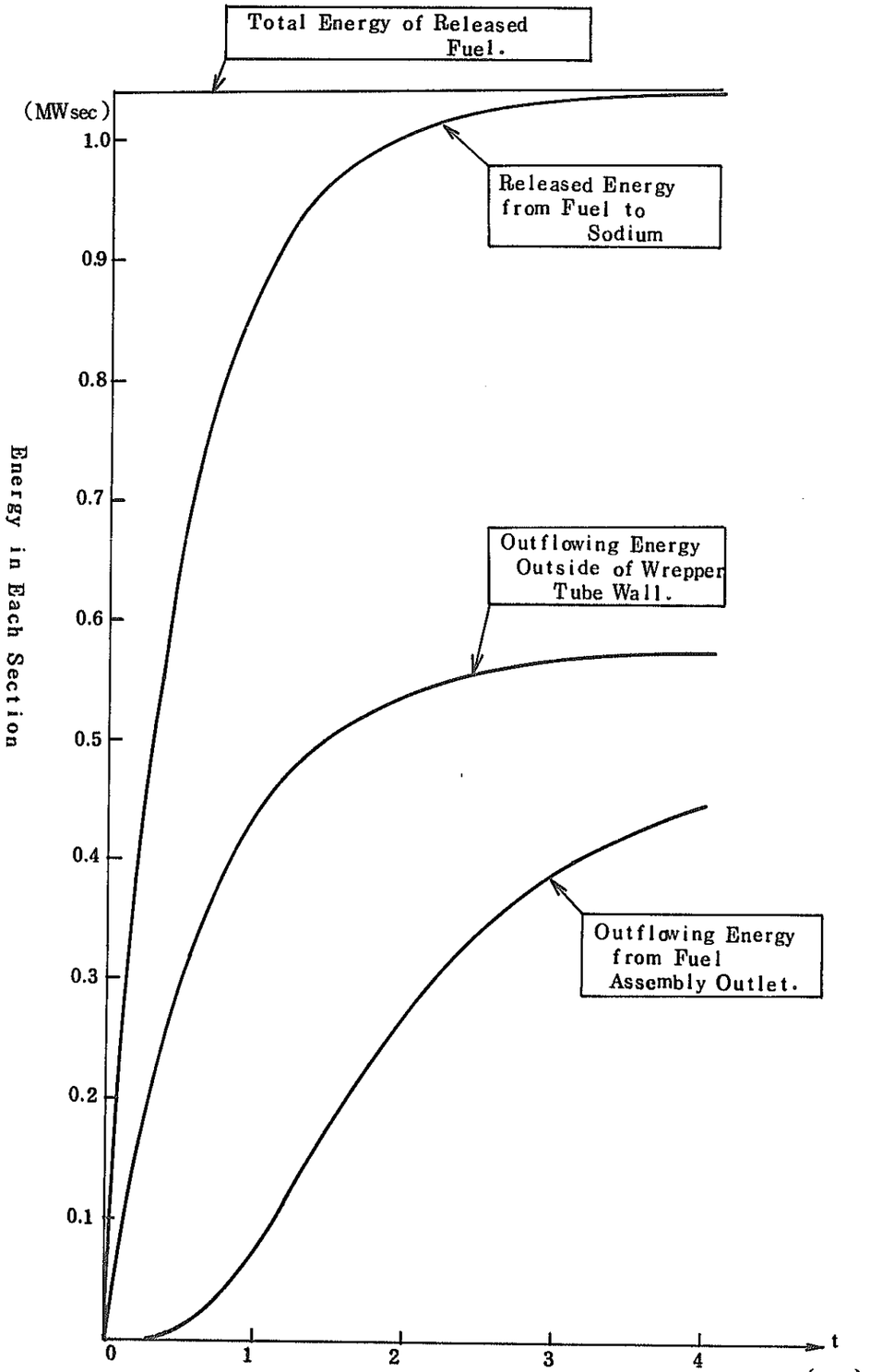

Fig. III-19. Energy Fluctuation in Each Section Following Molten Fuel Release. (Case 11)

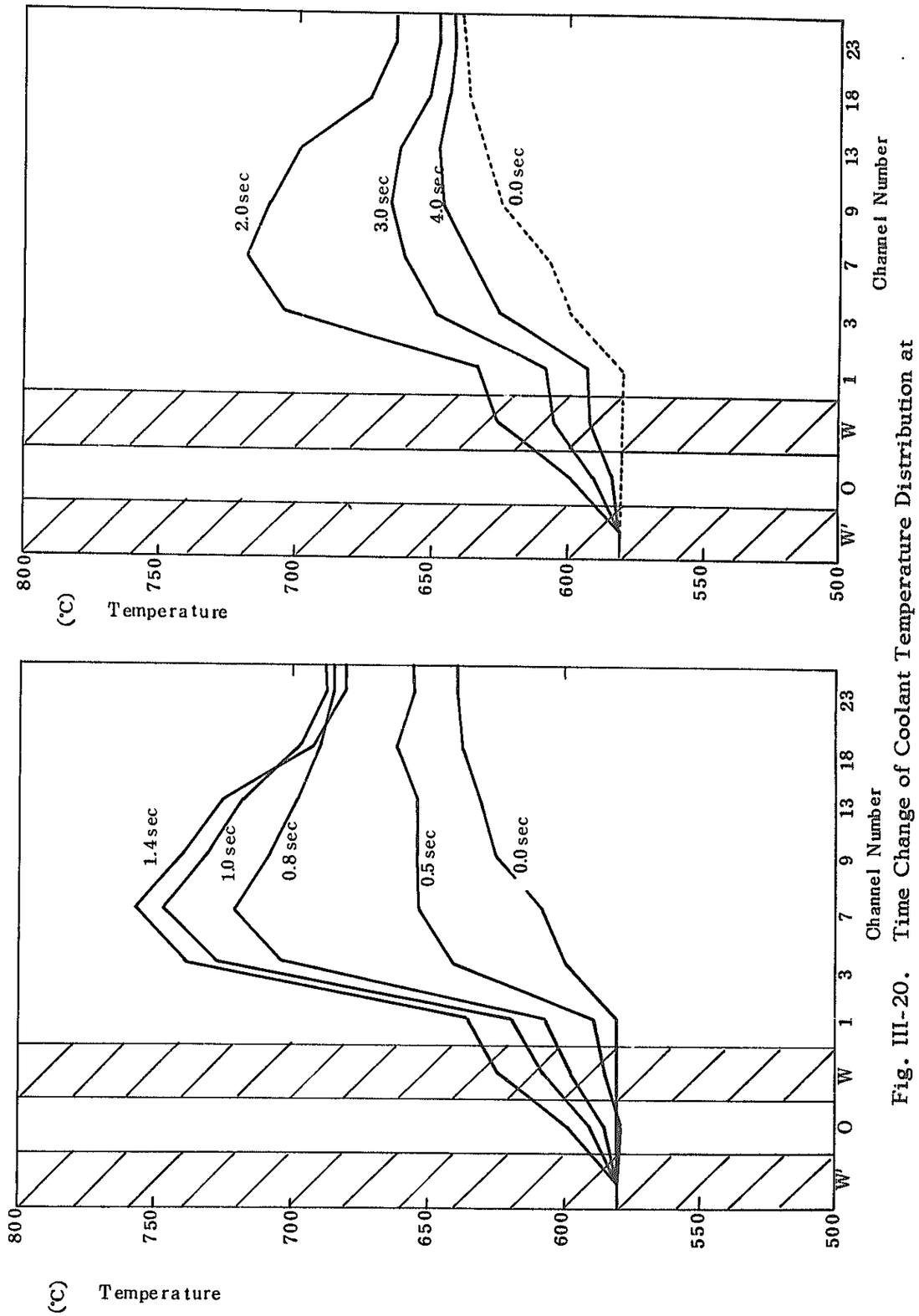

Fig. III-20. Time Change of Coolant Temperature Distribution at Fuel Assembly Outlet Following Molten Fuel Release

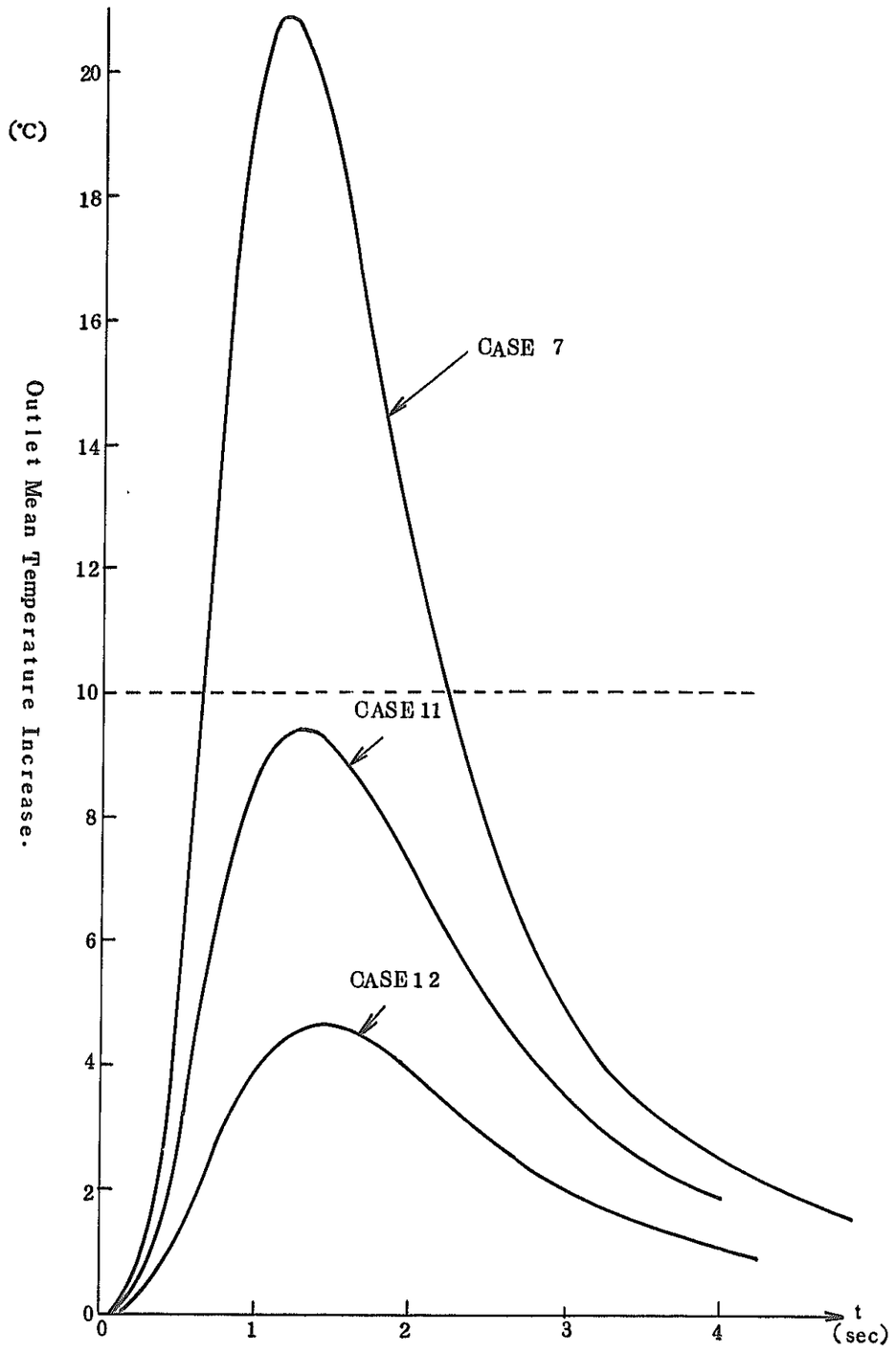

Fig. III-21. Time Change of Outlet Mean Temperature Increase Following Molten Fuel Release

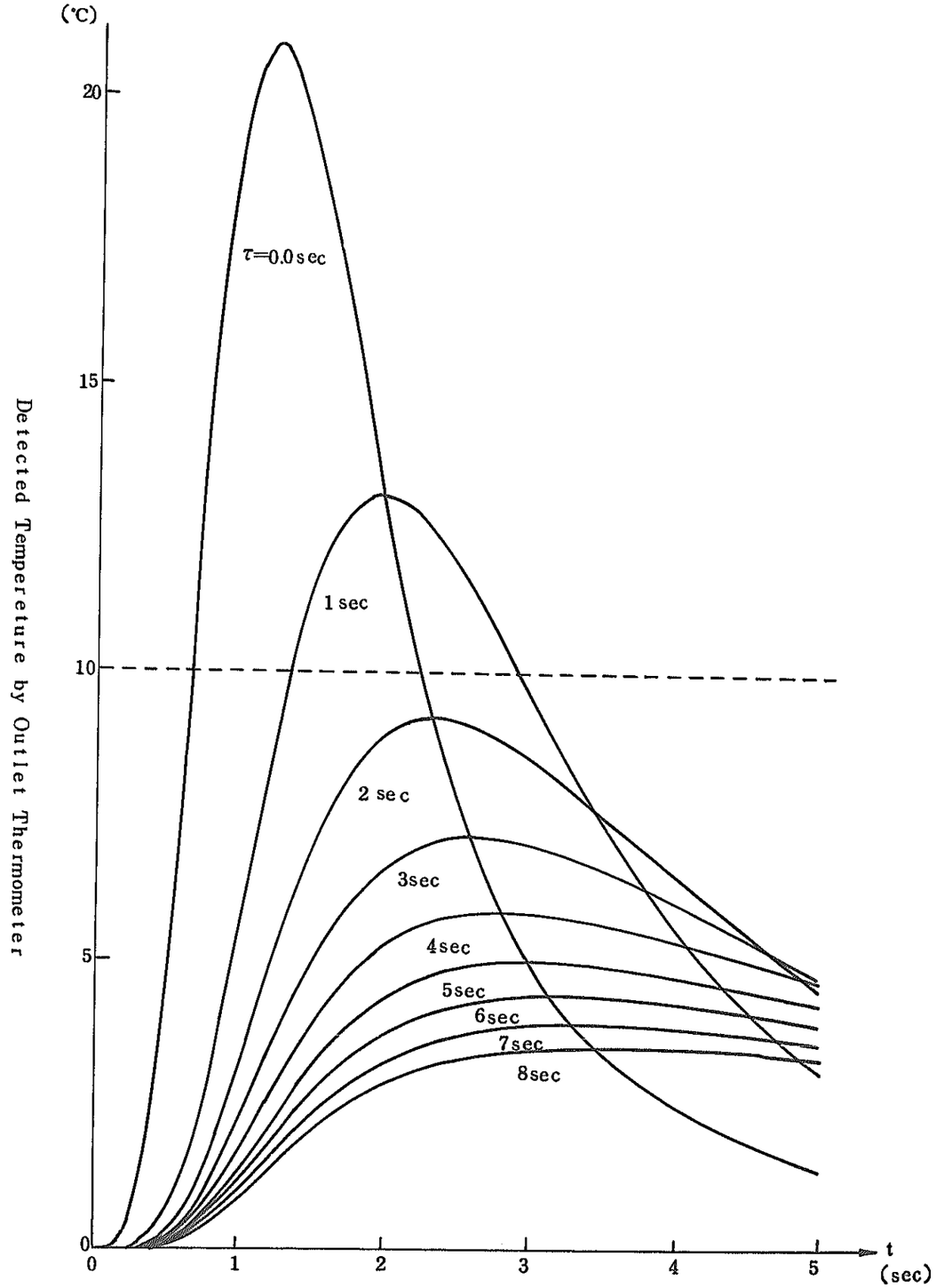

Fig. III-22. Detection Characteristics of Outlet Thermometer at Molten Fuel Release (Case 7)

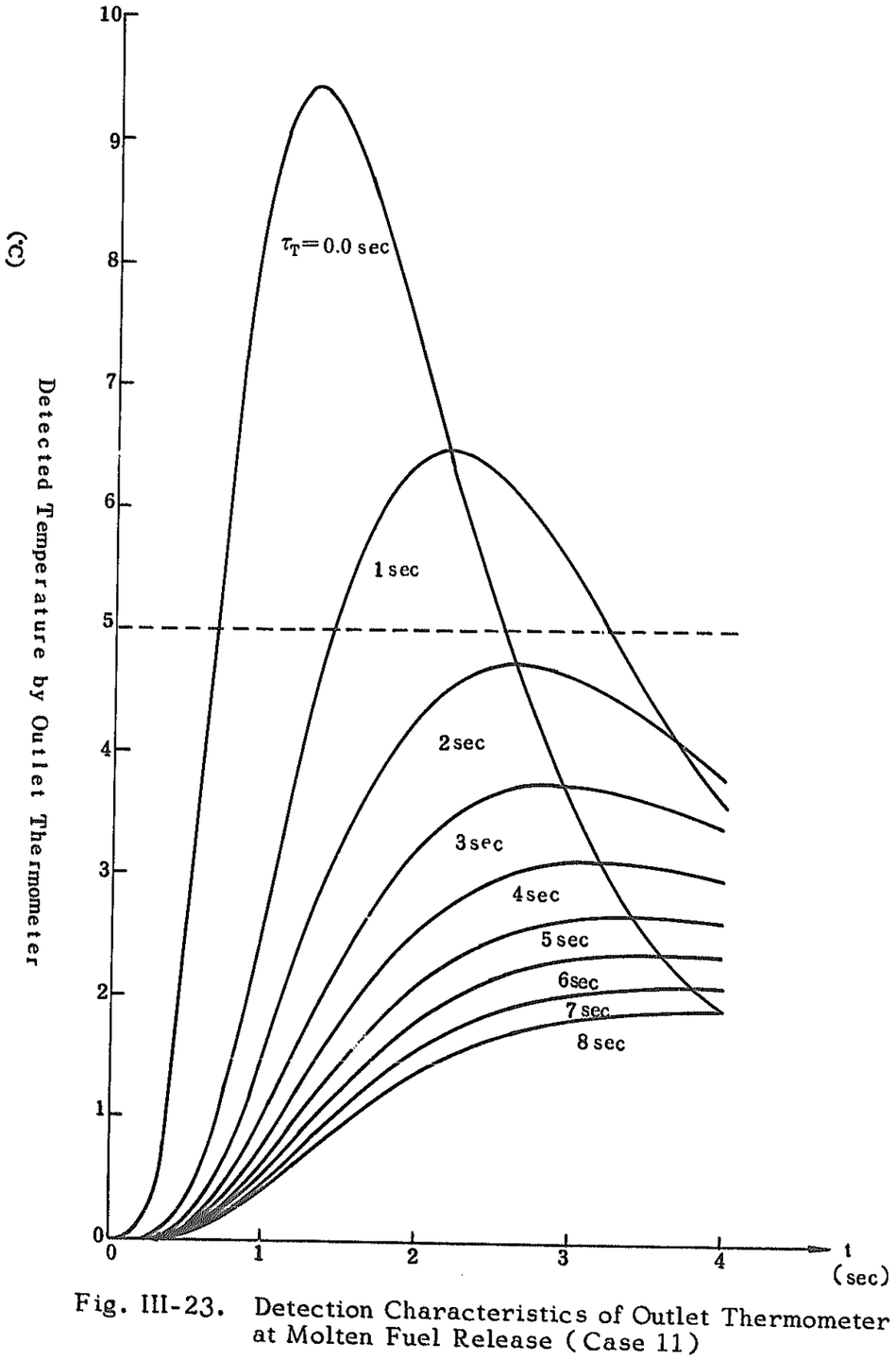

Fig. III-23. Detection Characteristics of Outlet Thermometer at Molten Fuel Release (Case 11)

IV. Conclusion and Future Problems

Summarizing the results of the above two analyses, the following conclusion may be made under the present analytical model.

(A) Analysis of Flow Variation by Local UO_2-Na Interaction

(1) Under a molten fuel release of about a 10g level, even if a local Na boil takes place, it disappears within several 10 msec.

(2) Under a molten fuel release of about a 50g level, although Na voids may develop to the full length of the core, they disappear in 200 ~ 300 msec.

(3) Under a molten fuel release of more than 100g, Na voids vibrate in the space for a cycle of 200 ~ 300 msec, while voids also remain for a prolonged time.

(4) The space behavior of Na voids is greatly influenced by the peripheral temperature, void condensation heat transfer rate, fuel grain size, UC_2-Na (vapor) heat transfer rate, and the mix ratio of non-condensed gas.

(5) Flowmeters with the time constant not longer than 100 msec can detect flow fluctuation in the case of more than 100g of released fuel.

(B) Analysis of Thermal Propagation Behavior in Fuel Assembly Following Local Molten Fuel Release

(1) The thermal propagation behaviors in the fuel assembly are greatly influenced by the coolant flow behaviors in the fuel released region and its peripheral zone.

(2) When the coolant flow rate in each flow channel is maintained at a nominal flow, the radial direction thermal propagation is minimal.

(3) Thermal release from the released molten fuel to sodium will nearly complete within 1 second, while the outlet temperature

will strengthen its repondency one second thereafter.

(4) The upper fuel plenum plays a role of heat moderator at the time of a violent heat release accident.

(5) The outlet temperature response is poor when the UO_2-Na thermal transfer coefficient has substantially declined (0.1W/cm ℃) by gas blanketing in the periphery of the released fuel.

(6) In the event of a fuel release near the wrapper tube, the outlet temperature response substantially declines because of the thermal outflow outside the wrapper tube wall.

(7) The effect of the parameters of released fuel particle size, UO_2-Na mixture ratio in the fuel released region, and the intra-subchannel coolant mixture ratio is small to the outlet mean temperature response. But the effect of the released fuel rate is the greatest.

(8) Thermometers of several 2 ~ 3 sec time constant are capable of detecting the released thermal energy when the released molten fuel quantity is more than 2 Kg. But if it is less than this quantity, detection may sometimes become difficult according to the release condition.

As the future R & D, further studies on the following items are considered necessary:

(1) For the analysis of localized UO_2-Na interaction, Na voids space movements (r, Z) shall be handled two dimensionally.

(2) For the analysis of the thermal propagation in the fuel assembly, the thermal mix effect from the change of fluid by a local Na void production is considered.

(3) At the time of fuel release nearby the wrapper tube wall, the thermal propagation effect in the adjacent fuel assembly should

be considered.

(4) By conducting analysis of the initial accidental phenomena leading to a fuel release, the released molten fuel rate and the fuel released region should be sought and determined.

(5) By seeking the possibility of the fuel failure propagation in the fuel assembly and its propagation velocity following the outbreak of a fuel release accident, a study must be developed to clarify at what point the reactor should be scrammed in order to prevent the fuel failure propagation further in the adjacent fuel assemblies.

(6) In order to analyze the phenomena of this kind of local accidents and to verify the detection conditions, it is essentially necessary to undertake a series of extensive out-pile and in-pile experiments and tests are essential.

Words of Appreciation

Hereby is expressed our deep appreciation for the advice and assistance extended to us in relation to the present experimental work by the members of the FBR Safety Research Technical Committee of PNC.